ABSTRACT

Name: Tigabu Kassa

Department: Chemistry and Biochemistry

Title: Production, Characterization, and Applications of Stereoselective Antibodies to α-Hydroxy acids

Major: Chemistry

Degree: Doctor of Philosophy

Approved by:

Date:

Dissertation Director

12/05/2007

NORTHERN ILLINOIS UNIVERSITY

ABSTRACT

While enantiomers, i.e., mirror-image-like stereoisomers, contain the same atoms and functional groups, differences in the three-dimensional arrangement of those atoms or groups may result in different biological activities. Regulatory agencies such as the US Food and Drug Administration require quantitative detection and characterization of individual enantiomers of chiral drugs and their metabolites because the pharmacodynamic, pharmacokinetic, and toxicological properties of enantiomers may differ. Therefore, separation and detection of enantiomers are crucial to the understanding of their biological roles. Antibodies raised against chiral haptens have the potential of discriminating between enantiomers, which makes them one of only a few tailor-made types of chiral selectors. In this dissertation, antibodies were raised against D- and L-α-hydroxy acids, respectively. Both polyclonal antibodies from rabbits and monoclonal antibodies from murine hybridomas were produced that stereoselectively bind to a wide range of α-hydroxy acids, including both aromatic and aliphatic α-hydroxy acids. No detectable interaction was seen with the "opposite" enantiomer. Further studies confirmed that the hydroxyl/carboxyl/ hydrogen triad about the stereogenic center is essential for antibody binding as no interaction was observed with structurally closely related compounds such as α-amino acids. Conversely, previously produced stereoselective anti-α-amino acid antibodies

bound only to α-amino acids of the correct configuration and not to α-hydroxy acids. The remarkable stereoselectivity and class specificity of these antibodies enabled the development of fluorescence-based immunoassays for the simultaneous detection of D-phenylalanine, L-phenylalanine, D-phenyllactic acid, and L-phenyllactic acid using four antibodies, each of which was labeled with a unique fluorophore. Furthermore, the utility of an anti-α-hydroxy acid antibody for enantiomer separation in chiral immunoaffinity chromatography was demonstrated.

NORTHERN ILLINOIS UNIVERSITY

PRODUCTION, CHARACTERIZATION, AND APPLICATIONS OF STEREOSELECTIVE ANTIBODIES TO α-HYDROXY ACIDS

A DISSERTATION SUBMITTED TO THE GRADUATE SCHOOL

IN PARTIAL FULFILLMENT OF THE REQUIREMENTS

FOR THE DEGREE

DOCTOR OF PHILOSOPHY

DEPARTMENT OF CHEMISTRY AND BIOCHEMISTRY

BY

TIGABU KASSA

DEKALB, ILLINOIS

DECEMBER 2007

Certification: In accordance with departmental and Graduate School policies, this dissertation is accepted in partial fulfillment of degree requirements.

Dissertation Director

12/05/2007

Date

ACKNOWLEDGMENTS

I would like to express my deepest gratitude to my advisors, Drs. Oliver and Heike Hofstetter, for their help including everything from ideas and advice to supplies and antibodies. I thank you for your mentorship, enthusiasm, and encouragement during these challenging years. Jodi Scaletta provided invaluable assistance with the care and use of animals for antibody production. Thank you to Jessica M. Kassa for assistance with chiral immunoaffinity chromatography. Steve Akkah and Judah J. Smith worked with me as undergraduates and helped with ELISAs. My gratitude is to Pauli Undesser for her support in the development of fluorescence-based immunoassays. To all of our research group—both past and present—it has been a joy to work and learn with you. I will treasure your friendships.

My heartfelt thanks to my friends and family. My parents, Kassa Zeleke and Taytu Hunde, have always supported me in every task I've undertaken. They taught me by example the importance of hard work and have always believed in me. My brothers, too, have been there to support me, to talk to and encourage me. Abebaw Zeleke, thank you for being like a father to me. Without your dedication, I could not have made it this far. My parents-in-law, Steve and Jane Pace—thank you for making me a part of your lives. I have learned so much from both of you. Thank you too for proofreading my dissertation. My wife, Jessica M. Kassa, I don't have words to express my appreciation. You are my best friend. I have learned so much discussing

and brainstorming with you. You have been my inspiration, struggling with me during these challenging years of research and study. I would not be here without you. Thank you for critiquing and editing my dissertation. Thank you my son, Elias, for your smiles, your affection, and your delight. You have brought so much meaning and joy to my life. I love being your father.

Funding for research, travel expenses for scientific conferences, stipends, and dissertation-related expenses was provided in part by the following institutions: the Department of Chemistry and Biochemistry, the Center for Biochemical and Biophysical Studies, the Graduate School, Rhotten A. Smith Fellowship, Diversifying Faculty Initiative Fellowship, and the National Institutes of Health.

DEDICATION

To my father

Abba Kassa Zeleke

TABLE OF CONTENTS

LIST OF TABLES

Table Page

LIST OF FIGURES

Figure Page

Figure Page

LIST OF ABBREVIATIONS

AA	α-Amino acid
AHA	α-Hydroxy acid
ATCC	American-type culture collection
BSA	Bovine serum albumin
cDNA	Complementary DNA
CDR	Complementarity determining region
CFA	Complete Freund's adjuvant
CSP	Chiral stationary phase
DMAP	4-dimethylaminopyridine
DMF	*N,N'*-dimethylformamide
DMSO	Dimethyl sulfoxide
DNA	Deoxyribonucleic acid
DSC	*N,N'*-disuccinymidyl carbonate
ELISA	Enzyme-linked immunosorbent assay
Fab	Antigen binding fragment
$F(ab')_2$	Immunoglobulin fragment obtained by pepsin digestion containing the hinge region and two V_HC_H1 and V_LC_L
Fc	Crystallizable fragment
FDA	US Food and Drug Administration
HAT	Cell culture medium supplement that contains hypoxanthine, aminopterin, and thymidine
HEPES	4-(2-hydroxyethyl)-1-piperazineethanesulfonic acid

HGPRT	Hypoxanthine-guanine-phosphoribosyl transferase
HPLC	High-performance liquid chromatography
HRP	Horseradish peroxidase
HS	Horse serum
IACUC	Institutional Animal Care and Use Committee
IC_{50}	Inhibitory concentration for 50% decrease in binding
IFA	Incomplete Freund's adjuvant
Ig	Immunoglobulin
IgA	Immunoglobulin A
IgD	Immunoglobulin D
IgE	Immunoglobulin E
IgG	Immunoglobulin G
IgM	Immunoglobulin M
IR	Infrared
KLH	Keyhole limpet hemocyanin
LDH	Lactate dehydrogenase
MIPs	Molecularly imprinted polymers
MS	Mass spectrometry
MSUD	Maple syrup urine disease
NADH	The reduced form of nicotinamide adenine dinucleotide
NMR	Nuclear magnetic resonance
OPD	1,2-Phenylenediamine

ORC	Office of Research Compliance
PAGE	Polyacrylamide gel electrophoresis
PBS	Phosphate-buffered saline
PEEK	Polyetheretherketones
PEG	Polyethylene glycol
PLA	Phenyllactic acid
ppm	Parts per million
RIA	Radioimmunoassay
RNA	Ribonucleic acid
RPMI-1640	Cell culture medium developed at Roswell Park Memorial Institute, hence the acronym RPMI.
RPMI-HAT-HS	Cell culture medium prepared from RPMI-1640 with supplements HAT and HS
SDS	Sodium dodecylsulfate
TEA	Triethylamine
Tk	Thymidine kinase
TLC	Thin-layer chromatography
UV	Ultraviolet
WAC	Weak affinity chromatography

CHAPTER I

INTRODUCTION

Stereoisomers are molecules that have the same constituents and structural formula but differ in the spatial arrangement of certain atoms or groups of atoms. Enantiomers are stereoisomers that are nonsuperimposable mirror images and rotate plane-polarized light equally in opposite directions. Separation and detection of enantiomers remains challenging since they share most of their chemical and physical properties, such as melting point, boiling point, and solubility.

Louis Pasteur, in 1848, first discovered enantiomers when he found that tartaric acid formed distinct crystals, which are comprised of its pure enantiomeric forms.[1] Ten years later, Pasteur also recognized that in a biological system, the metabolization of each enantiomer might be different.[2] A better understanding of the physiological basis of chiral discrimination in biological systems resulted from the work of Emil Fischer and contemporaries, who showed that proteins are able to distinguish between enantiomers.[3-6] Numerous examples of differences in the biological activity of enantiomers have been described. For example, Piutti discovered as early as in the 1880s that L-asparagine is tasteless while D-asparagine tastes sweet.[7] Enantiomers may also have a distinct odor. (*R*)-limonene has an odor of oranges while (*S*)-limonene has an odor of lemons. Although (*R*)-limonene is

extracted from oranges and (*S*)-limonene from lemons, their differences in odor had been attributed to impurities until Friedman and Miller synthesized the enantiomers of limonene in 1971.[8]

The enantiomers of drugs may also differ in their biological activities; one enantiomer may have a desired effect while the other may be toxic. For example, D-penicillamine is used to treat both heavy metal poisoning and Wilson's disease, which is a hereditary defect in copper metabolism;[9] it is also used to treat arthritis.[10] L-penicillamine, however, is toxic.[10] In other cases, the two enantiomers of a drug are used to treat different diseases. For example, (*S*)-thyroxine is used to treat thyroid deficiency while (*R*)-thyroxine decreases serum cholesterol.[11]

Since enantiomers of a drug can have such drastic differences in activity, the US Food and Drug Administration (FDA) issued a policy statement in 1992 requiring pharmacodynamic, pharmacokinetic, and toxicological studies of individual enantiomers of drugs.[12] Therefore, suitable techniques for the detection and separation of enantiomers are needed to evaluate the enantiomeric composition of synthetic products and to determine the stereochemistry of drugs and metabolites.[13]

A variety of methods have been developed for the detection and separation of enantiomers. The oldest method of enantiomer resolution is crystallization. While some enantiomers, like tartaric acid, can be purified directly by crystallization, others are first reacted with an optically pure compound to form diastereomers so as to aid in the formation of pure crystals.[14]

One of the most popular methods for both detection and separation of enantiomers remains chiral chromatography, which is more versatile and faster than crystallization. The two variants of chiral chromatography are known as the direct and indirect methods. In the indirect method, enantiomers are reacted with another enantiomerically pure compound, a chiral derivatizing agent, to form diastereomers, which can be resolved on standard "achiral" chromatographic supports due to differences in their chemical and physical properties.[15] Despite the fact that this method is used for both analytical- and preparative-scale enantioseparations, numerous limitations remain.[15] Appropriate functional groups must be available on the chiral target molecule. The chiral derivatizing agent should be cheap, readily available, and optically pure. The derivatization reaction should be quantitative, and available chromatographic columns should be able to separate the resulting diastereomer. In the case of preparative-scale separations, the diastereomer must be cleaved to yield the desired, optically pure product and the chiral derivatizing agent in high yields. Additionally, the reaction conditions for both derivatization and cleavage must be mild enough to prevent racemization of either the chiral derivatizing agent or the target molecule. Indirect separations are generally multistep and time-consuming processes.

In direct chromatographic methods, separations can be performed without chemical modification of the chiral target molecules. Instead, enantioseparations are achieved via the formation of transient pseudo-diastereomeric complexes between a so-called chiral selector and the individual enantiomers of a chiral compound.

Chromatographic separations exploit the difference in the free energies of the transient complexes of the two enantiomers.[16] The chiral selector can be immobilized to solid-phase support materials, thus producing a so-called chiral stationary phase (CSP); separations can be performed with an achiral mobile phase. Alternatively, the chiral selector can be used as a chiral mobile phase additive with an achiral stationary phase. In both approaches, the chiral selector and the enantiomer interact via a combination of noncovalent forces including hydrogen bonding between acidic and basic sites, electrostatic interactions between polar/charged sites, π-π interactions of aromatic groups, and van der Waals attraction between hydrophobic portions of the interacting chiral selector and the enantiomer. Because enantiomers differ in their three-dimensional structure, steric interactions may also play an important role in recognition by chiral selectors. A wide variety of chiral selectors are commercially available such as macrocyclic antibiotics, π-donor/π-acceptor systems, oligo- and polysaccharides, synthetic polymers, ligand-exchange selectors, crown ethers, and proteins like bovine serum albumin (BSA).[17] Many of these chiral selectors have also been used for enantiomer separations in capillary electrophoresis and capillary electrochromatography.[18,19] Other chiral discrimination methods that are used to detect the interaction between enantiomers and a chiral selector are based on techniques like nuclear magnetic resonance (NMR),[20] mass spectrometry,[21] or microarrays.[22] Because typical chiral selectors are not designed for a specific enantiomer, the interaction between the enantiomer and chiral selector must be determined experimentally or predicted using a model derived from experimental

results. The enantioselectivity of a given chiral selector, however, can only be usefully predicted for molecules closely related to the enantiomers used in the original experiments. Additionally, data obtained from such models is generally only qualitative in nature.[23,24]

In order to avoid the often time-consuming and expensive process of identifying an effective chiral selector by trial and error, three methods are currently being investigated to produce tailor-made chiral selectors with a predetermined specificity: molecularly imprinted polymers (MIPs),[25-27] DNA and RNA aptamers,[28-34] and antibodies.[35] MIPs have been used as chiral stationary phases in high-performance liquid chromatography (HPLC), capillary electrophoresis, capillary electrochromatography, sensors, and immunoassays.[36-38] MIPs, however, have heterogeneous binding sites with varying affinities, which typically leads to significant peak broadening and tailing.[39] This effect may be increased by slow mass transfer kinetics due to poorly accessible binding sites and irregular particles. Poorly accessible binding sites are typically a result of small pore sizes, whereas the most common preparation method for MIPs, bulk polymerization, leads to irregularly sized and shaped particles.[39] Irregular particles also contribute to high back pressures.[39] Furthermore, MIPs may show nonspecific interactions, especially in aqueous phases.[40]

More recently, DNA and RNA aptamers have been used for chiral separations in chromatography and capillary electrophoresis.[28-34] While stereoselective aptamers of both DNA and RNA were produced previously,[41-44] Peyrin et al. were the first to report the utility of stereoselective aptamers as CSP.[28] Aptamers are advantageous

because they can be synthesized chemically in a short time with high purity and because their binding selectivity can be manipulated by changing their sequence.[45] However, the systematic evolution of ligands by exponential enrichment procedures used to select for aptamers with desired binding properties can be expensive and time-consuming.[29] Column stability must still be improved to compete with standard chromatographic techniques. While one of the DNA aptamers used in HPLC lasted for at least five months,[28] another showed drastic deterioration after only two months.[29] Chromatographic conditions have typically been limited to the use of aqueous solvents, although with one RNA aptamer CSP, an organic modifier was added to the mobile phase.[30] Columns suffer from broad peaks and low efficiency due to slow kinetics.[28] Additionally, the high specificity of aptamers has usually limited separation applicability to a single pair of enantiomers.[32]

The third type of tailor-made chiral selectors are antibodies. These glycoproteins are produced by the humoral immune response of vertebrates.[46] Immunoglobulin G (IgG), specifically, is the class of antibodies most readily available from serum.[47] IgGs are comprised of two identical "heavy" and two identical "light" chains connected by noncovalent interactions and disulfide bridges, thus forming a "dimer of dimers."[48] IgG antibodies possess two binding sites, which are formed from the so-called complementarity determining regions (CDRs) at the N-termini of each heavy and light chain pair.[49] Since the sequences of the CDRs, and thus binding specificities, vary widely among antibodies, an animal is able to recognize millions of structurally different antigens. Because of this variability, the regions of the antibody

that contain CDRs are known as "variable domains."[49] Unlike the N-terminal variable regions of the heavy and light chains, the sequence and structure of the constant domains of an antibody are largely conserved.[50]

In principle, antibodies can be raised against any molecule; however, molecules smaller than 5,000 Da are typically not immunogenic. In the early 1900s, though, Karl Landsteiner realized that small molecules, known as haptens, can be conjugated to a carrier in order to elicit an immune response.[51] Because of their immunogenicity, proteins are most frequently used as carriers. The chemistry employed to couple the hapten to a carrier should result in an optimal, directed presentation of the target structure of the hapten on the carrier.[51] The carrier-hapten conjugate can then be used to immunize animals and, thus, produce the desired antibodies.[51,52] After immunization, many different B-cells are stimulated and secrete a wide variety of antibodies (i.e., polyclonal antibodies). Polyclonal antibodies can easily be obtained from the sera or interstitial fluid of mammals, such as rabbits; therefore, their production is cost-effective and efficient.[52] However, because polyclonal antibodies comprise a heterogeneous population of immunoglobulins, there will be antibodies against unrelated antigens as well as antibodies with differing affinities for the same antigen and antibodies of different subclasses and consequently different biological properties. Additionally, their production is highly dependent on the survival of the animal. Monoclonal antibodies can be used to overcome the limitations of polyclonal antibodies.

In 1975, the production of monoclonal antibodies was first pioneered by Milstein and Köhler, who fused myeloma cells with antibody-secreting B-cells *in vitro*, making immortalized monoclonal antibody-secreting cells, called hybridomas.[53-56] Because each hybridoma cell line secretes a unique antibody, monoclonal antibodies have the same specificity and affinity for an antigen. A population of such antibodies, therefore, has homogeneous binding properties. The myeloma cells commonly used for hybridoma production lack the gene for one of two enzymes: either hypoxanthine-guanine-phosphoribosyl transferase (HGPRT) or thymidine kinase (Tk). The myeloma cells, therefore, are unable to synthesize the nucleotides adenosine monophosphate and guanosine monophosphate (in the case of HGPRT-deficient cells) or thymidine monophosphate (in the case of Tk-deficient cells) via the salvage pathway. Instead, the myeloma cells rely on the *de novo* pathway for nucleotide synthesis. After fusion, the cells are cultivated in HAT medium, which contains hypoxanthine, aminopterin, and thymidine, to select for hybridoma cells. Unfused B-cells die after a few days since they are not immortal. Furthermore, the dihydrofolate analog, aminopterin, blocks the *de novo* pathway, which effectively kills unfused myeloma cells. The hybridoma cells, however, are able to synthesize nucleotides via the salvage pathway using the hypoxanthine and thymidine supplied in the media because the B-cells "contributed" their functional HGPRT and Tk genes. Because hybridoma cell lines contain the genes from the myeloma cells, these hybridoma cell lines are immortal. In theory, hybridoma cells can be cultured indefinitely or frozen for later use.

Typically, hybridoma cells are initially cultured in 96-well sterile microtiter plates following limiting dilution. In limiting dilution, the concentration of cells plated out should be low to increase the probability of monoclonality, yet sufficiently high to promote cell growth. Positive clones are selected by screening the cell-culture supernatant for antibodies with the desired binding characteristics. Assays commonly used for screening include enzyme-linked immunosorbent assay (ELISA), radioimmunoassay (RIA), immunofluorescence, cytotoxicity assays, and immunoprecipitation. Positive clones are subcloned by multiple rounds of limiting dilution to ensure monoclonality until virtually every well tested is positive. The hybridomas that secrete the antigen-specific antibody can then be cultured in bigger cell culture flasks and may be used to up-scale production either in bioreactors or through ascites production in the peritoneal cavity of mice.

Both polyclonal and monoclonal antibodies have become increasingly important tools in analytical biochemistry for "achiral applications."[57] However, even though Landsteiner, in 1928, demonstrated that antibodies may discriminate between stereoisomers, including enantiomers,[58] antibody stereoselectivity has found only limited use for "chiral" applications in, e.g., chromatography, extraction, immunoblotting, immunohistochemistry, immunoassays, and sensors.[35] In order to establish antibodies as chiral selectors for routine use, highly stereoselective and specific antibodies need to be produced against a wider range of chiral compounds. In addition, the utility of these antibodies in a variety of analytical techniques should be demonstrated.

The widest variety of applications using stereoselective antibodies have been developed by Hofstetter and Hofstetter.[35] They produced poly- and monoclonal antibodies against protein conjugates of *p*-amino-D- and -L-phenylalanine (Phe), respectively. These antibodies recognize not only the haptens but also other α-amino acids (AAs) of the correct configuration. That is, the anti-D-AA antibodies bind to D-AAs, whereas the anti-L-AA antibodies bind to L-AAs.[59,60] While the antibodies primarily recognize the amino/carboxyl/hydrogen triad about the α-carbon, the nature of the side chain is of less importance but affects the overall binding affinity. AAs most similar in structure to the hapten show the strongest binding to the antibodies. Therefore, aromatic AAs generally are bound more strongly than aliphatic AAs. However, AAs lacking the amino/carboxyl/hydrogen triad such as β-alanine or proline show no binding interaction with the antibody as determined by competitive ELISAs.[59] The anti-AA antibodies have been used for chiral discrimination of AAs in various bioanalytical techniques such as immunoassays, chromatography, and sensors.[35,59-71]

A primary objective of this dissertation was to produce stereoselective antibodies against the structurally related class of compounds, the α-hydroxy acids (AHAs). AHAs represent one of the most important classes of biologically relevant chiral molecules since they are involved in various biological processes.[72,73] They are abundant in nature and have been extracted from animal tissues, plants, and microorganisms.[74] Determination of the stereochemistry of AHAs is essential for understanding their exact roles in biochemical processes and to diagnose and monitor

certain diseases.[75] Metabolic acidosis, for example, results from an accumulation of organic acids in the blood.

One variant of metabolic acidosis, lactic acidemia, is caused by the abnormal accumulation of lactic acid in the blood.[76] The stereospecific detection of lactic acid enantiomers can be used to determine the nature and origin of the disease.[75] L-Lactic acidosis can be caused by, e.g., hypotension or as a side effect of drugs such as nucleoside reverse-transcriptase inhibitors.[77,78] Because nucleoside reverse-transcriptase inhibitors inhibit mitochondrial DNA polymerase γ, mitochondrial DNA cannot be properly replicated. The body, therefore, is forced to rely on anaerobic metabolism instead of oxidative phosphorylation, which in turn leads to the accumulation of lactic acid.[77,78] D-Lactic acidosis can be caused by short bowel syndrome and the overpopulation of bacteria such as *Lactobacillus* in the colon.[76]

Another variant of metabolic acidosis, maple syrup urine disease (MSUD), is caused by a deficiency of the branched-chain α-keto acid dehydrogenase complex. This deficiency results in the accumulation of branched-chain AAs as well as the corresponding α-keto acids and AHAs. It has been known that MSUD can result in neurological damages and mental retardation. The elucidation of the enantiomeric ratios of the relevant metabolites can be used to determine metabolic enzyme activities involved in MSUD.[79]

AHAs are also contained in a wide array of cosmetics such as creams and lotions. While these AHAs are intended to reduce wrinkles, spots, and other signs of aging and sun damage,[80] they also make users more sensitive to sunlight—specifically

ultraviolet light.[81] This, in turn, increases the risk of skin cancer. AHAs, therefore, are under increasing scrutiny by the FDA.[82] In fact, many scientists are advocating reclassification of AHAs as drugs by the FDA.[83]

In synthetic organic chemistry, enantiomerically pure AHAs are both important products and chiral building blocks.[84,85] For example, optically active ether-linked β-lactams have been synthesized via 4-bromo-2-hydroxybutanoic acid esters derived from (*R*)- or (*S*)-malic acid.[86] The ester forms of AHAs can also be used in reactions such as metal-catalyzed aldol and Michael reactions to synthesize bi- and tridentate phosphane and thioether ligands, thiodiglycols, and diglycols.[87,88] Many natural products have been synthesized from AHAs. For example, the phosphatase inhibitor motuporin, originally isolated from the marine sponge *Theonella swinhoei*, can be synthesized from D-mandelic acid.[89] Eremantholide A from *Ermanthus elaeagnus* can also be synthesized from D-lactic acid. This compound has been investigated *in vitro* as an antitumor agent in a range of cell lines.[90] Other examples of natural products include integerrimine and monocrotaline, which were previously isolated from a variety of plants, including the families Boraginaceae (all genera), Compositae (genera *Senecioneae* and *Eupatorieae*), and Leguminosae (genus *Crotalaria*). Both integerrimine and monocrotaline can be synthesized from (*R*)-malic acid.[91,92]

Because of their biodegradability and biocompatibility, poly-AHAs have recently become popular in biomedical and pharmaceutical applications.[93] Polylactic acid, polyhydroxybutyric acid, and polyglycolic acid have all been utilized as

polymeric drug carriers[94] and bioresorbable sutures.[95,96] Degradation of these biopolymers in living organisms, e.g., humans, occurs by either enzymatic or nonenzymatic hydrolysis resulting in both water-soluble and water-insoluble oligomers. Water-soluble oligomers are readily excreted, whereas water-insoluble oligomers are processed by macrophages.[97] Depending on the particular use of these poly-AHAs, the hydrolysis rates can be controlled by choosing suitable enantiomeric ratios. This is based on the fact that poly-L-lactic acid degrades more rapidly than poly-D-lactic acid. However, both poly-D- and poly-L-lactic acids are highly crystalline and, therefore, degrade more slowly than poly-D,L-lactic acid.[98] Additionally, functional groups can be included in the polymer to increase the hydrophilic nature, thus increasing degradation rates.[99,100]

Because chiral AHAs are used in such a wide variety of applications ranging from cosmetics to organic synthesis and biopolymers, their preparation is of considerable technological and commercial interest. Both enzymatic and nonenzymatic methods for the enantioselective synthesis of AHAs have been developed. One example of enzymatic synthesis is the oxidation of racemic 1,2-diols to enantiomerically pure L-α-hydroxy aldehydes by horse liver alcohol dehydrogenase, followed by conversion to L-AHAs catalyzed by aldehyde dehydrogenase.[101] Other examples include the reduction of carbonyl compounds by NADH-dependent oxido-reductases like lactic acid dehydrogenase (LDH).[102] LDH catalyzes the stereospecific reduction of pyruvate to either D- or L-lactate depending on the specificity of the enzyme used. Thus, LDH from a variety of sources such as

rabbit muscle, bovine heart, and lobster tail can be used to synthesize L-lactate.[103] Alternatively, LDH from *Leuconostoc mesenteroides* produces D-lactate.[104] Other enzymatic methods are used to synthesize structurally related compounds, which, in turn, can be converted to enantiomerically pure AHAs. Baker's yeast (*Saccharomyces cerevisiae*) has been used to convert α-keto esters to enantiopure α-hydroxy esters, which can easily be hydrolyzed to yield pure AHAs.[105] Nitrilases can be used to stereospecifically add a nitrile to aldehydes in order to produce α-hydroxy cyanohydrins. The cyanohydrins are then converted to chiral AHAs with retention of the stereochemistry by acid hydrolysis.[106]

Nonenzymatically, AHAs are synthesized via various asymmetric synthesis methods such as the reduction of α-keto acid-derived hemiacetals[107] or α-oxo esters,[108] asymmetric oxygenation of chiral imide enolates,[109] oxidation of terminal alkenes,[110] and asymmetric hydrogenation of both enol esters[111] and α-functionalized ketones.[112] Alternatively, chiral AHAs can be synthesized from the corresponding AAs by diazotization followed by acid hydrolysis.[113]

Despite the progress made in the asymmetric synthesis of AHAs, chiral discrimination remains important for testing the purity of not only synthesized AHAs but also those isolated from biological samples. Commonly, AHAs are separated into their enantiomers by chromatographic and electrophoretic systems using some of the same chiral selectors that are used to separate AAs; these include ligand-exchange selectors,[114] macrocyclic antibiotics,[115] π-donor/π-acceptor systems,[116] and proteins.[117]

Interestingly, crown ethers can only be used for AA separations and not for the separation of AHAs.[118]

Determination of lactic acid enantiomers is also carried out enzymatically using D- or L-lactic acid dehydrogenase, which converts either D- or L-lactic acid to pyruvate. Since lactic acid dehydrogenase is NADH dependent, the concentration of produced D- or L-lactic acid can be correlated to the concentration of NADH measured at 340 nm.[119] In 1998, McKendry et al. developed a chemical force microscopy method for the chiral discrimination of mandelic acid. [120] D- or L-Mandelic acid was immobilized on a gold surface while a Pirkle-type chiral selector was immobilized on an atomic force microscopy tip. Interaction between the immobilized chiral selector and the mandelic acid enantiomers on the gold surface resulted in measurable differences in adhesion and friction forces, which were then used to distinguish between the two enantiomers.[120]

The first objective of this dissertation was to produce both polyclonal and monoclonal antibodies that stereoselectively bind to the enantiomers of AHAs. In order to produce such antibodies, conjugates of *p*-amino-D- and *p*-amino-L-phenyllactic acid (PLA), respectively, and keyhole limpet hemocyanin (KLH) had to be synthesized and used to immunize rabbits and mice following the method developed by Hofstetter et al. for the production of anti-AA antibodies.[59]

The second objective of this work was to characterize the binding specificity and stereoselectivity of the produced antibodies using both noncompetitive and competitive ELISAs. The affinity of these antibodies to a variety of different AHAs

was to be tested in order to evaluate the influence of the nature of the side chain on the overall affinity.

Because AHAs and AAs are structurally very similar classes of compounds that differ only in one functional group linked to the stereogenic center, a further goal of this dissertation was to test these antibodies for their ability to distinguish between different classes of compounds. Additional ELISAs had to be performed to test the binding of anti-AHA antibodies to AAs and, conversely, the binding of previously produced anti-AA antibodies to AHAs. The anti-AHA antibodies were also to be tested for their ability to bind to other structurally related compounds in order to further evaluate their specificity.

The final objective of this dissertation was to demonstrate the utility of these antibodies in analytical applications such as chiral chromatography and immunoassays.

CHAPTER II

MATERIALS AND METHODS

Chemicals

D- and L-PLA, 2-hydroxyisocaproic acid, and L-Phe were purchased from Aldrich (Milwaukee, WI). The following chemicals were from Sigma (St. Louis, MO): 2-hydroxydecanoic acid, 2-hydroxyoctanoic acid, D-mandelic acid, D-Phe, and tyramine. D- and L-α-hydroxyisovaleric acid, L-lactic acid sodium salt, and L-mandelic acid were purchased from Fluka (Milwaukee, WI). All these compounds were of the highest purity available.

Complete Freund's adjuvant (CFA), incomplete Freund's adjuvant (IFA), bovine serum albumin (BSA), gelatin, and keyhole limpet hemocyanin (KLH) were from Sigma (St. Louis, MO). All horseradish peroxidase-conjugated goat anti-rabbit, goat anti-mouse, and donkey anti-goat secondary antibodies were purchased from Jackson Immuno Research Laboratories, Inc. (West Grove, PA). The mouse monoclonal antibody isotyping reagents were from Sigma (St. Louis, MO). Goat anti-mouse IgG DyLight™ 647-conjugated antibody, goat anti-rabbit DyLight™ 547-conjugated antibody, DyLight™ 547 NHS Ester, DyLight™ 647 NHS Ester, DyLight™ 800 NHS Ester, and DyLight™ 490 NHS Ester were from ThermoFisher

(formerly Pierce Biotechnology, Rockford, IL). All anti-AA antibodies used in this study were previously produced by Drs. Oliver and Heike Hofstetter.[59,60]

The following cell culture reagents were purchased through Sigma (St. Louis, MO): RPMI-1640 medium, HAT media supplement (50x), sodium pyruvate, sodium hydroxide, hydrochloric acid, D-glucose, sodium bicarbonate, HEPES, horse serum donor herd heat inactivated (HS), benzalkonium chloride, dimethyl sulphoxide, and polyethylene glycol (PEG, MW 1,300-1,600). Antibiotic-antimycotic was from Invitrogen (Grand Island, NY).

1,2-Phenylenediamine (OPD) was from Aldrich (Milwaukee, WI). *N,N'*-disuccinymidyl carbonate (DSC) and 4-dimethylaminopyridine (DMAP) both were from NovaBiochem (La Jolla, CA). *N,N'*-dimethylformamide (DMF) was from Sigma-Aldrich (Milwaukee, WI).

Other salts were purchased from Fisher Scientific (Fair Lawn, NJ) and were of analytical grade. Preparation of buffers and cell culture media is described in the Appendix. Organic solvents were from Aldrich (Milwaukee, WI) and were all of reagent grade. All water was deionized using a Milli-Q water purification system from Millipore (Bedford, MA); ultrapure water for cell culture use came from the Core DNA Analysis Lab of NIU's Department of Biological Sciences.

Materials

Ninety-six-well MaxiSorp polystyrene microtiter plates were from Nunc (Rochester, NY); 96-well Immulon Immunoassay microplates were from Dynex Technologies (Chantilly, VA). A comparison of the two types of plates showed no significant difference in ELISA results. Nucleosil silica (100-3) was obtained through Alltech Associates, Inc. (Deerfield, IL). PEEK tubing (0.75 mm), a 2 μm frit-in-a-ferrule and a high-pressure-adjustable-back pressure regulator set to 43 bars were from Upchurch Scientific (Oak Harbor, WA). Sepharose CL4B was purchased from Pharmacia (Uppsala, Sweden). Centriplus centrifugal filter devices with molecular weight cut-offs of 30 and 100 kDa, respectively, were from Millipore (Bedford, MA). The Melon™ Gel IgG purification kit, 4-20% Precise™ protein gels (12-well), BupH™ Tris-HEPES-SDS running buffer, GelCode® blue stain reagent, and Reacti-Bind™ White Opaque 96-well plates were from ThermoFisher (formerly Pierce Biotechnology, Rockford, IL).

Twelve-week-old female New Zealand white rabbits and eight-week-old female BALB/c mice were both purchased from Harlan (Indianapolis, IN). The P3x63AG8 myeloma cell line was from ATCC (Manassas, VA).

Twelve- and 24-well tissue culture plates and 25, 250, and 600 mL tissue culture flasks were from Falcon (Franklin Lakes, NJ); 96-well cell culture plates and 25 cm^2 cell culture flasks were from Corning, Inc. (Corning, NY). Petri dishes as well as both 2 and 10 mL serological pipets were from Fisher Scientific (Fair Lawn, NJ).

A Nalgene™ cryo 1°C freezing container was purchased from Nalgene (Rochester, NY).

Instruments

The purifier class II biosafety cabinet model 3620904Δ was from Labconco (Kansas City, MO) and was installed and certified by Air Contamination Technologies (Chicago, IL). The inverted microscope Nikon ECLIPSE TS 100 for cell culture use was from Fryer Company, Inc., Scientific Instruments (Huntley, IL). The lab line CO_2 incubator model 460 was purchased from Fisher Scientific (Fair Lawn, NJ). The Locator 4 cryo biological storage system was from Thermolyne (Dubuque, Iowa). The GS-6R and Model J2-21 centrifuges came from Beckman Coulter (Fullerton, CA); the lyophilizer model line FreeZone 4.5 and rotary evaporator were both from Labconco (Kansas City, MO). The 200 MHz nuclear magnetic resonance (NMR) instrument was from Bruker Biospin Corp. (Billerica, MA). The FT-IR Genesis spectrophotometer was from Mattson (Madison, WI). The ATAGO polarimeter model AP-300 used for determination of optical rotations was from National Microscope Exchange (Carnation, WA). The Esquire 3000 ion trap mass spectrometer (MS) was fitted with an electrospray source and came from Bruker Daltonics, Inc. (Billerica, MA). The 1000/500 model power supply for gel electrophoresis was from BioRad (Hercules, CA). The RP-1 model peristaltic pump was purchased from Rainin (Emeryville, CA). The plate reader with FLOUstar 403 Galaxy control and evaluation

software came from BMG Labtechnologies (Offenburg, Germany). Alltech Slurry Packer model 1666 fitted with a 20 mL reservoir was from Alltech (Deerfield, IL). The chromatography system was from Hitachi (Naperville, IL) and consisted of an L-7400 UV detector fitted with a semi-micro flow cell, an L-7100 pump, a degasser, and a D-7000 interface. System Manager V 4.0 software was used for both instrument control and data collection. The Rheodyne 7725i injector, also from Hitachi (Naperville, IL), was fitted with a 5 μL injection loop.

Synthesis of Immunogens

p-Nitro-D- and -L-Phenyllactic Acid

p-Nitro-D- and -L-PLA were each synthesized separately from D- and L-PLA as follows (Figure 1): 500 mg of D- or L-PLA were mixed with three parts of concentrated sulfuric acid at room temperature. The solutions were then cooled on ice. One part of concentrated nitric acid was added dropwise to the cooled solutions while stirring. After ten minutes, 10 mL of cold water were added to the reaction mixtures; 3M ammonium hydroxide was used to adjust the pH to 9. The product, *p*-nitro-D- or -L-PLA, were first lyophilized, then recrystallized from methanol, and finally purified by thin-layer chromatography (TLC) using 1-butanol:water:acetic acid (4:1:1) as solvent.

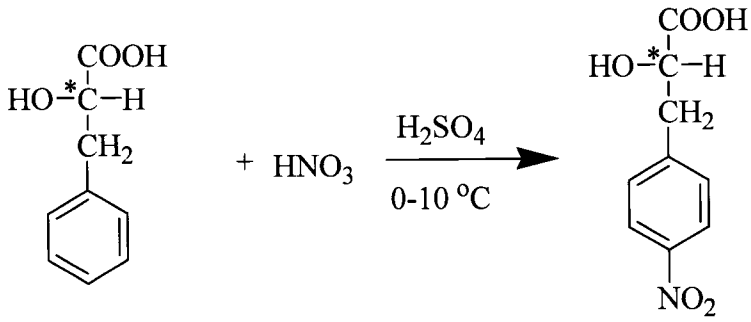

Figure 1: Nitration of D- or L-phenyllactic acid.

p-Amino-D- and -L-Phenyllactic Acid

p-Nitro-D- and -L-PLA were hydrogenated to *p*-amino-D- and -L-PLA, respectively (Figure 2). Four hundred mg of *p*-nitro-D- and -L-PLA were each dissolved separately in methanol, and 40 mg of palladium-charcoal hydrogen catalyst was added to the reaction mixtures. A hydrogen-filled balloon was connected to each of the reaction vessels. *p*-Nitro-D- and -L-PLA were hydrogenated at atmospheric pressure for two days under continuous stirring. The products were lyophilized, recrystallized from methanol, and purified by TLC using 1-butanol:water:acetic acid (4:1:1) as solvent.

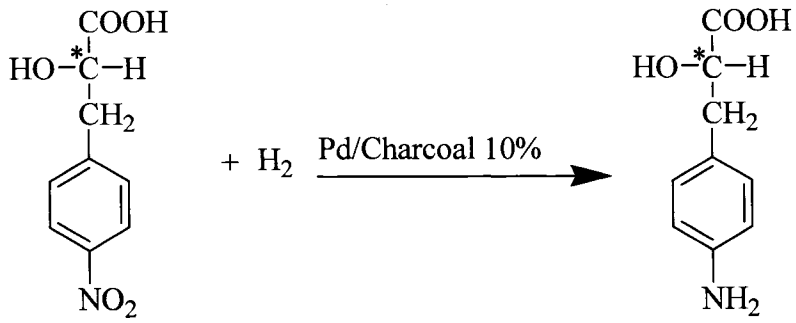

Figure 2: Hydrogenation of *p*-nitro-D- or -L-phenyllactic acid.

p-Azo-D- and -L-Phenyllactic Acid-Tyramine Conjugates

p-Azo-D- and -L-PLA-tyramine, respectively, were synthesized by modifying the method of Tabachnick and Sobotka (Figure 3).[121] *p*-amino-D- and -L-PLA (15 mg each) were dissolved separately in 1 mL of 0.1 M hydrochloric acid and cooled on ice. An equimolar amount of sodium nitrite was added to the solutions of *p*-amino-D- and -L-PLA while stirring continuously. Aliquots of tyramine (60 mg each) were dissolved in 100 mM borate buffer, pH 8.5, and added to each of the *p*-amino-PLA solutions. The pH was adjusted to 8.5 with 0.1 M sodium hydroxide. The mixture was allowed to react overnight at room temperature. The resulting *p*-azo-D- and -L-PLA-tyramine conjugates were first lyophilized, then recrystallized from methanol, and then purified by TLC using 1-butanol:water:acetic acid (4:1:1) as solvent.

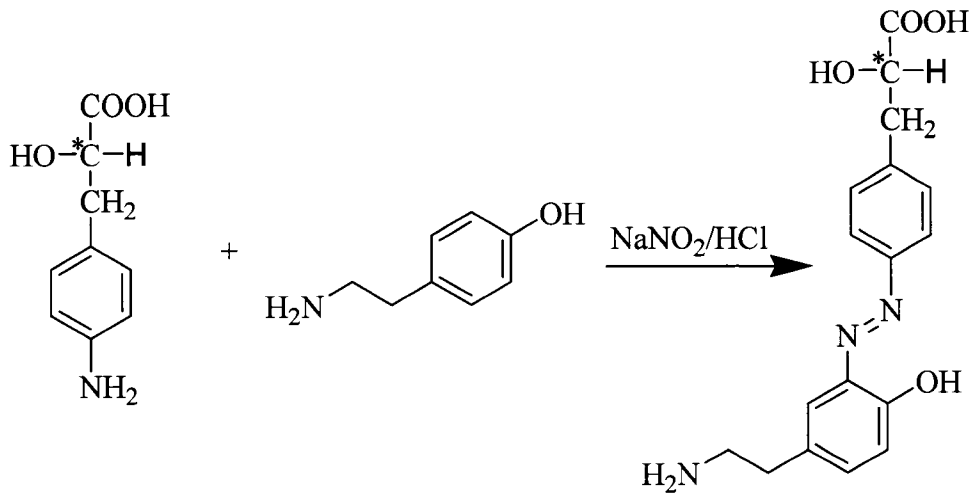

Figure 3: Diazotization reaction resulting in the formation of *p*-azo-D- and -L-phenyllactic acid tyramine conjugates.

Hapten-Carrier Conjugates

p-Amino-D- and -L-PLA were separately coupled to the proteins KLH and BSA via diazotization (Figure 4). Thirty mg of *p*-amino-D- or -L-PLA were dissolved in 2 mL of 0.1 M hydrochloric acid. The solution was cooled on ice, and an equimolar amount of sodium nitrite was added while stirring continuously. Sixty mg of protein were dissolved in 2 mL of 100 mM borate buffer (pH 8.5) and cooled on ice. After ten minutes, the reaction mixture was added dropwise to the cooled protein solution. The pH was readjusted to 8.5 by the addition of 0.1 M sodium hydroxide. The reaction was allowed to proceed overnight at 4°C. Following diazotization, the protein conjugates, *p*-azo-D- and -L-PLA-KLH, and *p*-azo-D- and -L-PLA-BSA were extensively dialyzed against phosphate-buffered saline (PBS) at 4°C.

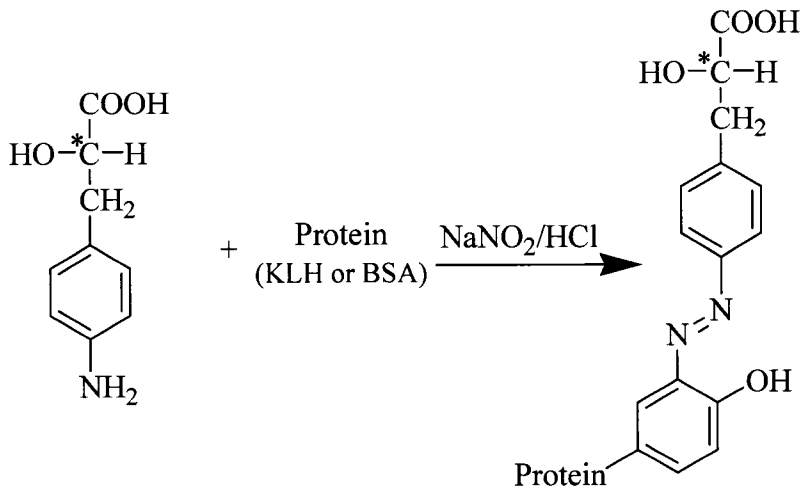

Figure 4: Coupling of *p*-amino-D- and -L-phenyllactic acid to tyrosine residues of the proteins KLH or BSA.

Protein concentrations were determined spectrophotometrically by measuring the absorbance at 280 nm. The hapten density was calculated based on the absorbance of the protein conjugates at 370 nm using the extinction coefficient of the *p*-azo-PLA-tyramine conjugate, which was determined independently from recrystallized samples.

Antibody Production

All animal and cell culture work was performed in accordance with Northern Illinois University's Institutional Research Compliance Guidelines. Institutional Animal Care and Use Committee (IACUC) approval was obtained for all work with animals (ORC #217 and ORC #258 for rabbits, and ORC #218 and ORC #262 for mice, respectively).

Polyclonal Antibody Production

For the first immunization (week 0), 100 μg of *p*-azo-D-PLA-KLH and *p*-azo-L-PLA-KLH, respectively, in complete Freund's adjuvant were injected subcutaneously at multiple sites in the back of rabbits #73 and #65, respectively. The rabbits were each given booster injections of 100 μg of *p*-azo-D- or -L-PLA-KLH in incomplete Freund's adjuvant after two weeks. Final immunizations were given after four weeks using 100 μg of the respective immunogens in PBS. Interstitial fluid samples were taken biweekly beginning with a pre-immunization sample at week 0. The samples were collected from wiffle balls implanted under the skin of the rabbits. Final blood samples were taken after sacrificing the animals.

Monoclonal Antibody Production

Five eight-week-old BALB/c mice were immunized with *p*-azo-D-PLA-KLH while another five mice were immunized with *p*-azo-L-PLA-KLH. Fifty to100 μg of the respective immunogen in complete Freund's adjuvant were injected intraperitoneally. The mice were given booster injections two weeks later with 50-100 μg of the respective immunogen in incomplete Freund's adjuvant. Booster injections of 50-100 μg of immunogen in PBS were given four weeks after the initial immunization and also three to four days before harvesting the spleens. Serum

samples were collected from the tail of each mouse and tested for antibody production and stereoselectivity using competitive and noncompetitive ELISAs. The procedure for ELISAs is described in Chapter II in the section Enzyme-Linked Immunosorbent Assay. Mice showing good immune responses were chosen for monoclonal antibody production.

In preparation for hybridoma production, myeloma cells were grown in RPMI-1640 medium until the culture contained $2x10^7$ cells.

The chosen mouse was anesthetized with carbon dioxide and terminated by cervical dislocation. The mouse was then prepped for surgery by disinfection with 70% ethanol. An incision was made along the left side of the abdomen. The abdominal cavity was sprayed with 70% ethanol and allowed to air-dry. The spleen was excised and removed with forceps. After the spleen was cleaned of connective tissue in a Petri dish filled with RPMI medium, it was transferred to a new Petri dish filled with RPMI medium and pulled apart into individual cells with sterile forceps. The cells were suspended with a Pasteur pipette and transferred to a sterile Falcon tube. Noncellular debris was allowed to settle for ten minutes on ice. The cell suspension was then transferred to another Falcon tube. Following centrifugation at 200 x g for 5 minutes at room temperature, the supernatant was discarded. The cells were resuspended in 10 mL of fresh RPMI-1640 medium, and two aliquots of cells were removed for a cell count.

Myeloma cells were centrifuged at 200 x g and resuspended in fresh medium at a concentration of 10^7 cells/mL. The splenocytes and myeloma cells were mixed at a

ratio of 5 to 1. The cells were suspended in 40 mL of medium and then centrifuged at 200 x g. The supernatant was discarded. A solution of 1.4 g PEG in 2 mL of medium at 37°C was added dropwise. The cell pellet was gently resuspended without breaking apart small clumps of cells. RPMI-1640 medium was added dropwise at a rate of about 1 mL/min for five minutes. Another 10 mL was added over the next five minutes. A final 20 mL was added over another five minutes. The cells were centrifuged again and resuspended in 15 mL of RPMI-HAT-HS medium. Following a cell count, limiting dilution was performed by adding RPMI-HAT-HS medium to achieve a final cell concentration of $5x10^5$ cells/mL. The final cell suspension was aliquoted into sterile 96-well polystyrene plates (100 μL/well).

Cells were incubated at 37°C and 5% CO_2. As the medium began to change color, the supernatant was collected and screened for antibody production using noncompetitive ELISA. Positive clones were transferred to sterile 24-well plates and fed with RPMI-HAT-HS medium. Once cells reached high enough density, a portion of the cells was frozen while the other was used for subcloning. To freeze cells, 1 mL aliquots of cells in medium containing 5% DMSO were transferred to cryovials and frozen in a cryo freezing container at -20°C. After 4 hours, the cells were transferred to a liquid nitrogen cryo freezer for storage. For subcloning, the cells were diluted by a factor of ten, and 100 μL aliquots were pipetted onto sterile 96-well plates. Second and third rounds of limiting dilutions were performed to ensure that selected cell lines are monoclonal. Monoclonal cell lines were grown in successively larger cell culture

plates and flasks, respectively, to increase the number of cells. Once monoclonal cell lines were established, cells were frozen as described above.

Antibody Purification

Antibody Precipitation

For polyclonal antibodies, interstitial fluid samples were centrifuged at 200 x g for 30 minutes while blood samples collected in serum separator tubes were first allowed to clot and then centrifuged at 200 x g for 30 minutes. Antibodies from either interstitial fluid or serum were precipitated by dropwise addition of saturated ammonium sulfate at 4°C to a final concentration of 45%.

Monoclonal antibodies were purified from cell culture supernatant. For that, supernatant was first centrifuged to remove any remaining cells and then concentrated to a tenth of the original volume using a Centriplus centrifugal filter device with a 100,000 Da molecular weight cut-off. Antibody was then precipitated from concentrated supernatant using 50% aqueous ammonium sulfate.

The precipitated antibody was washed three times with 45% chilled ammonium sulfate for polyclonal antibodies and 50% chilled ammonium sulfate for monoclonal antibodies. The antibody was then dissolved in PBS and dialyzed extensively against the same buffer at 4°C. The purity of the antibody was confirmed

using sodium dodecyl sulfate-polyacrylamide gel electrophoresis (SDS-PAGE), which was performed following the manufacturer's instructions.

Purification of Antibodies Using Melon™ Gel

Antibody samples still containing traces of albumin after ammonium sulfate precipitation were purified using the Melon™ Gel IgG purification kit. Serum samples from rabbits D#73 and L#65 were diluted 1:10 in Melon™ Gel purification buffer following precipitation. Antibody samples from cell culture supernatant were first concentrated and precipitated as described above. After adjusting the total protein concentration to 15-20 mg/mL using PBS, samples were diluted 1:10 in Melon™ Gel purification buffer. Melon™ Gel spin columns were prepared by pipetting 200 µL of 50% Melon™ Gel slurry at room temperature into the column and washing twice with Melon™ Gel purification buffer. Five hundred µL of diluted antibody samples from serum or cell culture supernatant were then incubated with the Melon™ Gel slurry in spin columns for five minutes at room temperature. The filtrate containing the purified antibody was obtained by centrifugation at 5,000 x g for one minute. The Melon™ Gel slurry was then regenerated using the Melon™ Gel regeneration buffer. Larger samples were purified using gravity-flow columns as follows: the Melon™ Gel slurry was pipetted into a plastic column and washed with 10 column volumes of Melon™ Gel purification buffer. Four milliliters of 50% Melon™ Gel slurry was used to purify 40 mL of diluted antibody sample. The antibody sample was applied to

the column, and 1 mL fractions were collected until absorbance readings at 280 nm approached the baseline. The columns were regenerated by washing with 10 column volumes of Melon™ Gel regeneration buffer followed by 10 column volumes of Melon™ Gel purification buffer. The purity of the antibody was confirmed using SDS-PAGE, which was performed following the manufacturer's instructions.

Affinity Chromatography

Stationary Phase Preparation

Sepharose CL4B was first washed successively with 1:3 (v:v) acetone:water, 1:1 (v:v) acetone:water, 3:1 (v:v) acetone:water, and dry acetone. Two batches of 14 g of Sepharose CL4B were each activated with a solution of 1.65 g of DSC and 1.35 g of DMAP dissolved in 20 mL of DMF following the procedure of Wilchek and Miron.[122] The reaction was allowed to proceed overnight at 4°C while the Sepharose CL4B was kept suspended by end-over-end rotation. Both batches of activated stationary phase were successively washed with dry acetone, 5% acetic acid in 1,4-dioxane, methanol, and finally isopropyl alcohol. In order to determine the number of active groups, an aliquot of 4.0 mg activated Sepharose was hydrolyzed using 1 mL of 0.25 M ammonium hydroxide. The absorbance of a 1/10 dilution of the aqueous phase was then determined spectrophotometrically at 261 nm.[122]

In order to immobilize *p*-amino-D- or -L-PLA via its side chain, 200 mg of tyramine in 30 mL of PBS was added to each batch of activated Sepharose and allowed to react for 4 hours at 4°C. The stationary phase was then washed successively with PBS, 100 mM Tris buffer (pH 7), PBS, 1 M NaCl, and again with PBS. Twenty mg of *p*-amino-D- or -L-PLA was dissolved in 1 mL of 0.1 M HCl, and an equimolar amount of sodium nitrite was added. After ten minutes, the reaction mixture was slowly added to the suspension of stationary phase. The pH was adjusted to 8.5 with 0.1 M sodium hydroxide. The reaction was allowed to proceed overnight at 4°C.

The prepared stationary phase was washed extensively with each of the following: PBS, 1 M NaCl, 10 mM triethylamine (TEA), 100 mM TEA, 0.1 M sodium hydroxide, 100 mM citric acid, 1M hydrochloric acid, and 6 M guanidinium/HCl. Following each of the above washing solutions, the stationary phase was washed with water. The stationary phase was stored in water containing 0.01% sodium azide at 4°C when not in use.

Determination of Elution Conditions

In order to determine suitable elution conditions for particular antibodies, microtiter plates were coated and blocked as described in Chapter II in the section Enzyme-Linked Immunosorbent Assay. Antibody-containing samples were added to the plate (100 μL/well) at a dilution that had previously resulted in absorbance values

of at least 0.8 as determined by noncompetitive ELISA; the plate was incubated at 37°C for 2 hours. One of the following solvents was added to each row of the plate: PBS, water, 100 mM ammonium hydroxide, 10 mM ammonium hydroxide, 100 mM glycine/HCl (pH 2.5), 100 mM citric acid, 10% 1,4-dioxane, 4 M sodium chloride, 6 M guanidinium/HCl, 1 M acetic acid, 10 mM sodium hydroxide, 10 mM TEA, or 100 mM TEA. After incubation for ten minutes at room temperature, the plate was washed with PBS/Tween 20. Secondary antibody and color formation steps were carried out as described in Chapter II in the section Enzyme-Linked Immunosorbent Assay.

Affinity Purification of Antibodies

The affinity stationary phase material was washed with 100 mM TEA, water, and PBS, respectively. The precipitated and dialyzed antibody was then incubated with the affinity stationary phase for two hours at room temperature under continuous rotation. The suspension was gently poured into a glass column. The flow-through was collected in a 50 mL Falcon tube. The column was then washed thoroughly with PBS until no significant levels of protein were detected. This was followed by washing the column with PBS containing 1 M sodium chloride to remove any nonspecifically bound protein. After washing the column again with PBS, the antibody was eluted using 10 mM TEA (pH 12). Fractions of 1 mL collected during the elution step were immediately neutralized with 27 μL of 100 mM citric acid.

Fractions containing significant protein levels were combined and dialyzed extensively against PBS. The purified protein solutions were concentrated using Centriplus centrifugal filter devices with a 10 kDa molecular weight cut-off. After the purification, the stationary phase was washed extensively with 100 mM TEA and with water.

Enzyme-Linked Immunosorbent Assay

Ninety-six-well Maxisorp polystyrene microtiter plates were coated with 1 μg/mL solutions of antigen in 50 mM carbonate buffer, pH 9.6. A third of the plate was coated with 100 μL/well of either *p*-azo-D-PLA-BSA, *p*-azo-L-PLA-BSA, or underivatized BSA. The proteins were allowed to adsorb overnight at 4 °C. After this and each of the succeeding steps, plates were washed three times with PBS/Tween20. Unoccupied spaces on the plastic surface were blocked with a 1% gelatin solution in PBS/0.05% Tween 20 (250 μL/well) by incubation at 37°C for 2 hours. For noncompetitve ELISAs, serial dilutions of the antibody-containing samples were prepared in PBS. One hundred μL samples were applied per well and incubated for 2 hours at 37°C. After washing, horseradish peroxidase (HRP) labeled goat anti-rabbit $F(ab')_2$ secondary antibody, for polyclonal antibodies, or HRP labeled goat anti-mouse $F(ab')_2$ secondary antibody, for monoclonal antibodies, was applied at a 1/10,000 effective dilution in PBS. One hundred μL was applied per well and the plate was again incubated for 2 hours at 37°C. The substrate solution was prepared by adding

8 mg of OPD and 13 μL of 30% hydrogen peroxide to 20 mL of citrate/phosphate buffer. One hundred μL of the OPD solution was added per well; HRP converts OPD to 2,2-diamino-azo-benzene, a colored product. The reaction was stopped by acidification with 1 N sulfuric acid. Absorbance readings were taken at 492 nm in a plate reader.

For competitive ELISAs, the plates were coated and blocked as described above for noncompetitive ELISAs using either *p*-azo-D- or -L-PLA-BSA for anti-D-AHA antibodies and anti-L-AHA antibodies, respectively. Serial dilutions of competitor were applied in triplicate onto the plate (50 μL/well in PBS), followed by addition of antibody at a constant concentration in PBS (50 μL/well). The secondary antibody and color formation steps were carried out as described for noncompetitive ELISAs.

ELISAs using the anti-AA antibodies were performed following the same protocols except that *p*-azo-D-Phe-BSA, *p*-azo-L-Phe-BSA, and underivatized BSA were used as coatings.

Isotype Determination

Ninety-six-well MaxiSorp polystyrene microtiter plates were coated and blocked as described for noncompetitive ELISAs. One hundred μL/well of monoclonal antibody to be tested in PBS were applied to twelve wells at a dilution that had previously resulted in absorbance values of at least 0.8; plates were incubated for

2 hours at 37°C. After washing three times with PBS/Tween 20, each of the six isotype-specific reagents from the isotyping kit was applied in duplicate (100 μL/well; 1/500 in PBS). The plate was incubated for 30 minutes at room temperature and then washed three times with PBS/Tween 20. One hundred μL of peroxidase-labeled donkey anti-goat antibody were added to each well at a dilution of 1/5,000 in PBS and incubated for 30 minutes at room temperature. The color formation step was carried out using OPD as substrate following the procedure described for noncompetitive ELISAs.

Fluorescence Immunoassay

Development of a Fluorescence Immunoassay Using ELISA

Ninety-six-well Maxisorp polystyrene microtiter plates were coated with 100 μL/well of a mixture of *p*-azo-D-PLA-BSA and *p*-azo-D-Phe-BSA. Both of the antigens were in 50 mM carbonate buffer, pH 9.6; each antigen was at a concentration of 1 μg/mL. The proteins were allowed to adsorb overnight at 4 °C, and plates were washed and blocked as described for noncompetitive ELISAs. Serial dilutions of competitor were applied in triplicate onto the plate (50 μL/well in PBS alone or in PBS containing 10 mM D-Phe or 10 mM D-PLA), followed by addition of antibody at a constant concentration in PBS (50 μL/well). Antibodies used were anti-D-AHA polyclonal antibody from rabbit #73 (anti-D-AHA 73), the anti-D-amino acid antibody

secreted by the clone 67.36 (anti-D-AA 67.36), or a mixture of both antibodies as indicated in the section Fluorescence Immunoassay Development in Chapter III. The secondary antibody and color formation steps were carried out following the same procedure as described for noncompetitive ELISAs.

Development of a Fluorescence Immunoassay Using Fluorophore-Labeled Secondary Antibodies

Reacti-bind™ white opaque 96-well plates were coated and blocked as described for noncompetitive ELISAs. Serial dilutions of anti-D-AHA 73 (100 μL/well) were applied and incubated for 2 hours at 37°C. After washing the plate, goat anti-rabbit IgG Dylight™ 547-conjugated antibody was added onto the plate at a dilution of 1:250 in PBS (100 μL/well). The plate was incubated at room temperature for 30 minutes. The plate was again washed three times with PBS/Tween 20 and then rinsed with PBS. One hundred μL/well of PBS were applied onto the plate prior to measuring. The fluorophore was excited at 557 nm and fluorescence emission was measured at 570 nm utilizing the "fluorescence mode" of the plate reader.

The same procedure was used for anti-D-AA 67.36 except that plates were coated with the *p*-azo-Phe-BSA conjugates, and goat anti-mouse IgG Dylight™ 647-conjugated antibody was used as the secondary antibody. The fluorophore was excited at 652 nm; fluorescence emission was measured at 673 nm.

For competitive immunoassays, the plates were again coated and blocked as described for noncompetitive ELISAs using either *p*-azo-D-PLA-BSA or *p*-azo-D-Phe-BSA for detection of anti-D-AHA 73 and anti-D-AA 67.36, respectively. Serial dilutions of competitor were applied in triplicate onto the plate (50 μL/well), and antibody at a constant concentration in PBS was applied (50 μL/well). The washing and secondary antibody steps were carried out using the same procedure as described for noncompetitive fluorescence immunoassays.

Competitive fluorescence immunoassays were then repeated using both anti-D-AHA 73 and anti-D-AA 67.36 for the simultaneous detection of D-Phe and D-PLA. Plates were coated with a mixture of *p*-azo-D-PLA-BSA and *p*-azo-D-Phe-BSA with each antigen at a concentration of 1 μg/mL in carbonate buffer. The plates were washed and blocked as described for noncompetitive ELISAs. Mixtures of serial dilutions of D-Phe and D-PLA were both applied in triplicate onto the plate (25 μL/well for each competitior). A mixture of anti-D-AHA 73 and anti-D-AA 67.36 at a constant concentration was then applied to the plate (50 μL/well). After washing, a mixture of goat anti-mouse IgG Dylight™ 647-conjugated antibody and goat anti-rabbit IgG Dylight™ 547-conjugated antibody (1:250 in PBS; 100 μL/well) was then applied onto the plate. The plate was again washed three times with PBS/Tween 20 and then rinsed with PBS. One hundred μL/well of PBS were applied to the plate prior to measuring. The plate was first measured by exciting the Dylight™ 647 fluorophore at 652 nm and measuring fluorescence emission at 673 nm in order to detect the interaction between anti-D-AHA 73 and D-PLA. The plate was then

remeasured by exciting the Dylight™ 547 fluorophore at 557 nm and measuring fluorescence emission at 570 nm in order to detect the interaction between anti-D-AA 67.36 and D-Phe.

Conjugation of Fluorophores to Antibodies

Four antibodies were selected for conjugation to four different fluorophores: the anti-D-AHA antibody secreted by the clone 8E10.9 (anti-D-AHA 8E10.9), anti-D-AA polyclonal antibody, the anti-L-AHA polyclonal antibody from rabbit #65 (anti-L-AHA 65), and the anti-L-amino acid antibody secreted by the clone 18.3 (anti-L-AA 18.3), respectively. The compounds used for labeling the aforementioned antibodies were DyLight™ 547 NHS ester, DyLight™ 647 NHS ester, DyLight™ 800 NHS ester, and DyLight™ 490 NHS ester, respectively. Antibodies were first dialyzed against 50 mM sodium borate buffer, pH 8.5. Labeling was then carried out as follows: a 15-fold excess of DyLight™ 547 (24.3 μL of a 10 mg/mL solution in DMF) was added to 1.5 mL of anti-D-AHA 8E10.9 (at 2.25 mg/mL). A 7.5-fold excess of DyLight™ 647 (12.6 μL of a 10 mg/mL solution in DMF) was added to 1.5 mL of the anti-D-AA polyclonal antibody (at 2.25 mg/mL). A 6-fold excess of DyLight™ 800 (15.0 μL of 10 mg/mL solution in DMSO) was added to 1 mL anti-L-AHA 65 (at 1.4 mg/mL). A 5-fold excess of DyLight™ 490 (21 μL of a 10 mg/mL solution in DMSO) was added to 1.5 mL of anti-L-AA 18.3 (at 2.1 mg/mL). The solutions were briefly vortexed and the reactions were allowed to proceed at 4°C for 2

hours under continuous rotation. The reactions were carried out in the dark with all microcentrifuge tubes wrapped in aluminum foil to protect the fluorophores from light. After completion of the reactions, the solutions were dialyzed extensively against PBS in 2 L Erlenmeyer flasks wrapped in foil in order to remove unreacted dyes.

Antibody concentrations were determined spectrophotometrically by measuring the absorbance at 280 nm. The dye-to-protein ratio was calculated based on the absorbance of the protein conjugates at the following wavelengths: 494 nm for the DyLight™ 490-labeled anti-L-AA 18.3, 547 nm for the DyLight™ 547-labeled anti-D-AHA 8E10.9, 647 nm for the DyLight™ 647-labeled anti-D-AA polyclonal antibody, and 774 nm for the DyLight™ 800-labeled anti-L-AHA 65. The extinction coefficients of the respective dyes were taken from the manufacturer's product information.

Noncompetitive Fluorescence Immunoassay

Reacti-bind™ white opaque 96-well plates were coated and blocked as described for noncompetitive ELISAs. Serial dilutions of the DyLight™ 490-labeled anti-L-AA 18.3, the DyLight™ 547-labeled anti-D-AHA 8E10.9, the DyLight™ 647-labeled anti-D-AA polyclonal antibody, or the DyLight™ 800-labeled anti-L-AHA 65 were applied onto the plate (100 μL/well) and incubated for 1 hour at room temperature. The plate was washed three times with PBS/Tween 20 and then rinsed

with PBS. One hundred μL/well of PBS were applied to the plate prior to measuring. Excitation and emission wavelengths were as follows: DyLight™ 490: 491/518 nm, DyLight™ 547: 557/570 nm, DyLight™ 647: 652/673 nm, and DyLight™ 800: 770/794 nm.

Competitive Fluorescence Immunoassay

The plates were coated and blocked as described for noncompetitive ELISAs using *p*-azo-D-PLA-BSA for DyLight™ 547-labeled anti-D-AHA 8E10.9, *p*-azo-D-Phe-BSA for DyLight™ 647-labeled anti-D-AA polyclonal antibody, *p*-azo-L-PLA-BSA for DyLight™ 800-labeled anti-L-AHA 65, and *p*-azo-L-Phe-BSA for DyLight™ 490-labeled anti-L-AA 18.3. Serial dilutions of competitors were applied in triplicate to each plate (50 μL/well), and the respective labeled antibody was applied at a constant concentration (in PBS, 50 μL/well). The plates were washed three times with PBS/Tween 20 and then rinsed with PBS. One hundred μL/well of PBS were applied to the plate prior to measuring.

For the simultaneous detection of AA and AHA enantiomers, a mixture of *p*-azo-D-PLA-BSA, *p*-azo-D-Phe-BSA, *p*-azo-L-PLA-BSA, and *p*-azo-L-Phe-BSA was used to coat Reacti-bind™ white opaque 96-well microtiter plates (100 μL/well). All four of the antigens were in 50 mM carbonate buffer pH 9.6; each antigen was at a concentration of 1 μg/mL. The proteins were allowed to adsorb overnight at 4 °C, and plates were washed and blocked as described for noncompetitive ELISAs. Mixtures

of serial dilutions of D- and L-Phe and D-and L-PLA were applied in triplicate onto the plate (12.5 μL/well in PBS for each competitor) and antibody solution containing all four fluorophore-conjugated antibodies in PBS was applied at a constant concentration (50 μL/well). The plates were washed three times with PBS/Tween 20 and then rinsed with PBS. One hundred μL/well of PBS were applied to the plate prior to measuring. Plates were measured as described for the noncompetitive fluorescence immunoassay.

Chiral Immunoaffinity Chromatography

PEEK tubing (200 mm x 0.75 mm i.d.) was packed with 100-3 Nucleosil silica using an Alltech slurry packer fitted with a 20 mL reservoir. Ethanol (95%) was used as both the slurry and packing solvent. The pressure was gradually increased to 200 bars; packing continued until a constant flow rate was achieved. The column was then flushed successively with 95% ethanol, acetone, and dry acetone using a syringe pump. The silica was activated *in situ* with DSC according to the method of Wilchek and Miron.[122] DSC (84.5 mg) and DMAP (62.4 mg) in DMF (960 μL) were pumped onto the column at 1 μL/min. The column was flushed with dry acetone, 5% acetic acid in 1,4-dioxane, methanol, isopropyl alcohol, and briefly with water before the addition of antibody. Anti-D-AHA 73 (1.4 mL at 4 mg/mL in PBS) was applied to the column. Initially antibody was applied at 5 μL/min for 30 minutes and the remaining antibody was applied at 1 μL/min. The column was then flushed with PBS and 1M

NaCl to remove unbound antibody. The amount of immobilized antibody was estimated to be 80% of the total antibody applied by calculating the difference between the amount of antibody applied and the amount of antibody collected after immobilization as determined from UV-absorbance measurements at 280 nm.

Separations were carried out at room temperature using PBS as mobile phase. Five microliters of nonracemic mixtures of PLA were injected. The 100 μL/min flow rate was split before the injector using a back-pressure regulator. Other conditions are given in the section Chiral Immunoaffinity Chromatography in Chapter III.

CHAPTER III

RESULTS AND DISCUSSION

Synthesis and Characterization of Immunogens

Antibodies, an element of the humoral immune system of vertebrates, are a group of glycoproteins present in the serum and tissue fluids of all mammals and are secreted by B-lymphocytes. Although the primary purpose of antibody production is to protect an organism against pathogens, antibody production can be initiated against virtually any molecule as long as it contains a distinct antigenic site, called epitope, and/or can be coupled to a carrier molecule. Antibodies with desired binding properties can be produced against a wide range of compounds, which is essential for their application in bioanalytical techniques such as immunoassays.

Selection or synthesis of an appropriate immunogen is the first step in the production of antibodies. Molecules larger than 5 kDa are usually good immunogens as long as they are recognized as being foreign to the host animal. Thus, proteins and polypeptides with larger molecular weights are generally immunogenic and can be injected without any further modification. However, small molecules, i.e., those with less than 1 kDa, typically cannot elicit an immune response by themselves. In the early 1900s, Landsteiner realized that such molecules, called haptens, could be

rendered immunogenic if they are covalently linked to a carrier molecule such as a protein. Landsteiner, in his original experiments, prepared synthetic antigens by coupling diazonium compounds to serum proteins via tyrosine and histidine residues on the protein. Rabbits inoculated with the (artificially) prepared azo-proteins produced antibodies that recognized the attached hapten as detected by immunoprecipitation.[51]

The overall principles for the production of anti-hapten antibodies have remained essentially unchanged since Landsteiner's work,[35] although, since then, various other reactions for the conjugation of haptens to proteins have been established.[123,124] As any conjugation strategy must preserve the "immunogenicity" of the hapten, the point of attachment between hapten and carrier is critical. The specificity of anti-hapten antibodies, as Landsteiner demonstrated, is directed primarily toward the part of the hapten farthest away from the point of linkage to the carrier protein.[51] This principle of hapten accessibility was further elucidated by Michael Sela et al., who showed that, e.g., oligopeptides must be readily accessible on the surface and not in the interior of hapten-carrier conjugates.[125,126]

Similar observations were made with antibodies against protein antigens. For example, in myoglobin the antigenic regions are located at the areas of the molecule which are exposed on the outer surface.[127,128] Another example is lysozyme, in which the loop region, which is an immunodominant determinant in the molecule,[129-131] is exposed on the surface of the protein.[132] Thus, the fact that antibodies recognize epitopes on the surface must be considered in the design and synthesis of

immunogens. If antibodies are needed to discriminate between closely related compounds, functional groups on the hapten essential for distinguishing the molecule from other analogs and precursors should not be used for conjugation to carrier proteins.[133] Conversely, if cross-reactive antibodies are desired, the shared functional groups on the hapten should be exposed on the surface of the immunogen.[133]

Similarly, a chiral hapten should be conjugated to a carrier at a site away from the asymmetric center to optimize the stereospecificity of the antibodies produced.[134] In this way, the asymmetric center is exposed on the surface of the immunogen. Additionally, for chiral haptens, four possible combinations exist: either the racemate or the individual stereoisomers may be used for both the immunogen and for the screening assay, or alternatively, the racemate may be used for either the immunogen or the screening assay and the individual stereoisomers may be used for the other.[134] Regardless of whether racemic or enantiomerically pure haptens are used for the immunogen, a heterogeneous population of antibodies will be produced, which may include a range of selective and cross-reactive antibodies against the hapten in addition to antibodies which recognize the carrier. Racemic haptens are typically preferred for the production of antibodies that must recognize both enantiomers (e.g., for immunoassays of racemic drugs).[134] Alternatively, analogues which lack a chiral center may be used as haptens to produce antibodies for racemic assays.[134] Racemic haptens may also result in stereoselective antibodies; however, enantiomerically pure haptens improve the probability of producing stereoselective antibodies.[134,135] Landsteiner, who first produced stereoselective antibodies, conjugated, e.g., D-

tartanilic acid, a derivative of D-tartaric acid, to a protein to produce antibodies which could discriminate between D- and L- tartaric acid.[51]

Since a primary objective of this dissertation was to produce antibodies which stereoselectively bind to AHAs, the AHA hapten was conjugated to the carrier in such a way that the hydroxyl/carboxyl/hydrogen triad about the α-carbon is oriented on the outside of the immunogen. Thus, the shared functional groups of AHAs are exposed on the surface of the immunogen, which, ideally, results in antibodies that cross-react with a wide range of AHAs. Since these same functional groups are also unique to AHAs, the resulting antibodies should be specific to this group of compounds. Additionally, the probability of producing *stereoselective* antibodies is increased by exposing the chiral center of the hapten on the surface of the immunogen and by using enantiomerically pure haptens.

While a wide range of coupling chemistries may be used for conjugation of haptens to carrier proteins, the conjugation should be simple, reproducible, and result in an optimal presentation of the hapten on the surface of the immunogen.[124] Diazotization, a process by which an aromatic primary amine is converted to a diazonium compound, was used for preparation of the immunogens. In diazotization, sodium nitrite is added to a solution of the amine in aqueous acid solution at 0-5°C.[136] Reaction of the amine with nitrous acid gives a nitrosamine; tautomerization and loss of water lead to the diazonium cation, which is stabilized by delocalization of the positive charge at the ortho- and para-carbon atoms of the ring.[136] The great importance of diazonium compounds in immunogen preparation lies in their ability to

couple to tyrosine or histidine residues on proteins.[136] The diazotization reaction proceeds by electrophilic attack of the diazonium group at the electron-rich points on the target molecules to yield an arylazo group at the position para or ortho to hydroxyl or amino groups.[136] Diazotization results in an oriented presentation of haptens with excellent yields. Diazotization is also a relatively simple chemistry to use—particularly as no protecting groups are needed. The resulting azoproteins are deeply colored, which can provide visual confirmation of the completion of the reaction. This approach was previously used by Hofstetter et al. to produce stereoselective antibodies to α-amino acids.[35,59] Enantiomerically pure *p*-amino-D- or -L-Phe were coupled to KLH via diazotization, and the resulting conjugates were used as immunogens for the production of both polyclonal and monoclonal antibodies.[59,60] In this research, immunogens were produced by coupling the analogous *p*-amino-PLA to KLH. *p*-Amino-D- and -L-PLA were not commercially available and, therefore, were synthesized from D- and L-PLA, respectively, as described in Chapter II, section Synthesis of Immunogens.

In addition to being used for the production of the immunogens, *p*-amino-D- and -L-PLA, and their precursors, *p*-nitro-D- and -L-PLA were also used as competitors in competitive ELISAs as described in Chapter II, section Enzyme-Linked Immunosorbent Assay.

Synthesis and Characterization of Phenyllactic Acid Derivatives

p-Nitro-Phenyllactic Acid

The nitration of both D- and L-PLA, which was performed as described in Chapter II, section Synthesis of Immunogens, is a typical electrophilic aromatic substitution reaction. The nitronium ion is created by protonation of the hydroxyl group of nitric acid by sulfuric acid followed by the loss of water. The nitronium ion, an excellent electrophile, then reacts with phenyllactic acid forming an intermediate sigma complex, which results in loss of a proton, yielding *p*-nitro-D- and -L-PLA, respectively. Because alkyl groups are ring-activating substituents (ortho- and para-directing), nitration of PLA at the ortho and para positions are favored. The para-substituted product, however, is the major product because the ortho-substituted product is sterically hindered. The synthesis of *p*-nitro-PLA was confirmed by ^{1}H NMR, IR, and mass spectrometry.

^{1}H NMR spectra of *p*-nitro-D- and -L-PLA were recorded on a 200 MHz instrument using DMSO-d6 as solvent. The results in ppm for *p*-nitro-D-PLA are as follows: 8.16 (2H, d, J=7.9 Hz, 6-H and 8-H), 7.56 (2H, d, J=7.6 Hz, 5-H and 9-H), 4.25 (1H, dd, J=8.3 Hz, 4.3 Hz, 2-H), 3.10 (1H, d, J=4.2 Hz, 3a-H), 2.98, (1H, d, J=8.4 Hz, 3b-H), 2.52 (1H, s, 2-OH). The *p*-nitro-L-PLA results are as follows: 8.16 (2H, d, J=7.8 Hz, 6-H and 8-H), 7.54 (2H, d, J=8.3 Hz, 5-H and 9-H), 4.25 (1H, dd, J=8.4 Hz, 4.3 Hz, 2-H), 3.10 (1H, d, J=4.2 Hz, 3a-H), 2.98, (1H, d, J=8.3 Hz, 3b-H), 2.56 (1H, s,

2-OH). Two doublets in the aromatic region (8.16 and 7.5 ppm), which are characteristic of para-substituted benzene, were observed in the spectra of both enantiomers.

The presence of the nitro group was also confirmed by IR. The -N-O symmetric stretch was found at 1348 cm^{-1} and the -N-O asymmetric stretch was found at 1524 cm^{-1} for *p*-nitro-D-PLA. The -O-H stretch was found at 3113 cm^{-1}. For *p*-nitro-L-PLA, the -N-O symmetric stretch was found at 1344 cm^{-1}, the -N-O asymmetric stretch was found at 1516 cm^{-1}, and the -O-H stretch was found at 3119 cm^{-1}.

The purified *p*-nitro-D- and -L-PLA are both dark yellow. The melting point, optical rotation and mass (as determined by ESI-MS) are given in Table 1. The calculated mass of *p*-nitro-PLA is 211.05.

Table 1: Physical properties of synthesized *p*-nitro-phenyllactic acid

	melting point (°C)	Observed m/z	$[\alpha]_D^{25}$
p-nitro-D-PLA	135-138	210.9	+24.3°
p-nitro-L-PLA	133-137	210.9	-23.7°

p-Amino-Phenyllactic Acid

The catalytic hydrogenation of *p*-nitro-D- and -L-PLA to *p*-amino-D- and -L-PLA was carried out as described in Chapter II, section Synthesis of Immunogens. The hydrogenation reaction proceeds readily at room temperature and low pressures of hydrogen in the presence of a palladium-charcoal catalyst. The synthesis of *p*-amino-D- and -L-PLA was confirmed by ^{1}H NMR, IR, mass spectrometry, and reaction with ninhydrine.

^{1}H NMR spectra of *p*-amino-D- and -L-PLA were recorded in a 200 MHz instrument using DMSO-d6 as solvent. The *p*-amino-D-PLA results in ppm are as follows: 7.01 (2H, d, J=8.4 Hz, 6-H and 8-H), 6.71 (2H, d, J=8.4 Hz, 5-H and 9-H), 4.05 (1H, dd, J=7.8 Hz, 4.9 Hz, 2-H), 2.78 (1H, d, J=7.5 Hz, 3a-H), 2.64 (1H, d, J=7.4 Hz, 3b-H), 2.52 (1H, s, 2-OH). The results for *p*-amino-L-PLA in ppm are as follows: 7.01 (2H, d, J=8.4, 6-H and 8-H), 6.71 (2H, d, J=8.4, 5-H and 9-H), 4.05 (1H, dd, J=7.8, 4.9, 2-H), 2.78 (1H, d, J=7.5, 3a-H), 2.64, (1H, d, J=7.4, 3b-H), 2.52 (1H, s, 2-OH). The characteristic two doublets of *p*-substituted benzene are shifted downfield from those of the *p*-nitro-D- and -L-PLA in both spectra.

IR results confirmed the presence of the amino group for both the *p*-amino-D- and -L-PLA. The -C-N stretch was found at 1740.99 cm^{-1}; the -O-H stretch was found at 3144.29 cm^{-1} for the *p*-amino-D-PLA. For the *p*-amino-L-PLA, the -C-N stretch was found at 1741.45 cm^{-1} and the -O-H stretch was found to be 3221.82 cm^{-1}.

The presence of the amino group was also confirmed qualitatively by reaction with ninhydrine. The purified *p*-amino-D- and -L-PLA are both light yellow.

The melting point, optical rotation and mass (as determined by ESI-MS) are given in Table 2. The calculated mass of *p*-amino-PLA is 181.07.

Table 2: Physical properties of synthesized *p*-amino-phenyllactic acid

	Melting point (°C)	Observed m/z	$[\alpha]_D^{25}$
p-amino-D-PLA	180-184	182	+42.3°
p-amino-L-PLA	181-185	182	-40.9°

Synthesis and Characterization of Hapten-Protein Conjugates

The synthesized *p*-amino-D- or -L-PLA was separately coupled to the proteins KLH and BSA via diazotization. For that, the *p*-amino-D- or -L-PLA was reacted with nitric oxide to form the diazonium salt of PLA. Nitric oxide is obtained by reaction of sodium nitrite with hydrochloric acid to form nitrous acid, which degrades to nitric oxide. The diazonium salt of PLA, a good electrophile, reacts primarily with tyrosine residues on the KLH or BSA under basic conditions to form *p*-azo-PLA-BSA or -KLH conjugates. *p*-Azo-D- and -L-PLA-tyramine conjugates were synthesized following

the same procedure. The KLH conjugates were used for the immunization of both rabbits and mice, whereas the BSA conjugates were used in immunoassays as solid-phase coatings.

In order to determine the hapten density, i.e., the hapten-to-protein ratio, the appropriate extinction coefficient was determined from *p*-azo-D- and -L-PLA-tyramine conjugates. The *p*-azo-D- and -L-PLA-tyramines were dark red in color with an extinction coefficient of ε=10,000 $cm^{-1}M^{-1}$ at 370 nm. Using this value, the hapten-to-protein ratios presented in Table 3 were determined as described in Chapter II, section Synthesis of Immunogens.

Table 3: Hapten densities

hapten-protein conjugate	number of haptens
p-azo-L-PLA-KLH*	4
p-azo-L-PLA-BSA	2
p-azo-D-PLA-KLH*	3
p-azo-D-PLA-BSA	6

*expressed per subunit of KLH (approximate MW = 51,000)

It is known from the pioneering work of Landsteiner that the hapten density affects an animal's immune response. Generally, with too few haptens, only antibodies recognizing the carrier used for immunization are produced, whereas with too many haptens, the overall immune response may decrease.[137] Other researchers have found that higher hapten densities may produce a fast, primarily IgM-based immune response, and those antibodies often have a weaker affinity. Conversely, a lower hapten density can result in antibodies with higher affinity, although the immune response may be slower.[138,139]

Production and Characterization of Polyclonal Antibodies

Immune Response

The *p*-azo-D- and -L-PLA-KLH immunogens were used to inoculate rabbits #73 and #65, respectively, as described in Chapter II, section Antibody Production. Stereoselective antibodies were detected in noncompetitive ELISAs using the BSA conjugates of the *p*-amino-D- or -L-PLA as solid-phase coatings. It was found that antibodies from rabbit #73 (anti-D-AHA 73) bound to the *p*-azo-D-PLA-BSA coating while antibodies from rabbit #65 (anti-L-AHA 65) bound to the *p*-azo-L-PLA-BSA coating. No detectable binding to the opposite enantiomer or to BSA was observed in noncompetitive ELISAs using antibodies from either rabbit. Figure 5 shows time-dependent immune response plots for interstitial fluid samples determined at 1/10,000

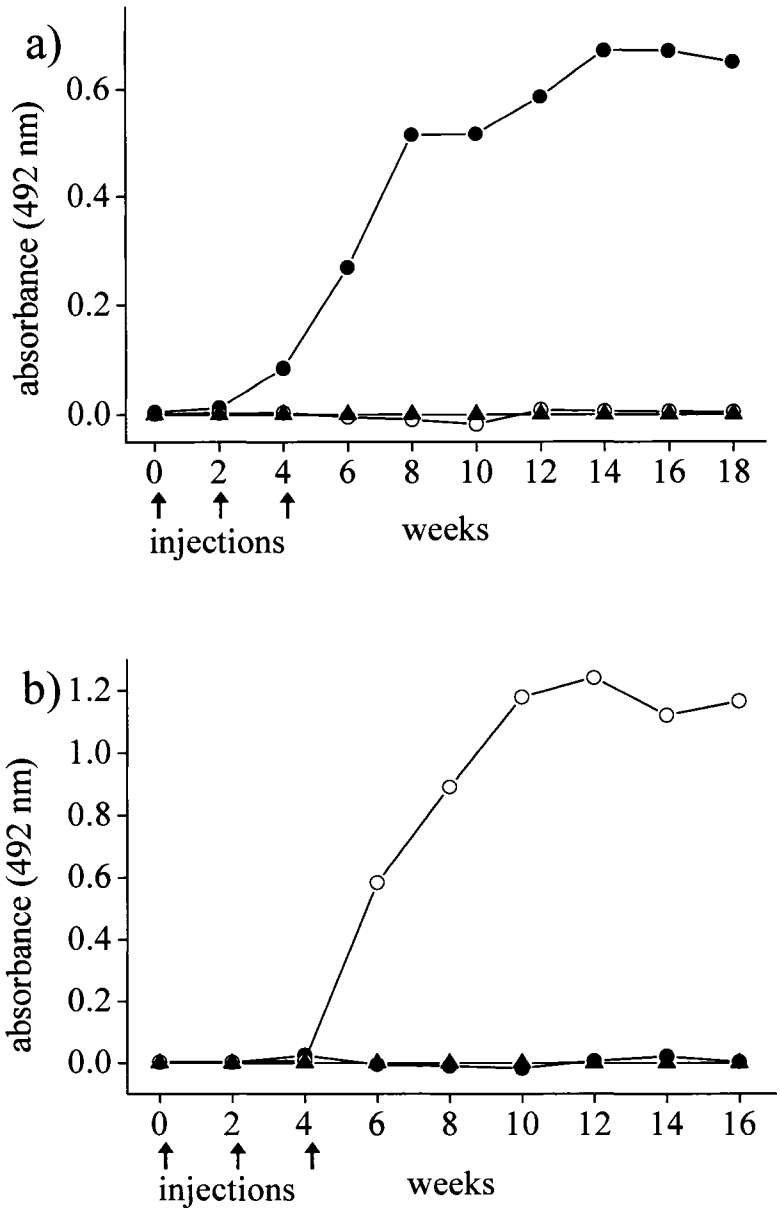

Figure 5: Immune responses of rabbits a) #73 and b) #65 following three injections with *p*-azo-D- and -L-PLA-KLH, respectively, in complete Freund's adjuvant, incomplete Freund's adjuvant, and PBS, respectively, at biweekly intervals (arrows). Antibody-containing interstitial fluid was tested in noncompetitive ELISA at 1/10,000 dilution on three different coatings, namely, *p*-azo-D-PLA-BSA (●), *p*-azo-L-PLA-BSA (○), and BSA (▲).

dilution for rabbits #73 and #65, respectively. Samples of interstitial fluid were obtained on a biweekly basis beginning with a pre-immunization sample of interstitial fluid obtained from each rabbit just prior to inoculation with the immunogen in CFA. At weeks 2 and 4, booster injections of immunogen in IFA and in PBS, respectively, were given. As expected, pre-immunization samples (week 0) showed no detectable immune response in noncompetitive ELISAs. However, by week 6, both rabbits #73 and #65 showed significant, stereoselective immune responses, which peaked by week 14 and 12, respectively.

The titer of each polyclonal antibody was determined by noncompetitive ELISAs for samples collected on a biweekly basis for 40 weeks. Sample binding curves of combined samples of interstitial fluid collected at weeks 6-18 were determined using noncompetitive ELISAs for both antibodies and are presented in Figure 6. The titers for these combined samples were found to be 1/100,000 for both anti-D-AHA 73 and anti-L-AHA 65.

Purification of Polyclonal Antibodies

Precipitation is commonly used as an initial step in the purification of proteins from crude mixtures. If a precipitating agent, such as saturated ammonium sulfate, is added to a crude mixture, the ammonium and sulfate ions compete with the protein for

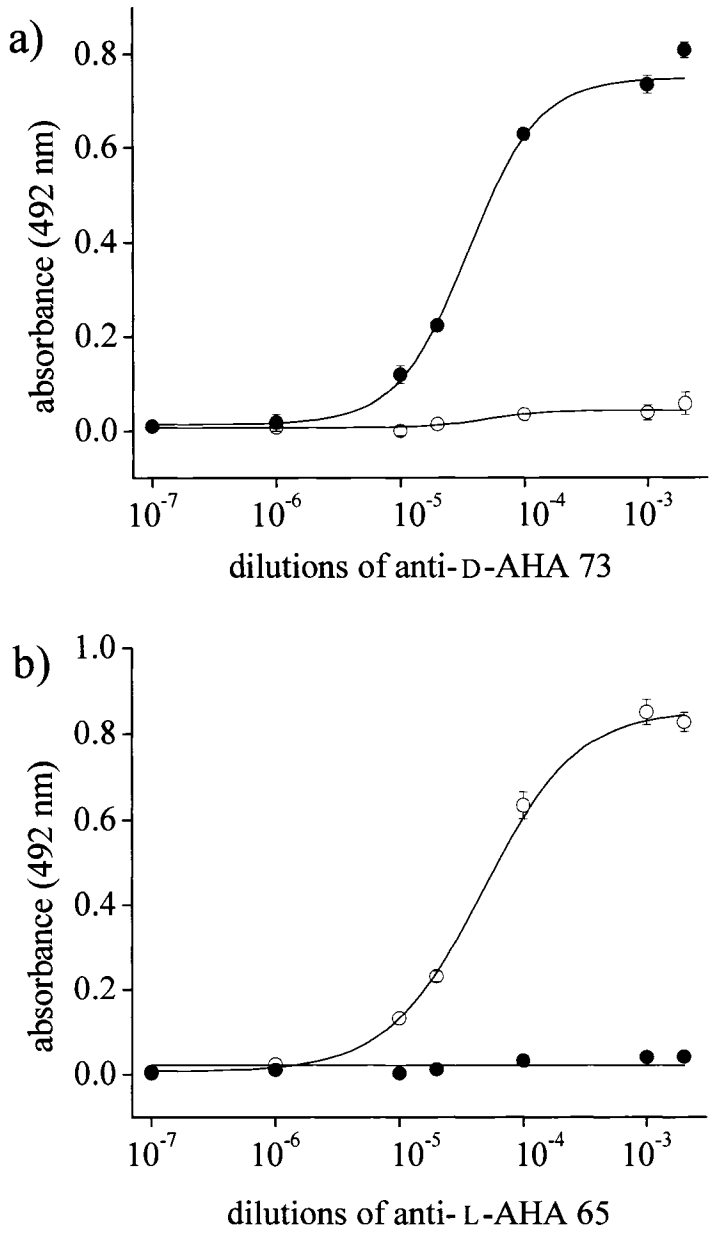

Figure 6: Noncompetitive ELISA results for a) anti-D-AHA 73 and b) anti-L-AHA 65 using interstitial fluid samples collected at weeks 6-18. *p*-Azo-D-PLA-BSA (●), *p*-azo-L-PLA-BSA (O), and BSA were used as solid-phase coatings. At each dilution, the values obtained with the BSA coating were subtracted from those obtained on the other two coatings. Data points represent means of triplicate determinations. Error bars are obscured by symbols.

water molecules, which decreases the solubility of the protein and results in precipitation.[140] Polyclonal antibodies precipitate when the concentration of ammonium sulfate reaches approximately 45%, whereas most other proteins found in serum or interstitial fluid remain in solution. Optimal separation is achieved by slow, dropwise addition of a saturated solution of ammonium sulfate. Typically, other proteins coprecipitate with antibodies; however, here the precipitate from interstitial fluid contained only antibodies as determined by SDS-PAGE. The procedure for antibody precipitation is found in Chapter II, section Antibody Purification. Figure 7 shows a nonreducing SDS-PAGE gel of anti-D-AHA 73 from interstitial fluid before and after ammonium sulfate precipitation; the nonreducing SDS-PAGE gel of the anti-L-AHA 65 was comparable.

Because antibody samples obtained from sera still contained impurities, they were further purified using the Melon™ Gel purification kit (Figure 8). More commonly, antibodies have been purified by ion-exchange, size-exclusion, or affinity chromatography. In size-exclusion chromatography, porous beads are used to separate molecules on the basis of size. In ion-exchange chromatography, molecules are separated on the basis of charge using either a cationic or anionic exchange resin. Ion-exchange and size-exclusion chromatography are used to purify a wide range of proteins, and separation conditions must be determined experimentally for optimal purifications. Because size-exclusion and ion-exchange resins do not specifically bind antibodies, antibodies may co-elute with other proteins.

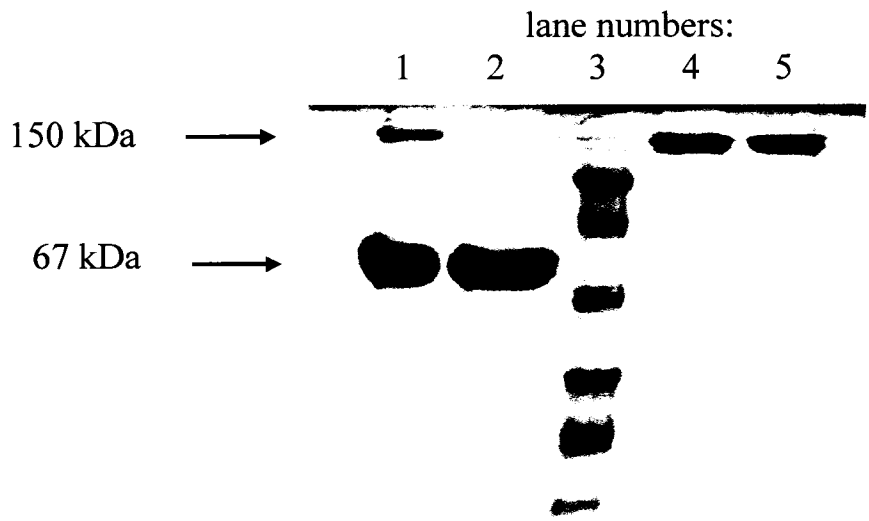

Figure 7: Nonreducing sodium dodecyl sulfate-polyacrylamide gel electrophoresis of interstitial fluid was used to determine the purity of samples before and after precipitation. Unpurified interstitial fluid (lane 1) was precipitated with 45% saturated ammonium sulfate. The precipitate only contained antibodies (lane 4). All contaminant proteins remained in the supernatant (lane 2), which contained no residual antibody. Lane 3 contains the MW marker and lane 5 is a positive control.

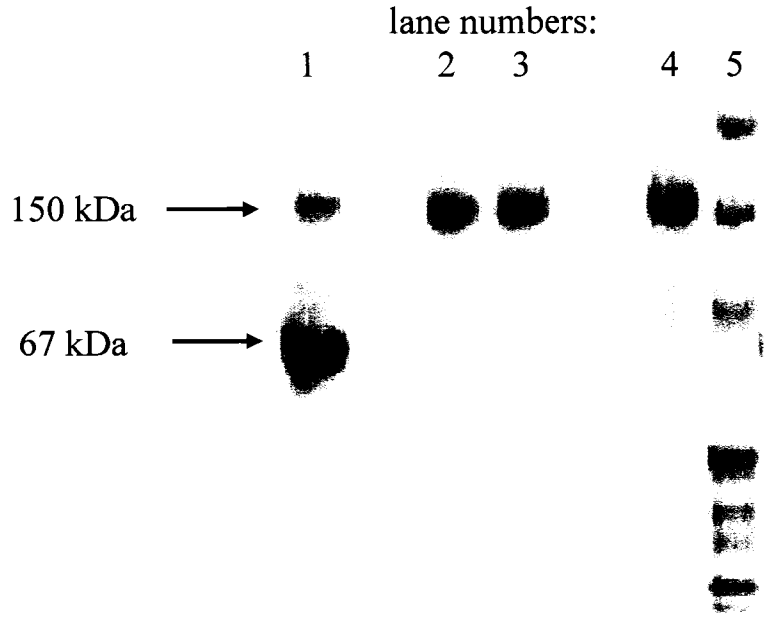

Figure 8: Nonreducing sodium dodecyl sulfate-polyacrylamide gel electrophoresis of serum was used to determine the purity of samples before and after precipitation and Melon™ Gel purification. Unpurified serum was precipitated with 45% saturated ammonium sulfate. The precipitate contained impurities (lane 1). The impurities were removed by further purification using Melon™ Gel (lane 2) followed by affinity purification (lane 3). Lane 4 is a positive control and lane 5 is the marker.

In contrast, proteins A, G, L, and, more recently, recombinant protein A/G are specifically used to purify immunoglobulins in affinity chromatography. Protein L, from the bacterium *Peptostreptococcus magnus*, binds to the light chains of most immunoglobulins.[141] Protein A, from *Staphylococcus aureus*, binds to the Fc region of immunoglobulins, primarily IgGs.[142] While native protein G is isolated from group G *Streptococci*, recombinant protein G is typically used for the purification of immunoglobulins. Protein G binds to the immunoglobulin Fc regions from a wider range of species than protein A and, in the recombinant version, has had the cell surface and albumin binding sites removed.[143,144] Protein A/G is a recombinant protein containing the Fc binding domains from both proteins A and G and, therefore, binds an even wider range of immunoglobulins, including all human and mouse IgG subclasses.[144] Harsh conditions are often required to elute the antibodies from protein A, G, L or A/G columns, which may denature the antibody. This procedure may also add a time-consuming dialysis or desalting step.

The Melon™ Gel, however, is designed to bind common serum proteins such as albumin and transferrin, but not antibodies. Antibodies can therefore be rapidly purified, e.g., in spin columns, without harsh denaturing conditions using a mild buffer at physiological pH. The purification buffer is also suitable for storage and downstream applications.

While ammonium sulfate precipitation and Melon™ Gel purification remove unwanted proteins from the antibody, the samples may still contain an array of antibodies against many different antigens. Affinity purification can be used to isolate

only those antibodies which bind to the desired antigen. In 1968, Pedro Cuatrecases, Chris Anfinsen, and Meir Wilchek first introduced affinity chromatography, which utilizes the immense power of biorecognition as a means of purification.[145] They successfully purified three enzymes, namely staphylococcal nuclease, α-chymotrypsin, and carboxypeptidase A, by immobilizing their respective inhibitors to activated Sepharose. Each of the proteins was eluted using acetic acid at pH 3.

Since that time, affinity purification has become a powerful tool in biomedical research and biotechnology as a separation system that exploits interactions between a protein and a specific ligand (e.g., enzyme-inhibitor, antibody-antigen, receptor-hormone, etc.) to isolate either the protein or its ligand. First, one of the two binding partners is immobilized. Second, the affinity matrix is equilibrated in a mild buffer such as PBS and the complementary binding partner is allowed to bind. Unbound and nonspecifically adsorbed material is then washed from the column with buffer. Alternatively, higher ionic strength buffer may be used for a more stringent washing. Finally, the bound analyte is eluted specifically using a competitive ligand, or nonspecifically by changing pH, ionic strength, or polarity. Commonly used elution buffers include acids, bases, organic solvents, and chaotropic salts. While specific elution with competitive ligands may avoid protein denaturation, it may be impractical or prohibitively expensive. Nonspecific elution conditions, however, may be ineffective or may denature proteins. To minimize denaturation, purified proteins should be neutralized immediately after elution and then dialyzed against a mild

buffer. Matricies containing proteins should also be washed with a mild buffer immediately after the purification.

For the purification of the polyclonal antibodies against D- or- L-AHAs, the hapten, i.e., *p*-amino-D- or -L-PLA, was immobilized on cross-linked Sepharose using the same chemistry (that is, diazotization) used for preparation of the immunogen. First, tyramine was immobilized on activated cross-linked Sepharose. The diazonium salt of *p*-amino-D- or -L-PLA was then reacted with the tyramine moiety to form a *p*-azo-D- or -L-PLA-tyramine conjugate. Since anti-hapten antibodies cannot be raised against free low-molecular weight haptens, even antibodies which are specific to the hapten may recognize a portion of the carrier or a linker that may have been used. Thus, if the hapten is immobilized on an affinity stationary phase using a different chemistry than that used for the immunogen production, the amount of specific antibody purified will most likely decrease. However, if the immunogen itself is used for affinity purification, nonspecific antibodies recognizing the carrier may also bind to the affinity stationary phase. Thus, the hapten should be immobilized on the stationary phase in a way that maximizes the amount of specific anti-hapten antibody and minimizes the amount of nonspecific antibody. Additionally, proteins should be avoided in stationary phase preparation because they are susceptible to denaturation and bacterial degradation. The *p*-azo-D- or -L-PLA-tyramine Sepharose stationary phase used here can specifically purify antibodies that recognize the hapten from those that may recognize the KLH carrier or other antigens. The stationary phase is also extremely durable because it contains no proteins. One batch of stationary phase was

prepared for purification of anti-D-AHA antibodies while another batch was made to purify anti-L-AHA antibodies as described in Chapter II, section Antibody Purification.

Determination of optimal elution conditions is essential for a successful affinity purification procedure. A binding buffer provides an environment favorable for the formation of the antibody-antigen complex, which is stabilized by noncovalent forces such as hydrophobic interactions, hydrogen bonds, van der Waals and Coulombic interactions, π-π interactions, etc. An elution buffer, in contrast, must sufficiently change the properties of the mobile phase to disrupt the antibody-antigen complex.[146,147] In order to find the optimal elution buffer that can liberate the bound antibody in a minimum volume, ten different elution conditions were tested in noncompetitive ELISAs as described for the anti-D-AHA 73 and the anti-L-AHA 65 antibodies in Chapter II, section Antibody Purification. The percent binding was calculated using the formula (A_{eb}/A_{ref}) x 100, where A_{ref} is the absorbance value for binding in the reference buffer PBS, and A_{eb} is the absorbance value after incubating with the respective elution buffer.[146] For both antibodies, acidic and basic conditions generally resulted in a significant decrease in the amount of bound antibody. Water and 4 M sodium chloride did not significantly decrease the amount of bound antibody. TEA showed the largest decrease in the percentage of bound antibody. While 100 mM TEA was more effective at eluting antibody, 10 mM TEA was chosen for elution to limit antibody denaturation. Figure 9 shows the ELISA results obtained with anti-D-AHA 73. Similar results were obtained with anti-L-AHA 65.

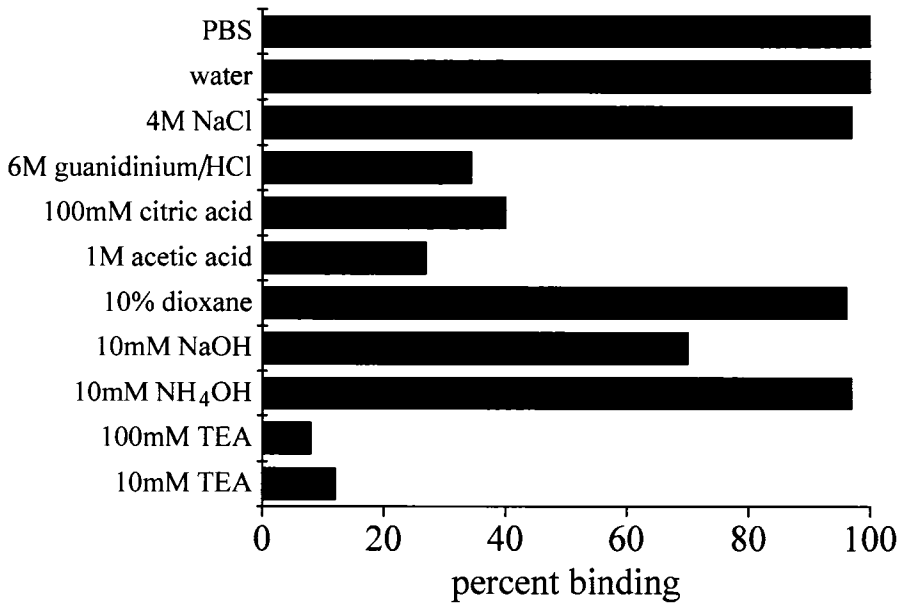

Figure 9: The efficacy of potential elution solvents for affinity purification was determined by noncompetitive ELISA. After binding of the primary antibody, the microtiter plate was incubated with the elution solvents for 10 min at room temperature. The antibody which remained bound was detected with HRP-labeled secondary antibody. PBS was used as a reference buffer.

After selection of the elution conditions, antibodies from the interstitial fluids and sera of both rabbits were further purified by affinity chromatography as described in Chapter II, section Antibody Purification. With each batch of antibody purified, the majority of antibody eluted from the column with the void volume and successive washings with PBS. Only a negligible amount of protein was removed by washing with 1 M sodium chloride. Specific antibody was eluted from the column with 10 mM TEA. For the purification shown in Figure 10, 130 mg of ammonium sulfate precipitated interstitial fluid containing anti-D-AHA 73 was applied to the column (bed volume: 15 ml) at a concentration of 8.7 mg/mL. Eleven mg of specific antibody were eluted from the column; both flow-through and eluted antibody were tested for activity in noncompetitive ELISAs (Figure 11). No apparent overloading of the column occurred as the flow-through contained no detectable specific antibody (not shown). The eluted antibody, on the other hand, still showed specific, stereoselective interaction indicating that the antibody retained activity after elution. The percentage of hapten-specific antibody was comparable to that observed in other studies[148,149] and ranged from 8–10% for both anti-D-AHA 73 and anti-L-AHA 65 from either interstitial fluid or serum.

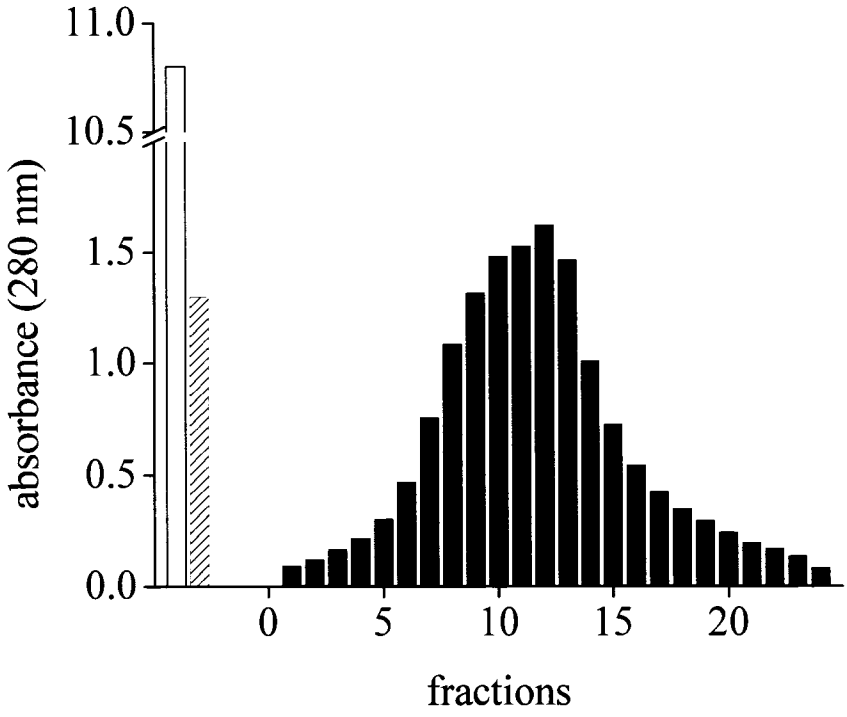

Figure 10: Affinity purification of anti-D-AHA 73 on CL4B Sepharose derivatized with *p*-azo-D-PLA-tyramine. One mL fractions were collected upon elution with 10 mM TEA and were measured at 280 nm (solid bars). Approximately 100 mg of the 130 mg of protein applied to the column did not bind to the column and were collected with the 13 mL of flow-through (open bar). Another 20 mg of protein were collected after washing with PBS (diagonally lined bar). Subsequent washing with PBS and 1 M sodium chloride did not remove any significant amounts of protein (not shown).

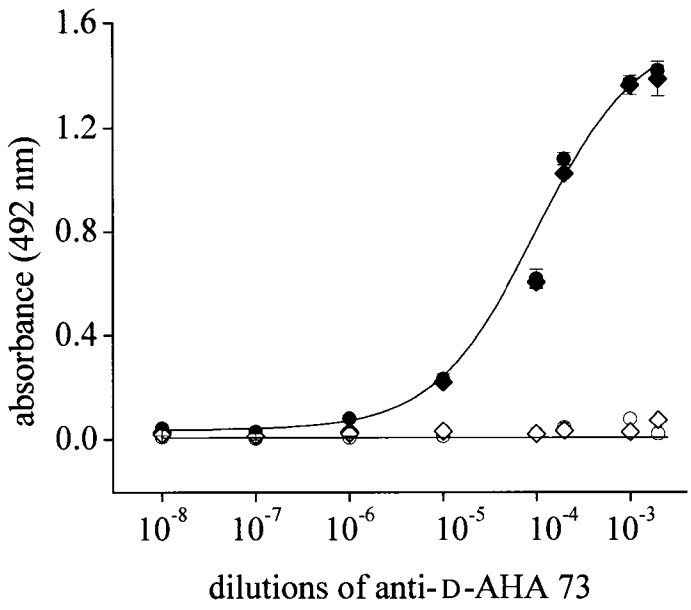

Figure 11: Noncompetitive ELISA results for anti-D-AHA 73 before (●,○) and after (◆,◇) affinity purification. The concentration of the purified antibody was adjusted to 1/10 of the concentration of antibody in the unpurified sample so that the concentration of specific antibody was the same in both samples. Filled and open symbols represent binding to *p*-azo-D-PLA-BSA and *p*-azo-L-PLA-BSA coatings, respectively. Values obtained with the BSA coating were subtracted. Data points represent means of triplicate determinations. Error bars are obscured by symbols.

Competitive ELISAs

Affinity-purified antibodies were characterized in competitive ELISAs using free AHAs as competitors as described in Chapter II, section Enzyme-Linked Immunosorbent Assays. In the earliest immunoassays, developed by Rosalyn Yalow and Solomon Berson, anti-insulin antibodies were shown to bind to insulin labeled with radioactive iodine. Unlabeled insulin could compete with and thereby decrease the binding of labeled insulin to the anti-insulin antibodies. Alternatively, antibodies were labeled with a radioactive isotope.[150,151] ELISAs eliminate the need for radioactive substances and are now more commonly used than RIAs.[152,153] Either the antibody or the antigen can be labeled with an enzyme such as horseradish peroxidase or alkaline phosphatase, each of which can convert a colorless substrate to a colored product. Commercially available enzyme-labeled secondary antibodies can also be used to detect the primary antibody. Protein antigens can be adsorbed directly onto the plastic surfaces of microtiter plates commonly used in ELISAs. Haptens, which may not adsorb directly onto microtiter plates, may be conjugated to a protein prior to application onto the plate. The protein, in this case, should not be the same protein used for immunization, so as to avoid binding of antibodies which recognize the carrier protein instead of the hapten. Addition of competitor can inhibit binding of the primary antibody to antigen-coated plates. In the case of a competitor that binds strongly to the antibody, only a small amount of competitor is needed to inhibit the

binding of antibody; conversely, larger amounts of competitor are needed if the competitor only binds weakly to the antibody.

Here, various free underivatized AHAs were used as competitors. The relative binding affinities of these AHAs were determined as IC_{50} values. The IC_{50} value is the concentration of inhibitor that leads to a 50% decrease in the amount of antibody bound to the plate. Absorbance values are converted to percent inhibition using the equation, percent inhibition = $[1-(A/A_0)] \times 100$, where A represents values in the presence of competitor (at a certain concentration), while A_0 is the absorbance in the absence of competitor.

As stated above, the extent of inhibition is strongly affected by the strength of interaction between antibody and competitor. Typically, the strongest binding affinities of anti-hapten antibodies are obtained with molecules which resemble the hapten. Because here the hapten, *p*-amino-D- or -L-PLA, was conjugated to the KLH carrier via diazotization, of all AHAs tested the *p*-azo-D- and -L-PLA-tyramine conjugates showed the strongest binding to the anti-D-AHA 73 and anti-L-AHA 65, respectively. The relative affinities of both antibodies for the respective *p*-azo-D- or -L-PLA-tyramine conjugates were found to be in the low micromolar range. *p*-Amino-PLA and PLA also bind with micromolar affinities as shown in Figure 12 and Figure 13, respectively. Aliphatic AHAs bound with weaker affinities, i.e., in the millimolar range. Lactic acid bound with the weakest affinity of all AHAs tested (Figure 14). Aliphatic AHAs with longer side chains bound more strongly than lactic acid. Despite their weak affinity, however, the aliphatic AHAs still were bound

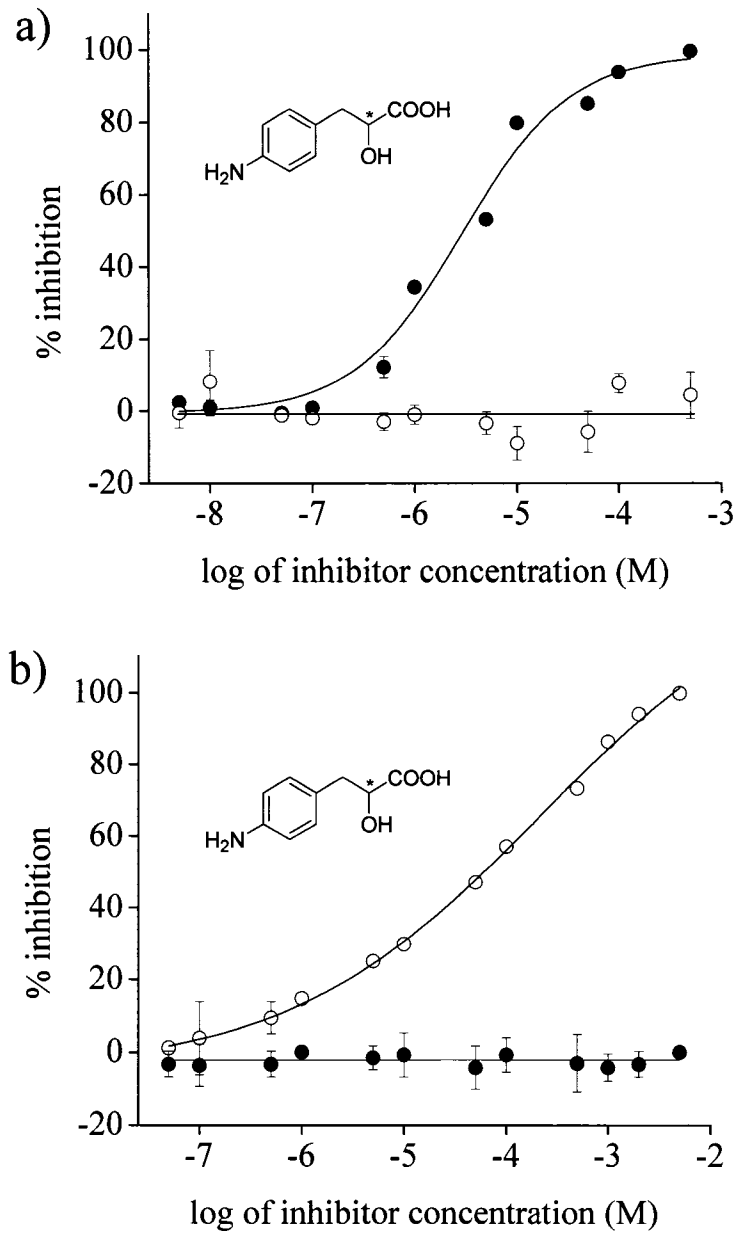

Figure 12: Competitive ELISAs performed with a) anti-D-AHA 73 and b) anti-L-AHA 65 using *p*-amino-PLA as competitor. Open circles (○) represent the L-enantiomer and closed circles (●) represent the D-enantiomer. Error bars indicate standard deviations of triplicate determinations. Missing error bars are obscured by symbols.

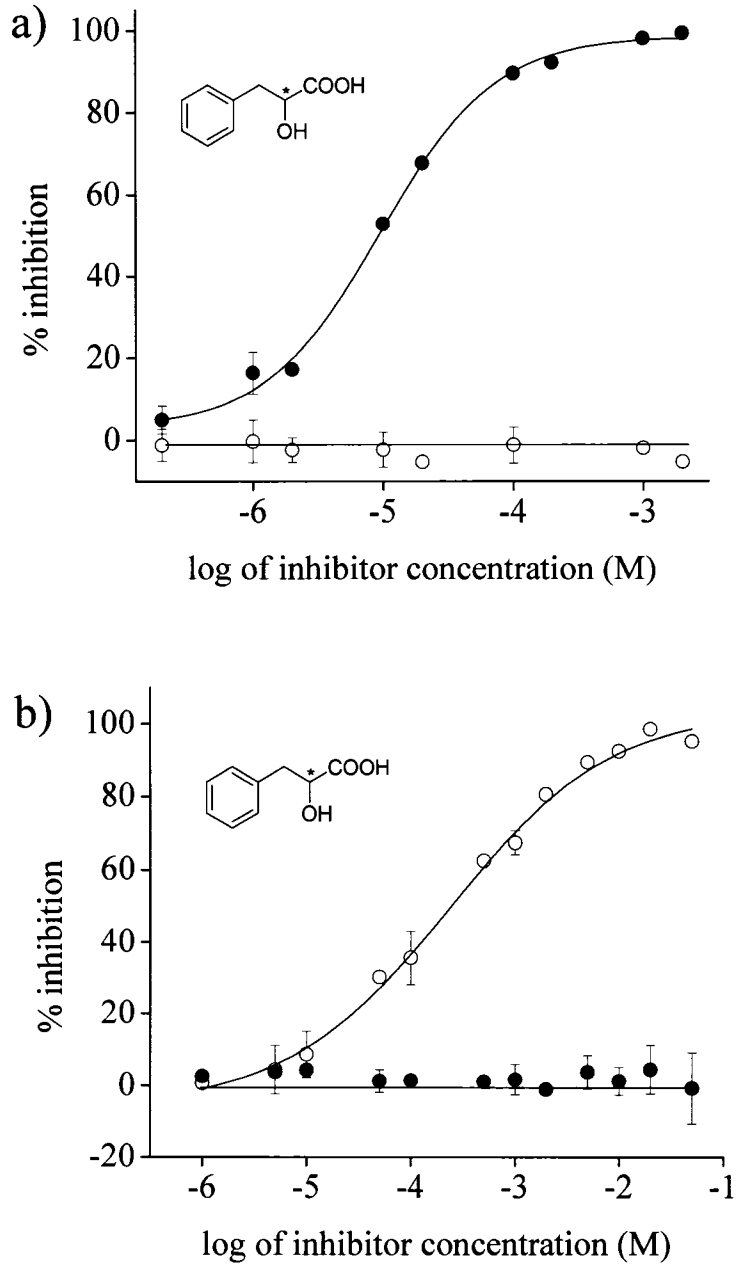

Figure 13: Competitive ELISAs performed with a) anti-D-AHA 73 and b) anti-L-AHA 65 using PLA as competitor. Open circles (O) represent the L-enantiomer and closed circles (●) represent the D-enantiomer. Error bars indicate standard deviations of triplicate determinations. Missing error bars are obscured by symbols.

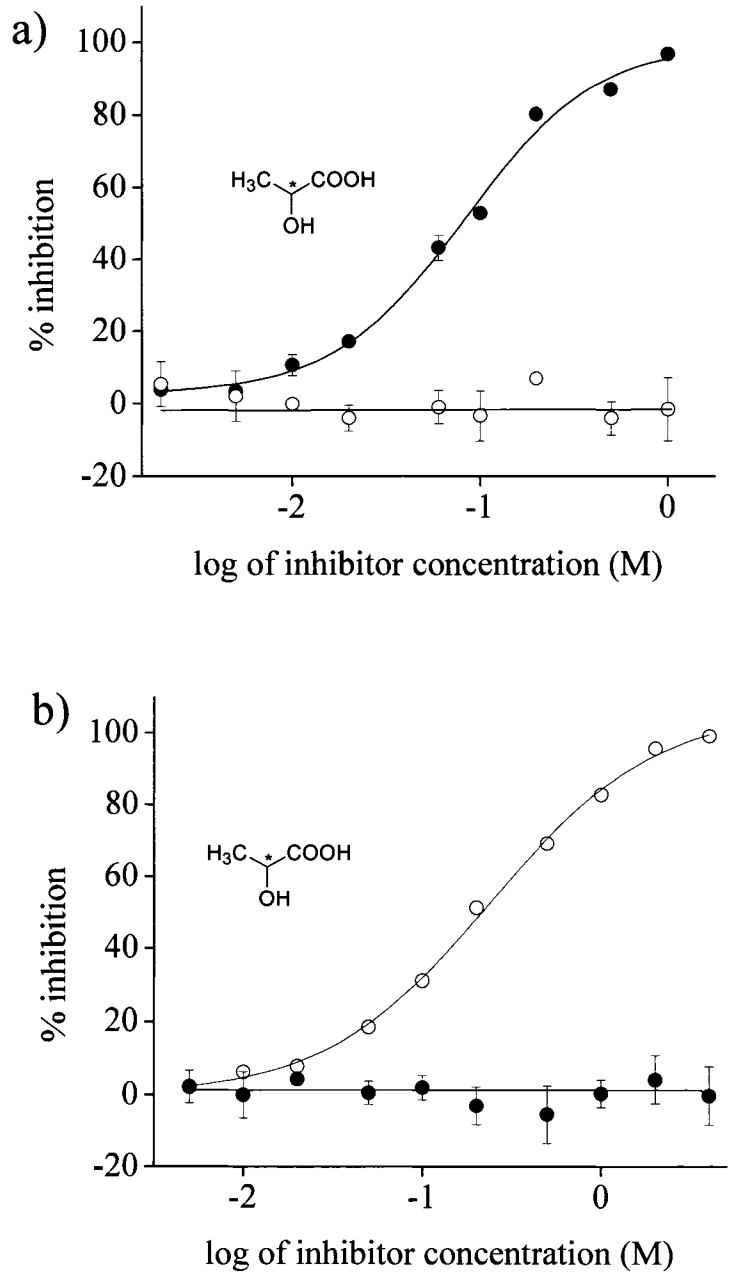

Figure 14: Competitive ELISAs performed with a) anti-D-AHA 73 and b) anti-L-AHA 65 using lactic acid as competitor. Open circles (○) represent the L-enantiomer and closed circles (●) represent the D-enantiomer. Error bars indicate standard deviations of triplicate determinations. Missing error bars are obscured by symbols.

stereoselectively by the corresponding antibodies. IC_{50} values determined in competitive ELISAs with various AHAs ranging from aromatic AHAs to lactic acid are given in Table 4 for anti-D-AHA 73 and in Table 5 for anti-L-AHA 65.

While the nature of the side chain affects the binding affinity, the hydroxyl/carboxyl/hydrogen triad about the stereogenic center is essential for stereoselective binding of AHAs to either antibody. Only AHAs of the correct configuration bind to the antibodies. No inhibition was observed using the "wrong" enantiomer as competitor in the range of concentrations tested. Since *p*-hydroxy-PLA, 2-hydroxyoctanoic acid, and 2-hydroxyisocaproic acid were only available as racemic mixtures, relative affinity values for these three AHAs were determined using the concentration of the correct enantiomer (i.e., half of the total AHA concentration). The simplifying assumption was made that the "wrong" enantiomer does not interact with the antibody.

The anti-AA antibodies described by Hofstetter and Hofstetter[35] also bound stereoselectively to a wide range of free AAs in competitive ELISAs. The influence of the side chain on the relative affinities showed a similar trend to the one observed here with the anti-AHA antibodies. The smallest IC_{50} values were obtained for AAs such as tyrosine and *p*-amino-Phe, whose structures resemble the hapten. Larger IC_{50} values were obtained for aliphatic AAs. Furthermore, aliphatic AAs with longer side chains, in general, had smaller IC_{50} values than those with shorter side chains.

While polycolonal antibodies were produced first because of the relatively short time until antibodies could be obtained and because fewer animals are typically

Table 4: Relative affinities of anti-D-AHA 73 to various α-hydroxy acids as determined by competitive ELISA

α-Hydroxy acid	Structure	IC_{50}
p-azo-D-PLA-tyramine[a]	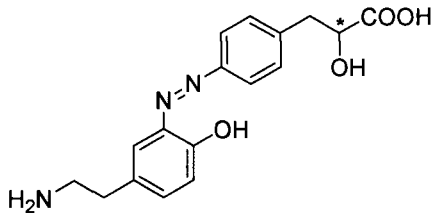	1.33 μM ± 0.18
p-hydroxy-D-PLA[h]	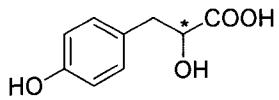	2.0 μM ± 0.1
p-amino-D-PLA[b]	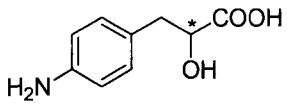	4.7 μM ± 1.7
D-PLA[c]	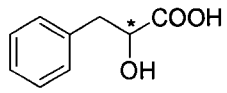	9.4 μM ± 0.1
p-nitro-D-PLA[d]	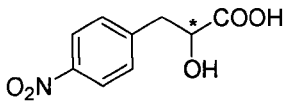	22.6 μM ± 0.6
D-mandelic acid[e]	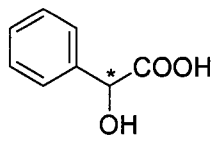	567.5 μM ± 7.8
D-2-hydroxyoctanoic acid[h]	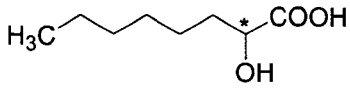	964.5 μM ± 2.1
D-2-hydroxyisocaproic acid[h]	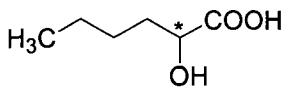	2.83 mM ± 0.04
D-2-hydroxyisovaleric acid[f]	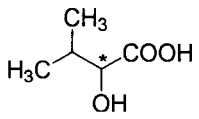	4.0 mM ± 1.0
D-lactic acid[g]	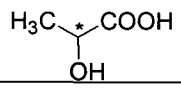	91.61 mM ± 0.02

Values represent means of three independent measurements. 50% inhibition was not reached with the opposite enantiomer using maximum concentrations as follows: a) 100 μM, b) 500 μM, c) 2 mM, d) 1 mM, e) 50 mM, f) 15 mM, g) 1 M, h) not determined.

Table 5: Relative affinities of anti-L-AHA 65 to various α-hydroxy acids as determined by competitive ELISA

α-Hydroxy acid	Structure	IC_{50}
p-azo-L-PLA-tyramine[a]	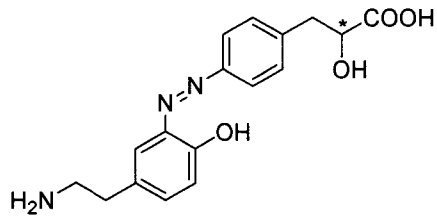	34.0 μM ± 3.8
p-hydroxy-L-PLA[f]	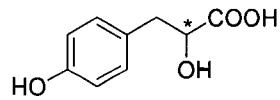	52.7 μM ± 5.2
p-amino-L-PLA[b]	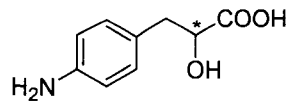	69.2 μM ± 6.2
L-PLA[c]	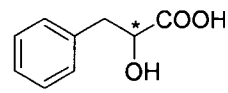	210 μM ± 4
p-nitro-L-PLA[c]	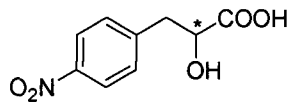	237 μM ± 2
L-mandelic acid[c]	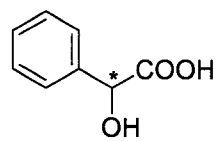	905 μM ± 3
L-2-hydroxyoctanoic acid[f.]	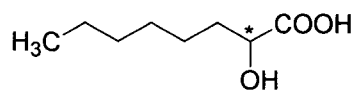	1.07 mM ± 0.07
L-2-hydroxyisocaproic acid[f]	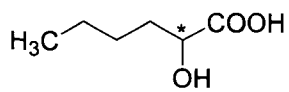	5.52 mM ± 0.12
L-2-hydroxyisovaleric acid[d]	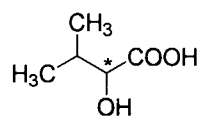	12.5 mM ± 0.6
L-lactic acid[e]	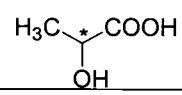	224.4 mM ± 5.7

Values represent means of three independent measurements. 50% inhibition was not reached with the opposite enantiomer using maximum concentrations as follows: a) 2 mM, b) 5 mM, c) 50 mM, d) 200 mM, e) 4 M, f) not determined.

needed to obtain positive results, monoclonal antibodies are ultimately more useful. Monoclonal antibodies are homogeneous and have a uniform binding specificity. Monoclonal antibodies can theoretically be produced indefinitely once a cell line is established, but continued production of polyclonal antibodies is dependent on an animal's survival. Additionally, monoclonal antibodies and their fragments can be used for structural analysis in X-crystallography. cDNA can also be obtained from monoclonal antibody-producing hybridomas for sequence determination.

Production and Characterization of Monoclonal Antibodies

Immune Responses and Selection of Mice

The production of monoclonal antibodies hinges on the fact that only one particular antibody molecule is produced by a given B-lymphocyte. Individual B-lymphocytes were shown to produce antibodies as early as 1958 by Nossal and Lederberg.[154] In 1963, Jerne and Nordin had developed the agar-gel plaque technique for visualizing single antibody-producing cells.[155] By 1967, Mäkelä demonstrated that the antibodies produced from such single immunocytes showed remarkable specificity for a single ligand.[156] In the same year, Green et al. used immunofluorescent techniques to prove that cells producing anti-hapten antibodies did not produce anti-carrier antibodies, and, likewise, the cells which produced antibodies against the carrier did not produce any anti-hapten antibodies.[157] Klinman, in 1969, confirmed

quantitatively that clones from a single B-lymphocyte produce homogeneous antibodies.[158] Because many B-lymphocytes respond when an animal is injected with an immunogen, multiple clonotypes are produced to yield a "polyclonal antibody." Klinman, in his subsequent experiments, estimated that a BALB/c mouse containing about 2 x 10^8 B-cells can, theoretically, generate 1-4 x 10^7 distinct clonotypes.[159] Theoretically, several different clonotypes could be produced for a given epitope, as one out of every 10,000 clonotypes may potentially produce antibody against a given epitope.[159,160] However, only few distinct antibodies are produced since only a few B-cell clones are activated.[52,161-163]

In "multiple myeloma," cancerous tumors of B-lymphocytes secrete monoclonal antibodies. While these antibody-secreting tumors had been known for years, the binding activity of such antibodies was unknown before 1967.[164] In fact, many researchers believed that they could not bind antigen.[164] Eisen et al., however, finally demonstrated that antibodies secreted from myeloma tumors could bind to an antigen, specifically DNP-lysine.[165] Since that time, more antibodies from myeloma tumors have been shown to bind to antigens.[166-169] In addition to naturally occurring myelomas, Michael Potter and C. R. Boyce found that myelomas can be induced in mice by intraperitoneal injections of mineral oil.[170,171] While cells from both naturally occurring and induced myelomas can be grown in cell culture, isolation of such myeloma cells producing antibodies with desired binding characteristics is impractical.[172] B-cells from an immunized animal secrete antibodies of known antigenic activity, yet they can only be maintained in tissue culture for a short time.

The hybridoma technology, pioneered by Köhler and Milstein, made it practical not only to isolate B-cells, which secrete monoclonal antibodies with known specificity, but also to grow those cells in culture.[53,54] Theoretically, unlimited quantities of homogeneous antibodies may be produced continuously from one cell line. Briefly, the animal, typically a mouse or rat, is first inoculated in order to stimulate B-lymphocytes that recognize the antigen; these cells will become antibody-producing plasma cells. Following subsequent booster injections, serum from test bleeds containing polyclonal antibodies is screened for antibodies with the desired binding properties. An animal with a good immune response is boosted with the immunogen just a few days prior to fusion. B-cells harvested from lymphoid tissues are then fused *in vitro* with an immortal, nonantibody-producing myeloma cell. Sendaii virus was originally used by Köhler and Milstein to fuse splenocytes and myelomas.[53,173] Since that time, polyethylene glycol (PEG) and electrofusion have both been used to fuse cells; however, today PEG is the most commonly used fusing agent.[174-177] As hybridomas are present only in small amounts in a cell mixture, which also includes unfused myeloma and B-lymphocytes, lymphocyte-lymphocyte, and myeloma-myeloma fused cells, the cells are grown in a selective medium containing HAT, in which only hybridoma cells survive. Detailed descriptions of the processes and methods involved in the production of monoclonal antibodies are given in Chapter I and Chapter II, section Antibody Production.

Initially, production of monoclonal antibodies by classical immunological methods requires essentially the same steps as the production of polyclonal antibodies.

Because immune responses may vary among animals, multiple mice or rats are typically inoculated. Polyclonal antibodies are typically obtained from immunized animals to select the animal with the optimal immune response for use in hybridoma production. Using multiple animals also provides an opportunity for repeated cell fusions should the first attempt be unsuccessful.

Because the goal of this part of the dissertation was to produce and characterize stereoselective monoclonal antibodies against AHAs, five mice were inoculated intraperitoneally with *p*-azo-D-PLA-KLH in CFA as described in Chapter II, section Antibody Production. Another five mice were inoculated with *p*-azo-L-PLA-KLH in CFA. Booster injections of the respective immunogen in IFA were given two weeks later. Four weeks after the first inoculation, each mouse was given a second booster injection of the respective immunogen in PBS. Serum samples were collected from the tail of each mouse one month after the second booster injection. These samples were tested for specific stereoselective antibody in noncompetitive ELISAs as described in Chapter II, section Enzyme-Linked Immunosorbent Assay. Sample binding curves are presented in Figure 15 a) for samples from mouse #1 and mouse #2, which were inoculated with *p*-azo-D-PLA-KLH. Figure 15 b) shows sample binding curves for mouse #6 and mouse #60 inoculated with *p*-azo-L-PLA-KLH. The titers determined for serum samples of all mice were in the range between 1/10,000 and 1/100,000.

Typically, high serum titers are considered indicative of a good immune response. High titers, however, do not guarantee the presence of an antibody of high

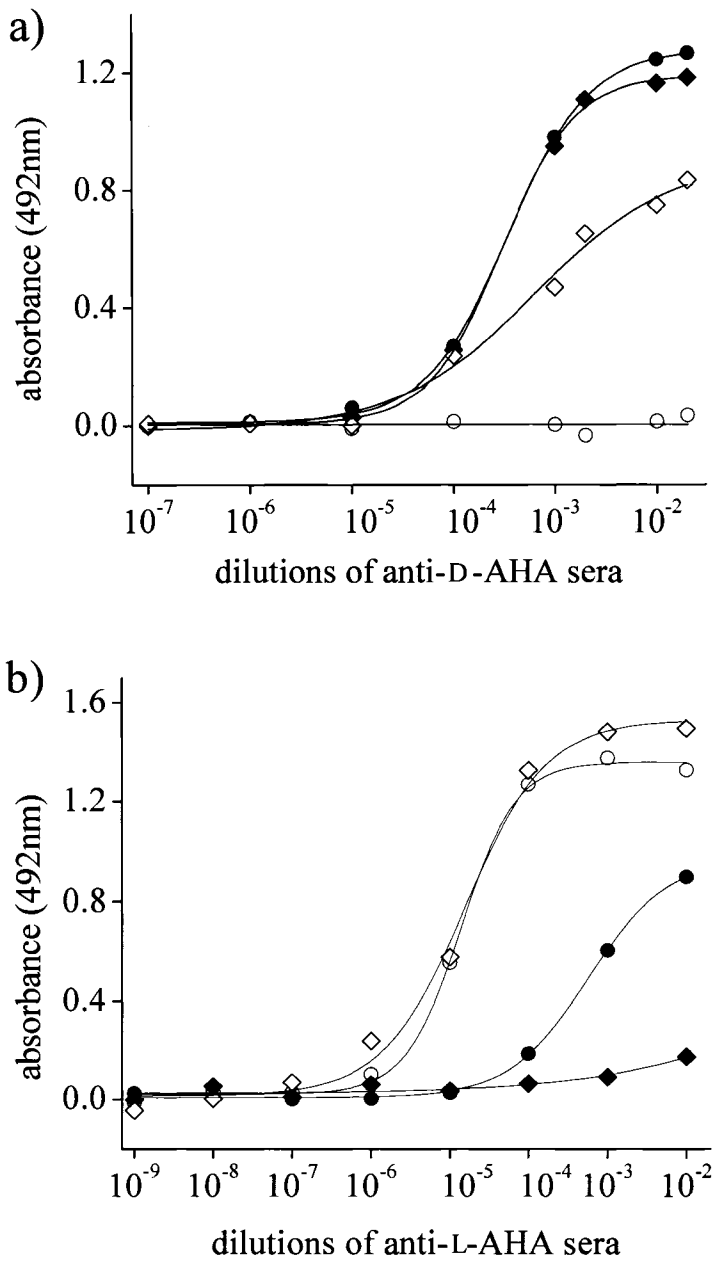

Figure 15: Noncompetitive ELISA results for polyclonal antibody-containing sera from mice inoculated with a) *p*-azo-D-PLA-KLH and b) *p*-azo-L-PLA-KLH. In graph a), mice #1 and #2 are represented by (●,○) and (◆,◇), respectively. In graph b), mice #6 and #60 are represented by (●,○) and (◆,◇), respectively. *p*-Azo-D-PLA-BSA (closed symbols), *p*-azo-L-PLA-BSA (open symbols), and BSA were used as solid-phase coatings. At each dilution, the values obtained with the BSA coating were subtracted from those obtained on the other two coatings.

affinity as the titer may be based on a high level of antibody production. The affinity of the antibody should, therefore, be tested in, e.g., a competitive ELISA. Mouse #1 had good titers and exhibited the most stereoselective immune response of all mice inoculated with *p*-azo-D-PLA-KLH. Of the mice inoculated with *p*-azo-L-PLA-KLH, mouse #60 exhibited the most stereoselective immune response and also had a good titer. Therefore, the polyclonal antibody-containing sera from these two mice were further tested in competitive ELISAs (Figure 16). An IC_{50} value of 15 μM was obtained for the binding of the polyclonal antibody from mouse #1 to D-PLA. For the serum sample from mouse #60, an IC_{50} value of 112 μM was obtained for the binding of the polyclonal antibody to L-PLA. As with the polyclonal rabbit antibodies, no inhibition was observed using the "wrong" enantiomer as competitor in the range of concentrations tested. The spleens from mice #1 and #60 were harvested for fusion to produce hybridoma cells because both mice had good stereoselective immune responses.

Production and Selection of Hybridomas

Mouse #1 and mouse #60 were given booster injections of *p*-azo-D-PLA-KLH and *p*-azo-L-PLA-KLH, respectively, in PBS three to four days prior to harvesting their spleens as described in Chapter II, section Antibody Production. Splenocytes from each mouse were fused separately with P3x63AG8 myeloma cells. Within an hour after fusion, formation of fused cells could be observed upon microscopic

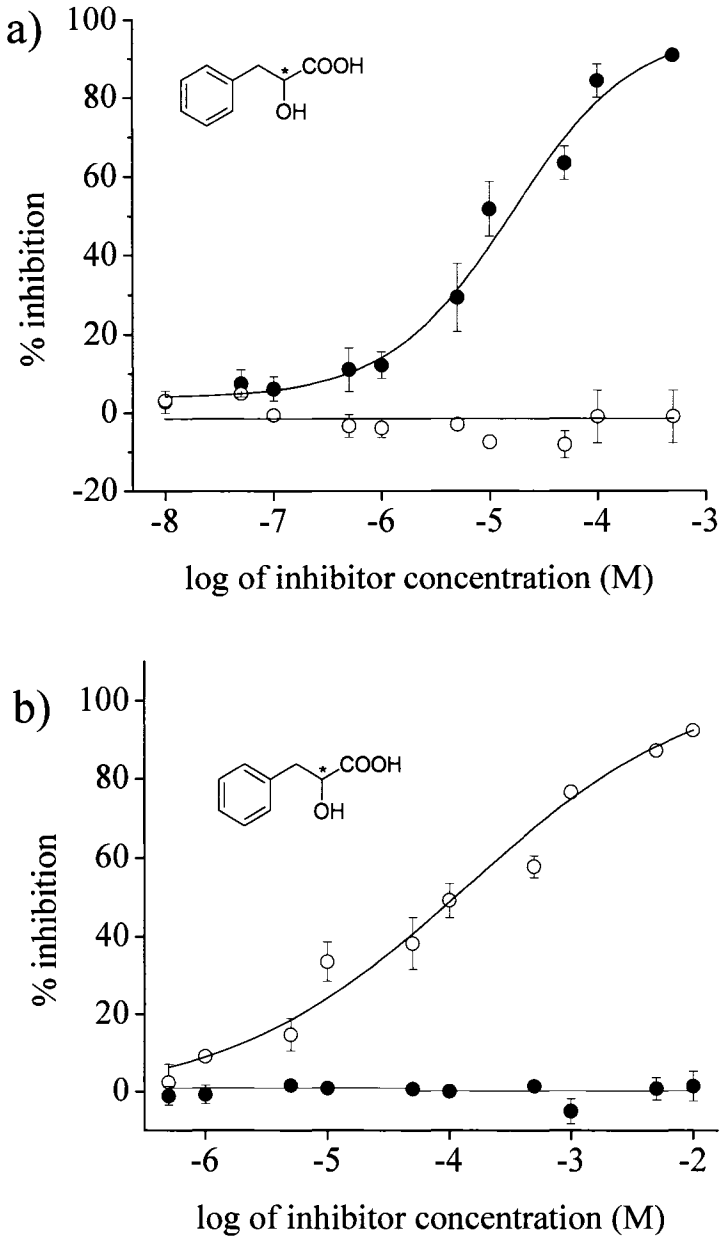

Figure 16: Competitive ELISAs of polyclonal antibody-containing sera from a) mouse #1, which was inoculated with *p*-azo-D-PLA-KLH, and b) mouse #60, which was inoculated with *p*-azo-L-PLA-KLH using PLA as competitor. Open circles (O) represent the L-enantiomer and closed circles (●) represent the D-enantiomer. Error bars indicate standard deviations of triplicate determinations. Missing error bars are obscured by symbols.

examination (Figure 17a). After being exposed to the HAT selective medium, multiple clumps of growing hybridoma cells could be seen after about one week (Figure 17b). Two weeks after fusion, the medium in some of the wells began to change color, indicating a pH change due to by-products of cellular metabolism, typically lactic acid. The supernatant was collected from the wells when the medium changed color. The samples were then tested in noncompetitive ELISAs as described in Chapter II, section Enzyme-Linked Immunosorbent Assay. Within a month, the bottoms of most of the wells were covered with a layer of cells (Figure 17c). By two months, the supernatant from most wells had been tested for specific antibody. Supernatant from any wells not previously tested were tested at this time and the culture plates were discarded to prevent infection.

Of the hybridomas produced from the splenocytes of the mouse inoculated with *p*-azo-D-PLA-KLH, eight produced antibodies that exhibited strong stereoselective binding to the *p*-azo-D-PLA-BSA coating; no significant binding to *p*-azo-L-PLA-BSA or BSA coatings was observed in noncompetitive ELISA (Figure 18). One clone, 0D11, secreted antibodies exhibiting significant cross-reactivity to the *p*-azo-L-PLA-BSA coating.

Nine hybridomas of those produced from the splenocytes of the mouse inoculated with *p*-azo-L-PLA-KLH produced antibodies that bound strongly to the *p*-azo-L-PLA-BSA coating (Figure 19). One of these antibodies, anti-L-AHA 5F12, also exhibited strong binding to the *p*-azo-D-PLA-BSA coating. None of these nine antibodies showed significant binding to the BSA coating.

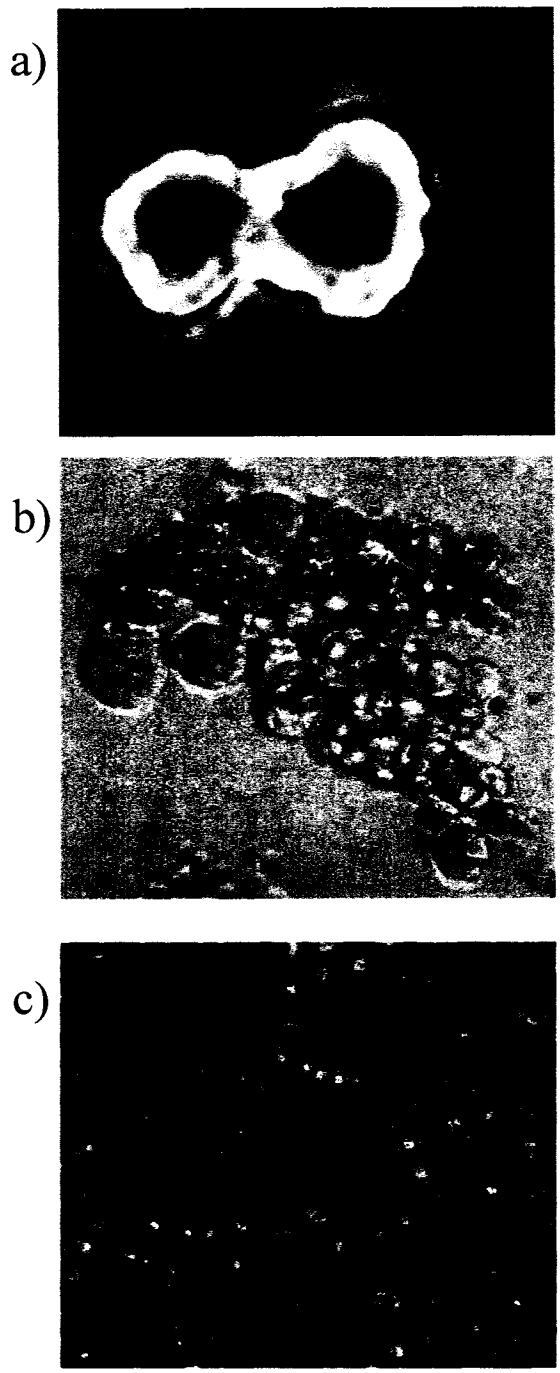

Figure 17: Hybridomas are grown in cell culture after they are produced by fusing lymphocytes and myeloma cells. a) Cells begin to fuse within an hour of treatment with polyethylene glycol (400 x magnification). b) Clumps of growing cells can be seen in about one week (200 x magnification); however, cell debris from dying cells is also seen. c) Cells cover the bottoms of many of the wells one month after fusion (200 x magnification).

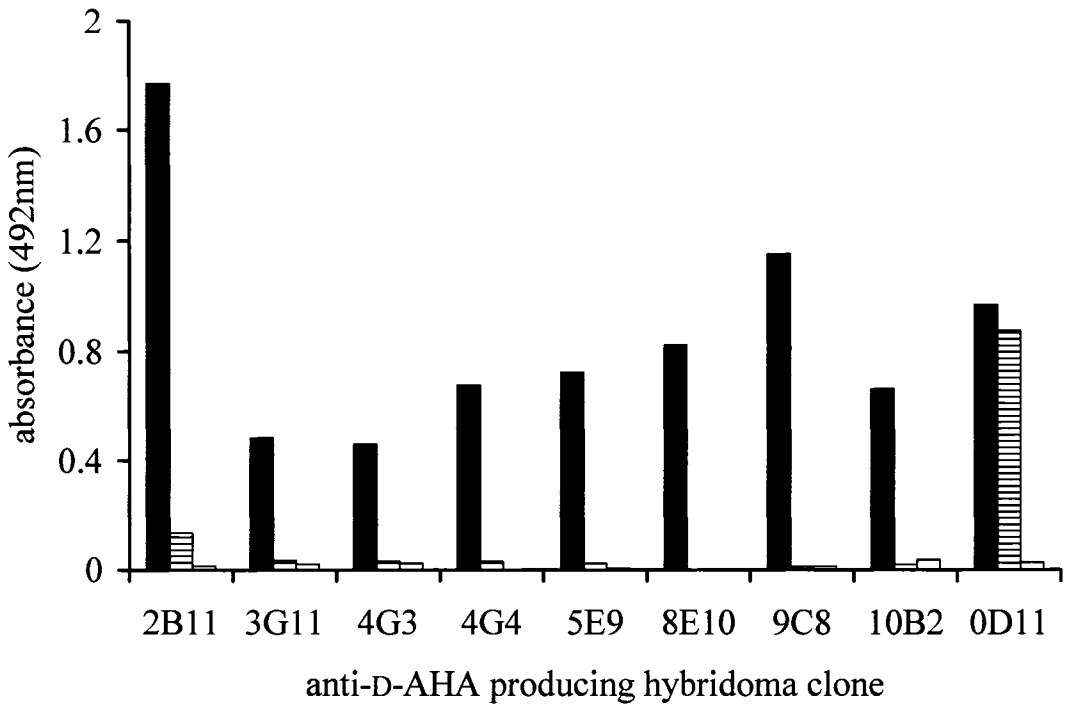

Figure 18: Cell culture supernatants were screened for antibodies that bind to *p*-azo-D-PLA-BSA coating (solid bars) in noncompetitive ELISA. The antibody-producing hybridomas were produced by fusing splenocytes from mouse #1, which was inoculated with *p*-azo-D-PLA-KLH. Cell culture supernatants were also screened against *p*-azo-L-PLA-BSA (horizontally lined bars) and BSA (open bars) coatings.

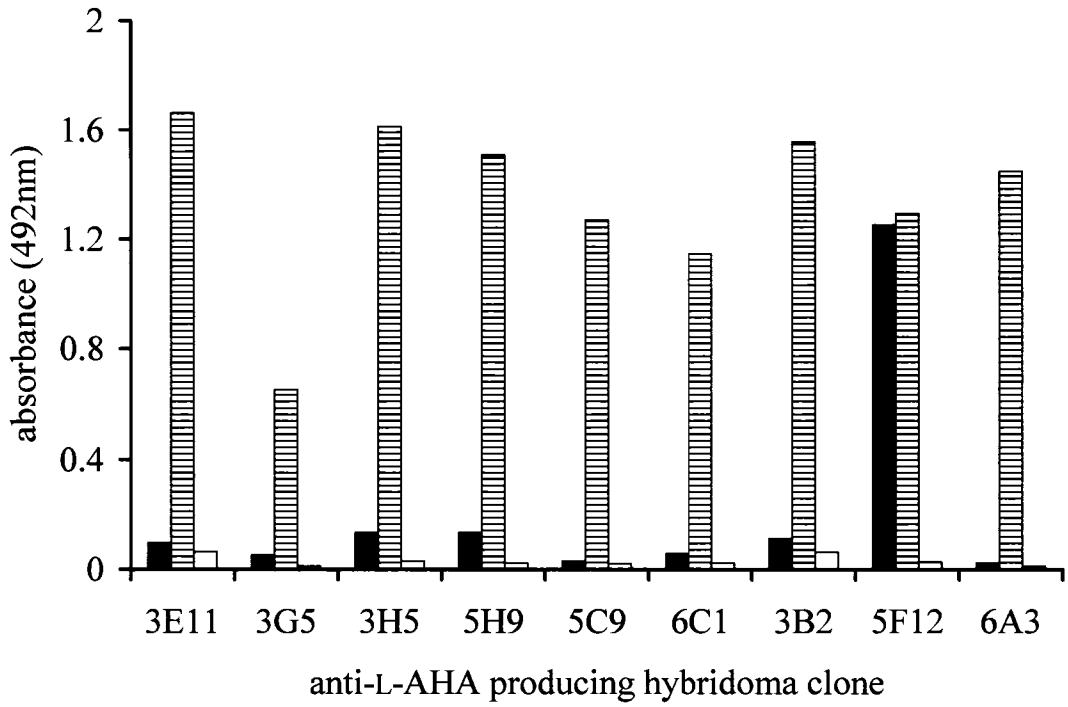

Figure 19: Cell culture supernatants were screened for antibodies that bind to *p*-azo-L-PLA-BSA coating (horizontally lined bars) in noncompetitive ELISA. The antibody-producing hybridomas were produced by fusing splenocytes from mouse #60, which was inoculated with *p*-azo-L-PLA-KLH. Cell culture supernatant was also screened against *p*-azo-D-PLA-BSA (solid bars) and BSA (open bars) coatings.

Characterization of Monoclonal Antibodies

While noncompetitive ELISAs represent an efficient method for initial screening of antibody-producing clones, competitive ELISAs are more useful to determine affinities of secreted antibodies. The aforementioned eighteen monoclonal antibodies were further characterized by competitive ELISAs as described in Chapter II, section Enzyme-Linked Immunosorbent Assay, using PLA as inhibitor. IC_{50} values were determined from competitive ELISAs using both D-and L-PLA as inhibitors. All IC_{50} values, determined with the "correct" enantiomer, were in the micromolar range between 5 μM and 551 μM (Table 6). The "wrong" enantiomer, in the range of concentrations tested, did not bind to any of the antibodies except anti-D-AHA 0D11 and anti-L-AHA 5F12. These two antibodies, which bound to both *p*-azo-D- and -L-PLA-BSA coatings in noncompetitive ELISAs, were inhibited by both D- and L-PLA in competitive ELISA (Figure 20), which provided further confirmation of their cross-reactivity. IC_{50} values for anti-D-AHA 0D11 were 279 μM and 425 μM for D-PLA and L-PLA, respectively (Figure 20a). The IC_{50} value for anti-L-AHA 5F12 was 353 μM for both enantiomers of PLA (Figure 20b).

In most vertebrates, there are five distinct classes of immunoglobulins that differ from each other in size, overall charge, amino acid composition, carbohydrate content, and immunological function. The five immunoglobulin classes are

Table 6: Relative affinities of various monoclonal antibodies to phenyllactic acid as determined by competitive ELISA

Antibody	IC_{50}	Antibody	IC_{50}
anti-D-AHA 2B11	175 μM	anti-L-AHA 3G5	551 μM
anti-D-AHA 3G11	169 μM	anti-L-AHA 3E11	220 μM
Anti-D-AHA 4G3	24 μM	anti-L-AHA 3H5	282 μM
Anti-D-AHA 4G4	189 μM	anti-L-AHA 6A3	154 μM
Anti-D-AHA 5E9	62 μM	anti-L-AHA 3B2	130 μM
anti-D-AHA 8E10	5.3 μM	anti-L-AHA 5H9	482 μM
Anti-D-AHA 9C8	145 μM	anti-L-AHA 6C1	529 μM
anti-D-AHA 10B2	40 μM	anti-L-AHA 5C9	298 μM

IC_{50} values were determined using the concentration of the "correct" enantiomer, i.e., D-PLA for anti-D-AHA antibodies and L-PLA for anti-L-AHA antibodies.

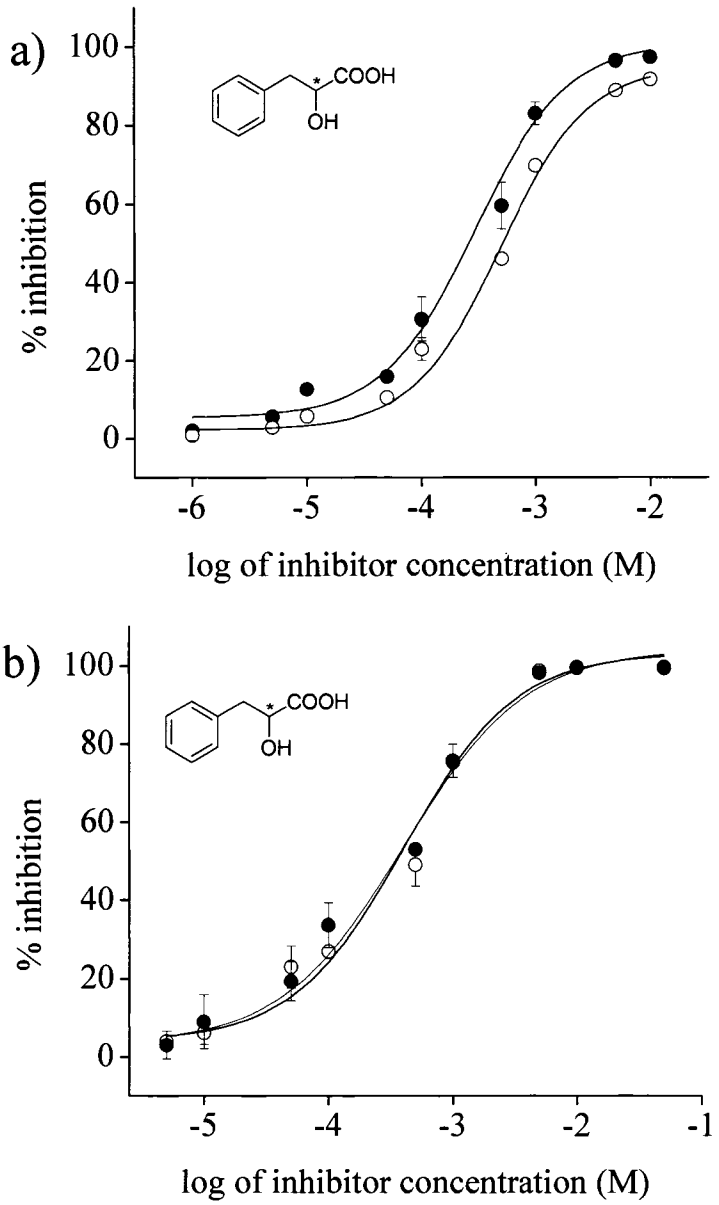

Figure 20: Competitive ELISAs using phenyllactic acid as competitor obtained with a) anti-D-AHA OD11 and b) anti-L-AHA 5F12. Open circles (○) represent the L-enantiomer and closed circles (●) represent the D-enantiomer. Error bars indicate standard deviations of triplicate determinations. Missing error bars are obscured by symbols.

designated IgM, IgG, IgA, IgD, and IgE. Primarily, each class is distinguished by unique amino acid sequences in the heavy chain constant region that confers class-specific structural and functional properties. These different classes can be isolated from serum using a combination of fractional precipitation and ion-exchange or size-exclusion chromatography.[178] Partial purification of antibodies from serum can be achieved by electrophoresis, which results in three fractions of globulins, designated α, β, and γ, and one fraction containing albumin.[179] Tiselius and Kabat determined that the γ-globulin fraction of serum contained antibodies (i.e., immunoglobulins) by raising antibodies against ovalbumin and analyzing serum using electrophoresis.[179] One aliquot of serum was reacted with ovalbumin and the precipitate containing antibody was removed. Another aliquot of serum was not reacted with antigen. Comparison of the two fractions revealed that the aliquot that had been reacted with antigen was significantly depleted in the γ-globulin fraction. It is now known that IgG antibodies are mostly found in the γ-globulin fraction while other classes of antibodies are found in the α and β fractions of serum.[180] IgG is the most abundant immunoglobulin in serum, accounting for 70-75% of the total immunoglobulin concentration. In mouse, there are four IgG subclasses, IgG1, IgG2a, IgG2b, and IgG3, which have dissimilar heavy chain amino acid sequences. In fact, some researchers consider these four IgG subclasses different classes, called IgF, IgG, IgH, and IgI.[181] The immunoglobulin classes and subclasses are encoded by different genes. The unique heavy chains of each class and subclass can be identified using anti-isotype antibodies, which are produced by inoculating an animal of one species

with an antibody of a particular class or subclass from a different species.[182] Isotype determination is important, e.g., for production of cDNA and sequence determination and certain purification methods. Therefore, the isotypes of the nine anti-D-AHA and nine anti-L-AHA antibodies were determined as described in Chapter II, section Isotype Determination. All antibodies were found to be of the IgG class (Table 7). Specifically, anti-D-AHA 0D11, anti-L-AHA 5C9, and anti-L-AHA 5F12 are IgG2b. However, the other fifteen antibodies are IgG1.

Purification of Monoclonal Antibodies

Two antibodies, anti-D-AHA 8E10 and anti-L-AHA 6A3, were purified for further characterization by ammonium sulfate precipitation, Melon™ Gel purification, and affinity purification as described in Chapter II, section Antibody Purification. Because antibodies are found in cell culture supernatant in relatively low concentrations, precipitation of antibody directly from cell culture supernatant may be unproductive. A higher fraction of antibody may be recovered if cell culture supernatant is first concentrated. Cell culture supernatants containing anti-D-AHA 8E10 and anti-L-AHA 6A3 were each concentrated as described in Chapter II, section Antibody Purification. Typically, 100 mL batches of cell culture supernatant were concentrated to 10 mL. Because the horse serum used in cell culture medium contains significant amounts of protein, the supernatant became increasingly viscous in the

Table 7: Isotypes of various monoclonal antibodies

Antibody	Isotype	Antibody	Isotype
anti-D-AHA 2B11	IgG1	anti-L-AHA 3G5	IgG1
anti-D-AHA 3G11	IgG1	anti-L-AHA 3E11	IgG1
anti-D-AHA 4G3	IgG1	anti-L-AHA 3H5	IgG1
anti-D-AHA 4G4	IgG1	anti-L-AHA 6A3	IgG1
anti-D-AHA 5E9	IgG1	anti-L-AHA 3B2	IgG1
anti-D-AHA 8E10	IgG1	anti-L-AHA 5H9	IgG1
anti-D-AHA 9C8	IgG1	anti-L-AHA 6C1	IgG1
anti-D-AHA 10B2	IgG1	anti-L-AHA 5C9	IgG2b
anti-D-AHA 0D11	IgG2b	anti-L-AHA 5F12	IgG2b

concentration process, making it impractical to concentrate supernatants by more than a factor of ten.

The antibody was precipitated from the concentrated cell culture supernatant using 50% saturated ammonium sulfate solution as described in Chapter II, section Antibody Purification. The proteins from horse serum including albumin and horse antibody coprecipitated with the murine antibodies (Figure 21). The antibodies were then further purified by Melon™ Gel in order to remove protein impurities like albumin and transferrin (Figure 22). While the manufacturer's instructions only describe purification of antibodies from serum, antibodies from cell culture supernatant could also be purified here using the same procedure once precipitated antibody was dissolved in PBS at concentrations between 15 and 20 mg/mL. After Melon™ Gel purification, the antibodies were concentrated to 5 mg/mL. Melon™ Gel purification, however, could not remove unwanted horse antibody. The anti-D-AHA 8E10 and the anti-L-AHA 6A3 were therefore isolated by affinity purification using the same *p*-azo-D- and -L-PLA-tyramine Sepharose, respectively, that was used for the affinity purification of the polyclonal rabbit antibodies. Possible elution buffers were tested in noncompetitive ELISA as described in Chapter II, section Antibody Purification. TEA was found to effectively prevent binding of both anti-D-AHA 8E10 and anti-L-AHA 6A3 to their respective antigens on the plate. Even if 100 mM TEA was more effective at eluting antibody, 10 mM TEA was chosen to prevent antibody denaturation. Binding, washing and elution steps using the

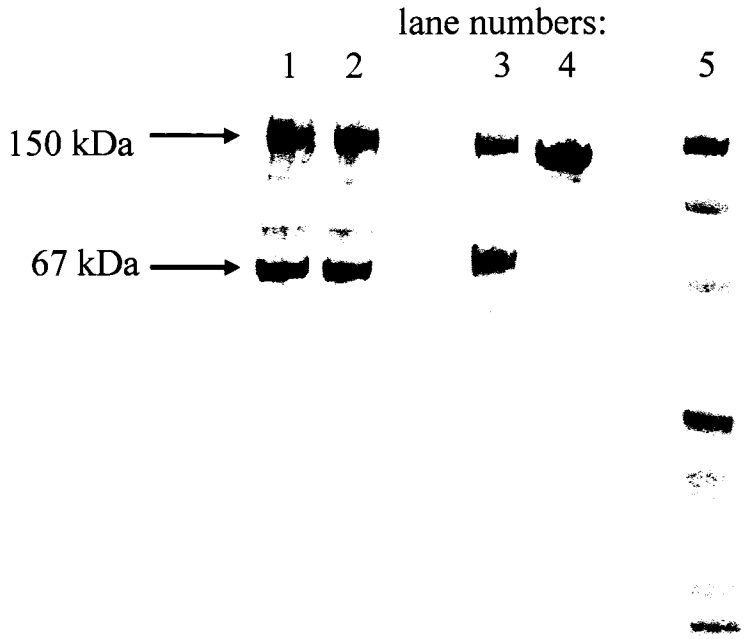

Figure 21: Nonreducing sodium dodecyl sulfate-polyacrylamide gel electrophoresis of concentrated cell culture supernatant containing anti-L-AHA 6A3 (lane 1). Supernatant was precipitated with 50% saturated ammonium sulfate. The precipitate still contained albumin in addition to both horse and murine antibodies (lane 3). The majority of protein in cell culture supernatant comes from horse serum (lane 2). Lane 5 contains the MW marker and lane 4 is a positive control.

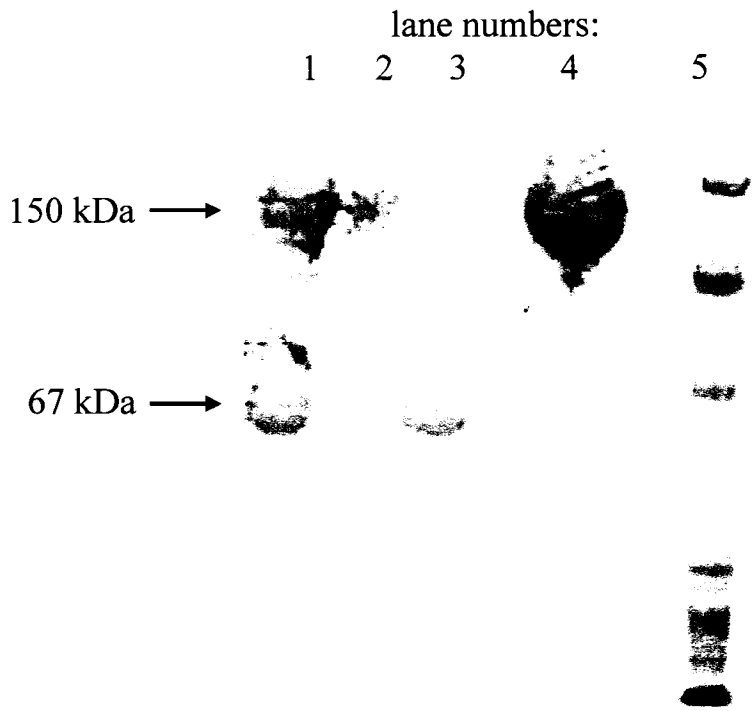

Figure 22: Nonreducing sodium dodecyl sulfate-polyacrylamide gel electrophoresis of anti-L-AHA 6A3 purified from cell culture supernatant by Melon™ Gel (lane 2). Melon™ Gel purification removed protein contaminates (e.g., albumin) that remained after precipitation with 50% saturated ammonium sulfate (lane 1). Such contaminating proteins bind to the Melon™ Gel resin and are eluted with the Melon™ Gel regeneration buffer (lane 3). Lane 5 contains the MW marker and lane 4 is a positive control.

monoclonal antibodies were analogous to the purification of polyclonal rabbit antibodies.

Following ammonium sulfate precipitation and Melon™ Gel purification, 80 mg of the antibody sample containing anti-D-AHA 8E10 at 5 mg/mL were applied to the column (bed volume: 15 mL) for the purification shown in Figure 23. Seven mg of specific antibody were eluted from the column. Similar to the polyclonal rabbit antibodies, the eluted antibody showed specific, stereoselective interaction indicating that the antibody retained activity after elution as determined by noncompetitive ELISA (not shown). The flow-through, however, contained no detectable specific antibody. Purification of anti-L-AHA 6A3 gave similar results following the same purification procedures. Six mg of specific anti-L-AHA 6A3 were obtained from 80 mg of precipitated Melon™ Gel purified cell-culture supernatant antibody. The concentration of hapten-specific antibody in cell-culture supernatant thus ranged from 60-70 μg/ml for both anti-D-AHA 8E10 and anti-L-AHA 6A3. Values are comparable to that observed in other studies.[183,184]

Competitive ELISAs

Anti-D-AHA 8E10 and anti-L-AHA 6A3 were further tested for their ability to bind to various free AHAs. Competitive ELISAs were performed as described in Chapter II, section Enzyme-Linked Immunosorbent Assay. The concentration of free AHAs required to inhibit antibody binding by 50% (IC_{50} value) was used to evaluate

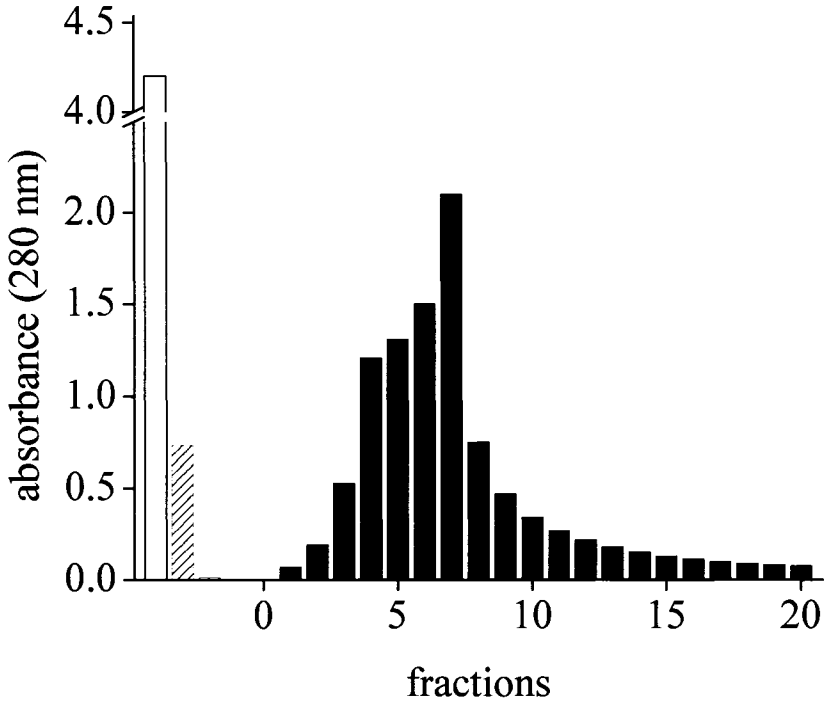

Figure 23: Affinity purification of anti-D-AHA 8E10 on CL4B Sepharose derivatized with *p*-azo-D-PLA-tyramine. One mL fractions were collected upon elution with 10 mM TEA and measured at 280 nm (solid bars). Approximately 60 mg of the 80 mg of protein applied did not bind to the column and were collected with the 20 mL flow-through (open bars). Another 13 mg of protein were collected after washing with PBS (diagonally lined bars). Subsequent washing with PBS and 1 M sodium chloride did not remove any significant amounts of protein (bars obscured).

the relative binding affinities for these compounds. As observed with the polyclonal antibodies, the strongest binding affinities were obtained with AHAs that resemble the hapten, such as *p*-amino-D- or -L-PLA; weaker binding affinities were obtained with aliphatic AHAs. Specifically, the *p*-azo-PLA-tyramine conjugates showed the strongest binding and lactic acid the weakest binding of all AHAs tested. The relative affinities of both antibodies for the respective *p*-azo-D- or -L-PLA tyramine conjugates were in the micromolar range while the relative affinities for the respective D- or L-lactic acid were in the millimolar range. Sample inhibition curves are given in Figure 24 for PLA and in Figure 25 for lactic acid. IC_{50} values of various AHAs determined in competitive ELISAs ranging from aromatic AHAs to lactic acid are given in Table 8 for anti-D-AHA 8E10 and in Table 9 for anti-L-AHA 6A3.

As previously described, the immunogen was designed to produce antibodies that recognize the hydrogen/carboxyl/hydroxyl triad about the alpha carbon of AHAs but are cross-reactive with regard to the side chain. The ELISA results confirmed that these antibodies in fact recognize a wide range of AHAs, including aliphatic AHAs, which differ significantly in their side chain structure from the hapten. As expected, aliphatic AHAs did bind more weakly than AHAs resembling the hapten. These results are in agreement with the results obtained with the polyclonal anti-D-AHA 73, anti-L-AHA 65, and the analogous anti-AA antibodies described by Hofstetter et al., which bind more strongly to amino acids resembling the hapten.[59,60]

The ability of both anti-AHA and previously produced anti-AA antibodies to bind various AHAs and AAs, respectively, is likely due to so-called "true cross-

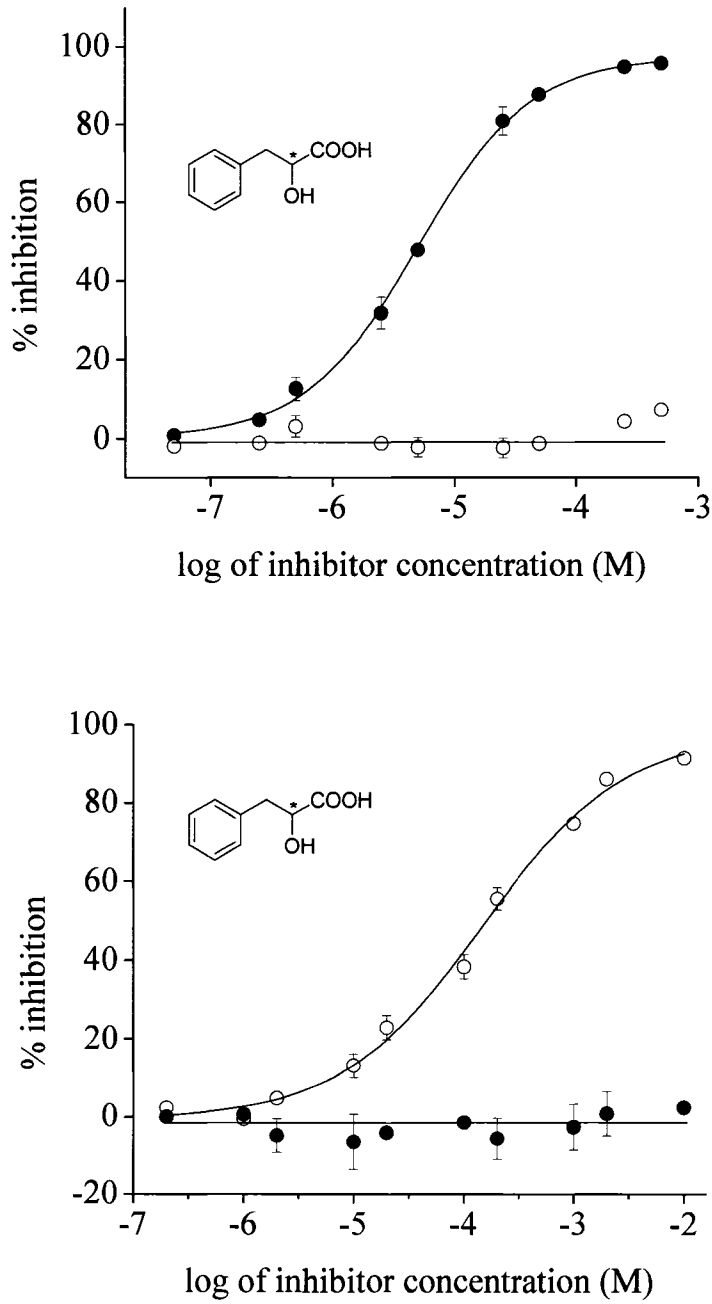

Figure 24: Competitive ELISAs performed with a) anti-D-AHA 8E10 and b) anti-L-AHA 6A3 using PLA as competitor. Open circles (O) represent the L-enantiomer and closed circles (●) represent the D-enantiomer. Error bars indicate standard deviations of triplicate determinations. Missing error bars are obscured by symbols.

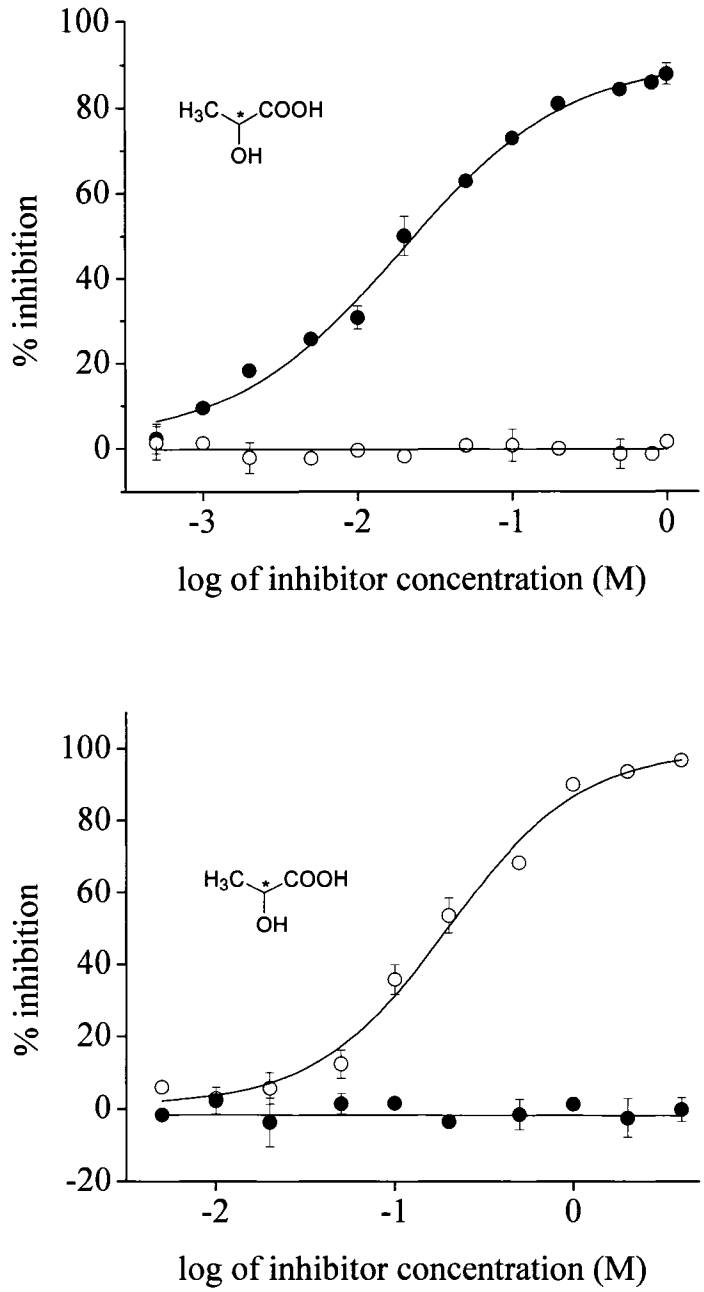

Figure 25: Competitive ELISAs performed with a) anti-D-AHA 8E10 and b) anti-L-AHA 6A3 using lactic acid as competitor. Open circles (O) represent the L-enantiomer and closed circles (●) represent the D-enantiomer. Error bars indicate standard deviations of triplicate determinations. Missing error bars are obscured by symbols.

Table 8: Relative affinities of anti-D-AHA 8E10 to various α-hydroxy acids as determined by competitive ELISA

α-Hydroxy acid	Structure	IC_{50}
p-azo-D-PLA-tyramine[a]	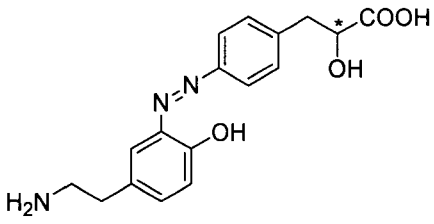	0.20 μM ± 0.03
p-hydroxy-D-PLA[h]	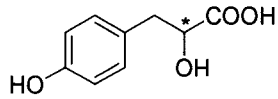	0.98 μM ± 0.31
p-amino-D-PLA[b]	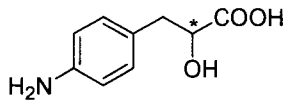	2.7 μM ± 0.6
D-PLA[c]	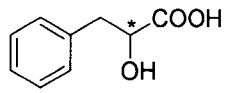	5.3 μM ± 0.8
p-nitro-D-PLA[d]	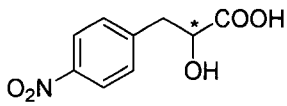	9.2 μM ± 1.3
D-2-hydroxyoctanoic acid[h]	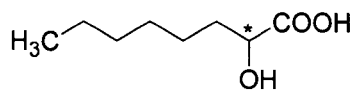	686.0 μM ± 1.2
D-2-hydroxyisocaproic acid[h]	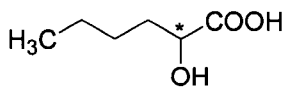	747.1 μM ± 2.8
D-2-hydroxyisovaleric acid[e]	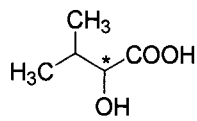	950 μM ± 1
D-mandelic acid[f]	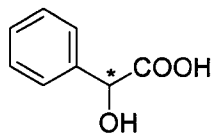	1.21 mM ± 0.02
D-lactic acid[g]	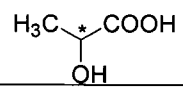	23.3 mM ± 0.8

Values represent means of three independent measurements. 50% inhibition was not reached with the opposite enantiomer using maximum concentrations as follows: a) 25 μM, b) 50 μM, c) 5 mM, d) 10 mM, e) 15 mM, f) 50 mM, g) 1 M, h) not determined.

Table 9: Relative affinities of anti-L-AHA 6A3 to various α-hydroxy acids as determined by competitive ELISA

α-Hydroxy acid	Structure	IC_{50}
p-azo-L-PLA-tyramine[a]	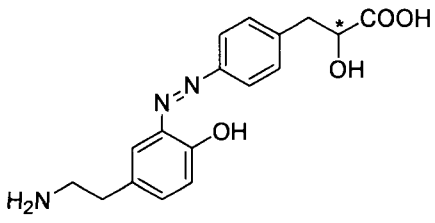	35.6 μM ± 0.1
p-hydroxy-L-PLA[g]	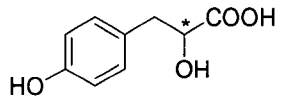	36.2 μM ± 1.4
p-amino-L-PLA[b]	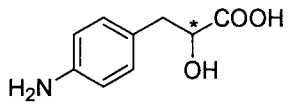	42.2 μM ± 1.6
L-PLA[c]	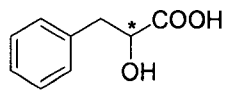	154.3 μM ± 1.2
p-nitro-L-PLA[c]	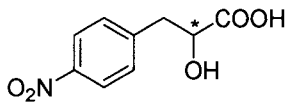	158.5 μM ± 2.1
L-2-hydroxyoctanoic acid[g]	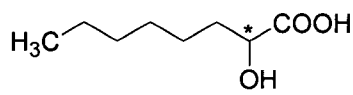	1.4 mM ± 0.1
L-mandelic acid[d]	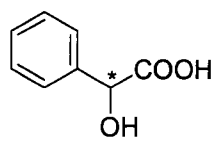	5.1 mM ± 0.1
L-2-hydroxyisocaproic acid[g]	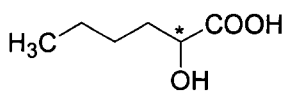	5.6 mM ± 0.2
L-2-hydroxyisovaleric acid[e]	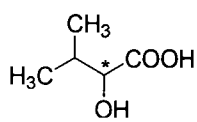	15.3 mM ± 0.3
L-lactic acid[f]	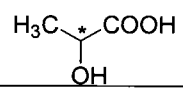	220.2 mM ± 0.4

Values represent means of three independent measurements. 50% inhibition was not reached with the opposite enantiomer using maximum concentrations as follows: a) 1 mM, b) 5 mM, c) 10 mM, d) 50 mM, e) 500 mM, f) 4M, g) not determined.

reactivity." As explained first by Berzofsky and Schechter[185] and later by van Regenmortel,[186] "true cross-reactivity" arises when the same antibody is able to recognize different compounds that are structurally related to the hapten. Typically, the antibody will bind more strongly to the hapten used for producing the antibody and structures resembling this hapten. The similarity of binding exhibited by polyclonal antibodies and monoclonal antibodies, furthermore, suggests that the ability of polyclonal antibodies to bind to a large variety of compounds is also based on "true cross-reactivity."

The "correct" configuration of the hydrogen/carboxyl/hydroxyl triad was also essential for binding of both anti-D-AHA 8E10 and anti-L-AHA 6A3. D-AHAs did not inhibit the binding of anti-L-AHA 6A3 to the solid-phase immobilized antigen, nor did L-AHAs inhibit anti-D-AHA 8E10 in the range of concentrations tested. As described in Chapter III, section Production and Characterization of Polyclonal Antibodies, the correct three-dimensional arrangement of the hydrogen/carboxyl/ hydroxyl triad is equally important for the binding of anti-D-AHA 73 and anti-L-AHA 65 antibodies. Similar observations were made by Hofstetter et al. for the binding of anti-AA antibodies, where the "correct" configuration of the hydrogen/carboxylate/ primary amino triad is essential.

In order to further investigate the specificity of anti-AHA antibodies, their interaction with structurally closely related molecules was examined next. This study included also a comparison with the anti-AA antibodies produced by Hofstetter et al.[59,60]

Comparison of Anti-AA and Anti-AHA Antibodies

AAs and AHAs are structurally related classes of compounds which, as their names indicate, have an amino group or a hydroxyl group, respectively, attached to the alpha carbon. At physiological pH, AAs are zwitter ions comprising a positively charged amino and a negatively charged carboxyl group. Because the hydroxyl group of AHAs is uncharged, AHAs with uncharged side chains have an overall negative charge at physiological pH, which is due to the deprotonated carboxylate group. While the polar hydroxyl group of AHAs can be either a hydrogen bond donor or a hydrogen bond acceptor, the amino group of AAs will act as hydrogen donor at physiological pH. However, reliable prediction of the specificity or cross-reactivity of antibodies raised against AAs and AHAs, respectively, merely based on the structural similarity or specific differences between these compounds, is not possible. Therefore, both noncompetitive and competitive ELISAs were performed to compare the class-specificity of anti-AA and anti-AHA antibodies. Furthermore, competitive ELISAs were performed to evaluate the effect of replacing the carboxyl or hydroxyl groups on the α-carbon using closely related molecules as competitors.

First, anti-AHA antibodies were tested for binding to *p*-azo-D- and -L-Phe-BSA coatings, respectively, as compared to their binding to *p*-azo-D- and -L-PLA-BSA coatings. No significant binding was detected on either "amino acid coating." As previously observed, the anti-AHA antibodies bound only to the "correct"

enantiomer of the *p*-azo-PLA-BSA coating. Figure 26a shows a sample binding curve for anti-L-AHA 65. Comparable results were obtained with anti-D-AHA 73, anti-L-AHA 6A3, and anti-D-AHA 8E10 antibodies. The anti-D-AA 67.36 and anti-L-AA 29.2 antibodies were tested likewise for binding to both the *p*-azo-D- and -L-Phe BSA coatings and the *p*-azo-D- and -L-PLA-BSA coatings. Also here, the antibody only bound to the correct antigen coating with regard to both the correct class and configuration. Thus, anti-D-AA 67.36 bound only to *p*-azo-D-Phe-BSA coating (Figure 26b), whereas anti-L-AA 29.2 bound only to the *p*-azo-L-Phe-BSA coating (not shown).

Competitive ELISAs using free AAs and AHAs as competitors were performed to confirm the class-specificity of these antibodies. Anti-D-AHA 73, anti-L-AHA 65, anti-D-AHA 8E10, anti-L-AHA 6A3, anti-D-AA 67.36, and anti-L-AA 29.2 were each tested in competitive ELISAs using four inhibitors: D- and L-Phe and D- and L-PLA. Each antibody only bound to the competitor of the correct configuration and class. No detectable interaction was seen with any of the other three competitors in the range of concentrations tested. For example, binding of the anti-D-AHA 73 was only inhibited by D-PLA and not by L-Phe, L-PLA, or D-Phe; anti-D-AA 67.36 was only inhibited by D-Phe and not by L-Phe, L-PLA, or D-PLA (Figure 27).

Both noncompetitive and competitive ELISAs confirmed the class-specificity and stereoselectivity of the six antibodies investigated in this study. The anti-D-AHA 8E10 and anti-L-AHA 6A3 antibodies were further investigated to test the importance of functional groups about the stereogenic center, i.e., the hydrogen/carboxyl/hydroxyl

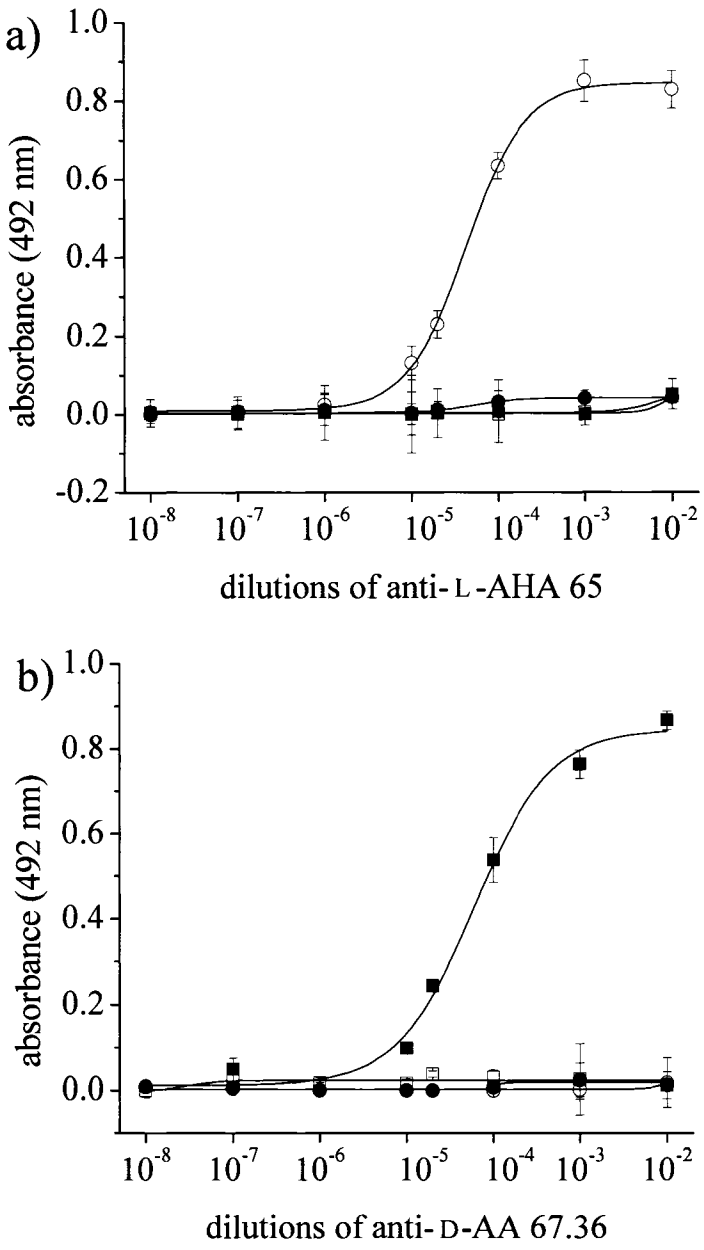

Figure 26: Noncompetitive ELISA results obtained with a) anti-L-AHA 65 and b) anti-D-AA 67.36. *p*-Azo-D-PLA-BSA (●), *p*-azo-L-PLA-BSA (○), *p*-azo-D-Phe-BSA (■), *p*-azo-L-Phe-BSA (□), and BSA were used as solid-phase coatings. At each dilution, the values obtained with the BSA coating were subtracted from those obtained on the other two coatings. Data points represent means of triplicate determinations. Error bars are obscured by symbols.

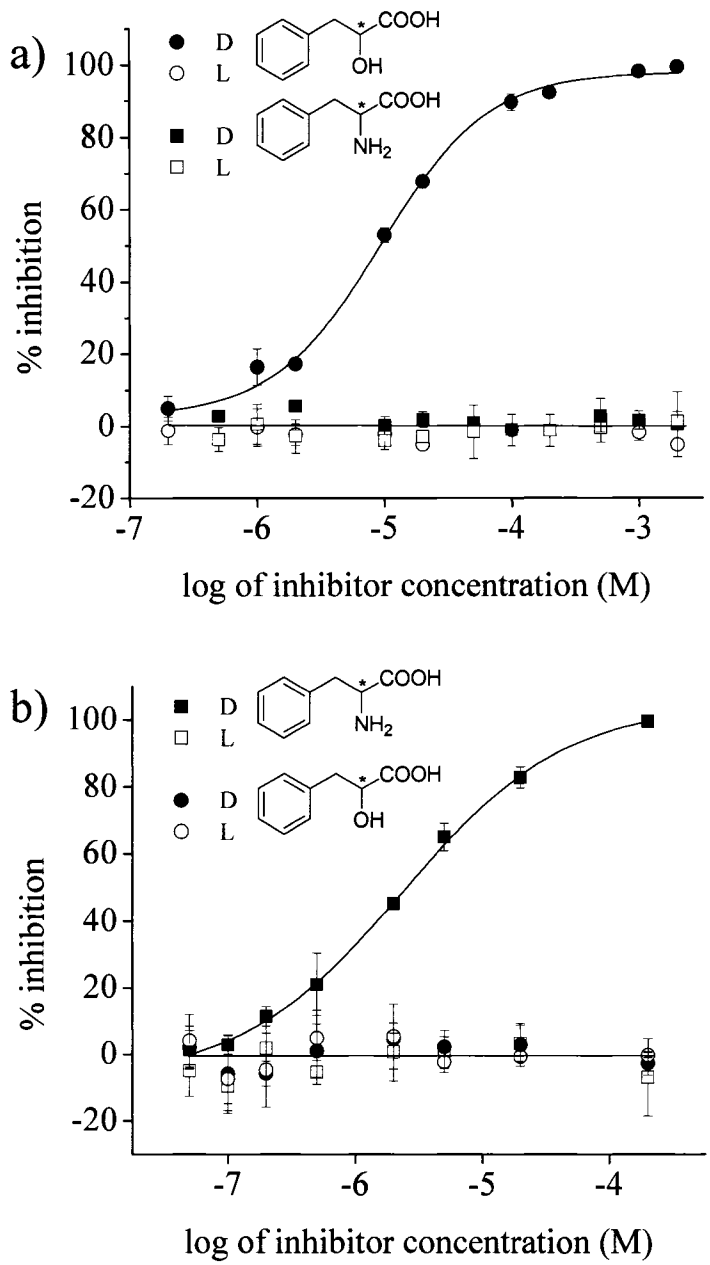

Figure 27: Competitive ELISAs performed with a) anti-D-AHA 73 and b) anti-D-AA 67.36 using PLA and Phe as inhibitors. Open circles (○) represent L-PLA, closed circles (●) represent D-PLA, open squares (□) represent L-Phe, and closed squares (■) represent D-Phe. Error bars indicate standard deviations of triplicate determinations. Missing error bars are obscured by symbols.

triad, for binding. Phenylpropionic acid and phenyllactic acid methyl ester were each used as competitors in further competitive ELISAs. While phenylpropionic acid, the dehydroxylated analog of PLA, is achiral, phenyllactic acid methyl ester, in which the carboxyl group of PLA is substituted by a methyl ester, is chiral. Both phenylpropionic acid and phenyllactic acid methyl ester lack the hydrogen/carboxyl/ hydroxyl triad of AHAs. Neither compound inhibited the binding of anti-D-AHA 8E10 to the *p*-azo-D-PLA-BSA coating or of anti-L-AHA 6A3 to the *p*-azo-L-PLA-BSA coating (Figure 28).

Historically, medicinal chemists have believed that the structural similarity of molecules would correlate with similar biological activities. Replacement of atoms or groups of atoms with closely related atoms or groups, therefore, has widely been used to modify the biological activity of potential enzyme inhibitors, receptor agonists, antagonists, and other biologically active molecules. Such "bioisosteric replacement" can indeed be an effective route to optimize so-called lead structures into therapeutically useful drugs and therapies.[187] Several parameters must be considered in the selection and modification of molecules.[187] In order to attain the needed biological activity, a given ligand must fit in the binding site of the corresponding biological macromolecule. The hydrophobic or polar surface areas within the binding site should likewise match. While exchange of one hydrogen bond donor for another, or of one hydrogen bond acceptor for another, may not significantly affect activity, exchange of a hydrogen bond donor for an acceptor or vice versa will most likely affect binding by several orders of magnitude. Although such considerations may

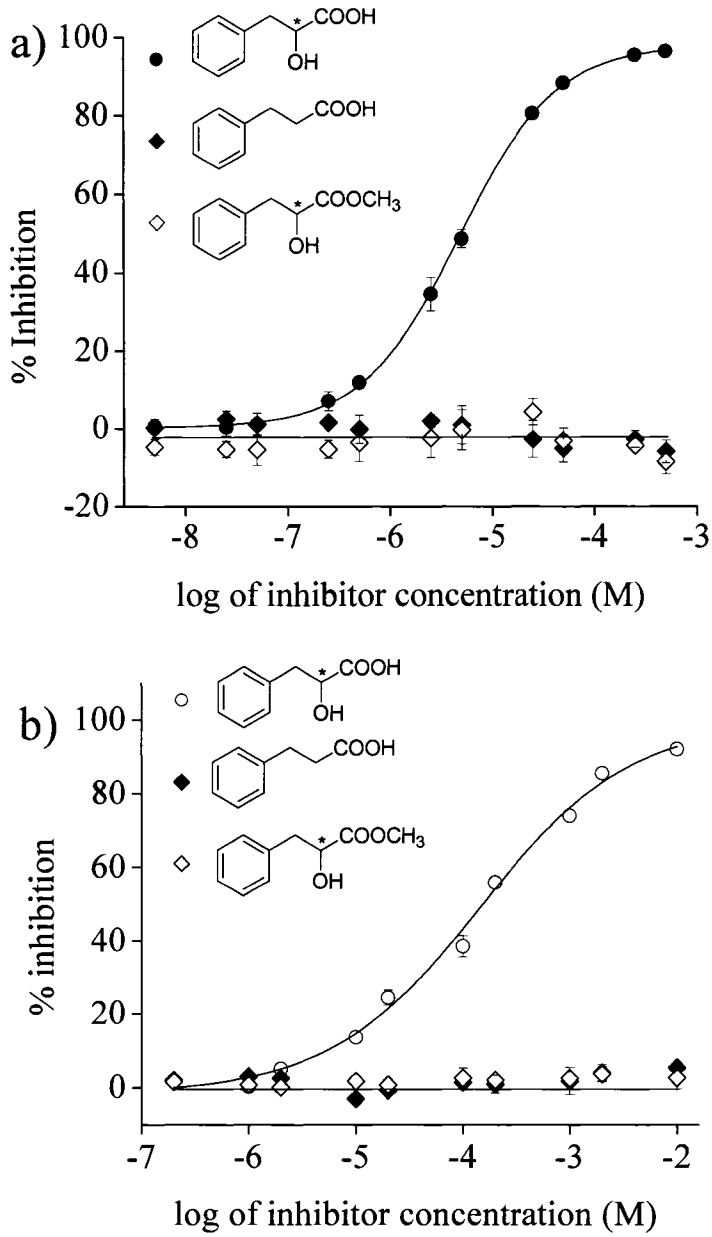

Figure 28: Competitive ELISAs performed with a) anti-D-AHA 8E10 and b) anti-L-AHA 6A3 using L-PLA (○), D-PLA (●), phenylpropionic acid (◆), and phenyllactic acid methyl ester (◇) as inhibitors. D-Phenyllactic acid methyl ester was used in a) and the L-enantiomer was used in b). Error bars indicate standard deviations of triplicate determinations. Missing error bars are obscured by symbols.

provide reasonable guidelines for bioisosteric replacements, several structure-function relationship studies showed that chemically similar molecules can have significantly different biological activities.[188-190] Hence, bioisosteric replacement of atoms or groups may result in decreased, increased, or unchanged biological activity.[187,190]

Arrhenius first described the binding of antibodies in chemical terms using mathematical descriptions from physical chemistry in the early 1900s.[191] However, chemical descriptions of antibody-antigen binding were limited because little was known about the structure of antigens. Landsteiner circumvented this problem by using anti-hapten antibodies to systematically study the effect of both an antigen's structure and its specific functional groups on antibody binding. Landsteiner studied the binding of anti-hapten antibodies to both the hapten and other closely related molecules using immunoprecipitation reactions.[51] Hapten analogs with modified stereochemistry and/or functional groups were used, first by Landsteiner and later by others, to identify structural features important for the binding of such antibodies. For example, one study by Pressman and Siegel of an anti-*p*-(*p*'-azophenylazo)-benzenearsonate antibody showed little difference between binding to *p*-(*p*'-aminophenylazo)-benzenearsonate and to *p*-(*p*'-hydroxyphenylazo)-benzenearsonate.[192] *p*-Amino-benzenearsonate and *p*-hydroxy-benzenearsonate both bound more weakly to the same anti-*p*-(*p*'-azophenylazo)-benzenearsonate antibody but with nearly the same binding affinity as each other.[192] No other studies comparing the effect of amino and hydroxyl functional groups of haptens on the binding of anti-

hapten antibodies have been found by the author. However, it should be noted that the amino and hydroxyl groups in Pressman and Siegel's studies were unlikely to interact in any significant way directly with antibody, as they were positioned away from the antibody binding site. The effect of substituting an amino group for a hydroxyl group or vice versa in inhibitors, antibiotics, and other ligands on their biological activity, though, has been investigated in a number of studies.

Functional groups in antibiotics are frequently modified in order to optimize their selectivity and to combat antibiotic resistance. Several aminoglycoside antibiotics have been studied, in which one or more hydroxyl groups were converted to an amine. Both the location and number of amino groups were found to possibly affect antibiotic activity in prokaryotes.[193,194] The 2',6'-diamino-substituted aminoglycoside antibiotics, for example, were the most potent inhibitors of protein synthesis. The 6'-amino-substituted antibiotics were still more effective than the 2'-amino-substituted ones, and the unsubstituted antibiotics were the least effective. Conversely, other studies using eukaryotic systems found that aminoglycosides with a hydroxyl group at the 6' position were more potent inhibitors.[195,196] Anthracycline antibiotics such as daunomycin, doxorubicin, and rebeccamycin derivatives which contain a 3'-amino group instead of a 3'-hydroxyl group or, for rebeccamycin, a 2'-amino group in place of a 2'-hydroxyl group bind more strongly to DNA.[197,198] No change in activity, however, was seen for cytotoxic and topoisomerase II activity with amino-substituted daunomycin and doxorubicin.[199] Amino-substituted rebeccamycin, likewise, does not affect the activity of topoisomerase I.[198]

Other important targets for chemical modification include inhibitors, hormones, and substrates. Kati et al., e.g., studied the binding of α- and β-amino acids and their analogous hydroxy acids for their ability to inhibit influenza virus neuraminidase. They found that 3-chloro-2-hydroxy-5-(*t*-butyl)-phenylgycine binds 360 times more strongly than its hydroxy acid analog.[200] 4-Hydroxy-1-(ethyl-isopropyl-carbamoyl)-3-hydroxy-pyrrolidine-3-carboxylic acid has a 2,600-fold weaker binding affinity than its β-amino analog.[200] Two hydroxyl groups of DANA (2,3-didehydro-2-deoxy-*N*-acetylneuraminic acid), another inhibitor of influenza virus neuraminidase, were converted to amino groups. A 100-fold increase in inhibition was seen for 4-amino-DANA while a 100-fold decrease was seen for 9-amino-DANA. 4,9-Diamino-DANA was only a slightly weaker inhibitor compared to DANA.[201] While 1-hydroxy-1,1-bisphosphonates and 1-amino-1,1-bisphosphonates both coordinate magnesium ions, the 1-amino derivatives were found to be better inhibitors of *Trypanosoma cruzi* targeting farnesyl pyrophosphate synthase than the 1-hydroxy-1,1-bisphosphonates.[202] Conversion of the primary amino group of the hormone oxytocin to a hydroxyl group resulted in a decrease of binding affinity to its receptor neurophysin.[203] However, the hydroxyl-substituted analog of oxytocin still had twice the activity of the corresponding deamino analog.[203] Glucose-6-phosphate and glucosamine-6-phosphate both bind to glucosamine-6-phosphate synthase. The 2'-hydroxyl group of glucose-6-phosphate and the 2'-amino group of glucosamine-6-phosphate each interact with the same amino acid residues of the enzyme according to the crystal structure.[204] Both phenyllactyl-tRNA^{Phe} and Phe-tRNA^{Phe} bind to the A site

of ribosomes in the same manner as determined by X-ray crystallography.[205] The ribosome still catalyzes the nulceophilic attack of either the amino or the hydroxyl group on the ester carbon of the P-site peptidyl-tRNA via the same mechanism, even though the catalytic rate is slower for the phenyllactyl-tRNA^{Phe}.[205]

Clearly, hydroxyl and amino groups are not universally interchangeable. Substitution of an amino group for a hydroxyl group or vice versa can have drastic effects on interactions of ligands with biological macromolecules, although some of the examples listed above also show that many interactions may remain largely unchanged, resulting in only small differences in affinity or activity. Thus, the effect of a substitution on a ligand is difficult to predict and multiple parameters may need to be studied to determine the full effect of a substitution. Continued progress in modeling and structural analysis coupled with binding assays promise to facilitate predictions in the future. For certain applications, however, understanding the effects of a substitution may be of less importance than knowing the nature and extent of the effect itself. Since the substitution of a hydroxyl group for an amino group resulted in a complete loss of all detectable binding of anti-AHA antibodies to AAs, the presence of AAs such as Phe had no effect on the binding of anti-AHA antibodies to AHAs such as PLA. Likewise, the presence of AHAs such as PLA had no effect on the binding of anti-AA antibodies to AAs. Therefore, the remarkable stereoselectivity and class-specificity of both the anti-AA and anti-AHA antibodies make their use for the simultaneous detection of AAs and AHAs appealing.

Fluorescence Immunoassays

The goal of this part of the dissertation was the development and optimization of immunoassays for the simultaneous detection of AA and AHA enantiomers using anti-AA and anti-AHA antibodies labeled with distinct fluorophores. Fluorophore-labeled antibodies were first used in 1941 by Coons et al. for the detection of *pneumococcus* in mammalian tissue using fluorescence microscopy.[206,207] Despite such early use in histology, fluorescence immunoassays weren't introduced until 20 years later when quantitative techniques and more fluorogenic compounds became available.[208] Fluorophore-labeled antibodies are now used in, e.g., pathology, histology, virology, microbiology, flow cytometry, and immunoassays. While a wide range of materials and compounds, including proteins (e.g., green fluorescent protein), minerals, lanthanides, and numerous organic compounds, may exhibit fluorescence properties, fluorescent organic compounds are most commonly used as labels in immunofluorescence. However, chelated lanthanides and fluorescent proteins have also been used successfully. Cost, quantum efficiency, hydrophobicity/hydrophilicity, stability, and suitability for the desired application should be considered in the selection of fluorophores. The DyLight™ fluorophores used in this study are well suited for applications such as immunoassays since they are more photostable, brighter, and less pH-sensitive than, e.g., fluorescein and rhodamine, which have historically been used in many biological and bioanalytical applications.

Two basic strategies have been employed in immunoassays for the detection of multiple analytes.[209,210] In one strategy, either an antigen or a capture antibody for each analyte is immobilized onto distinct solid supports.[210] Color-coded or fluorescent beads, microparticles of varying sizes, and even threads have been used as solid supports.[210] Spatial resolution of analytes can also be achieved using discrete spots on a single solid phase.[211] Alternatively, antibodies may be labeled with distinct tags for each analyte to be tested.[210] In order to develop fluorescence immunoassays for simultaneous detection of multiple analytes, the antibodies used in a given multianalyte immunoassay must be sufficiently specific for the desired application. Furthermore, fluorophores with sufficiently distinct emission spectra should be used for independent detection of multiple differently labeled antibodies within a mixture using appropriate filters. The DyLight™ fluorophores used in this study have unique emission ranges that can be measured independently. The specificity of the anti-AA and anti-AHA antibodies used in this dissertation has already been described in Chapter III, section Comparison of Antibody Binding. However, further studies were conducted to confirm that no change in antibody binding is seen when combinations of antibodies, antigen coatings and analytes are used together in the same sample.

Initial tests were performed by modifying previously established ELISA procedures. Noncompetitive ELISAs were conducted using mixtures of antigen coatings. In the previously established ELISAs, antigens were coated on the plate individually at concentrations of 1 μg/mL. For the modified ELISAs, microtiter plates were coated with mixtures of antigens in which each antigen was at a concentration of

1 μg/mL (not shown). Binding curves obtained on mixed coatings did not differ significantly from those obtained on individual coatings.

Competitive tests of anti-D-AHA 73 with D-PLA as competitor were carried out in the presence of the analogous AA, D-Phe, and anti-D-AA 67.36 antibody. The D-Phe was added to the mixture of primary antibodies and competitor so that its effective concentration was 10 mM. The anti-D-AA 67.36 was added to the same solution. Both antibodies were applied at constant concentrations. The appropriate effective concentrations were determined in noncompetitive ELISAs to result in absorbance readings of at least 0.8. HRP-labeled goat anti-rabbit $F(ab')_2$ secondary antibody was used to selectively detect anti-D-AHA 73 bound to the plate. Comparison of the inhibition curve and relative affinity with previous competitive ELISA results of anti-D-AHA 73 with D-PLA showed no significant difference (Figure 29). The presence of the other antibody and the D-Phe had no discernable effect on the interaction of anti-D-AHA 73 with D-PLA. A second set of competitive ELISAs using a mixture of anti-D-AHA 73 and anti-D-AA 67.36 were carried out using varying concentrations of D-Phe and a 10 mM effective concentration of D-PLA. Bound anti-D-AA 67.36 was selectively detected using HRP-labeled goat anti-mouse $F(ab')_2$ secondary antibody. Once again, the presence of the other antibody and competitor had no significant effect on the interaction of anti-D-AA 67.36 with D-Phe (Figure 29).

Thus, ELISAs were successfully used to establish that the binding of anti-D-AA 67.36 to D-Phe and of anti-D-AHA 73 to D-PLA were unaffected by the presence

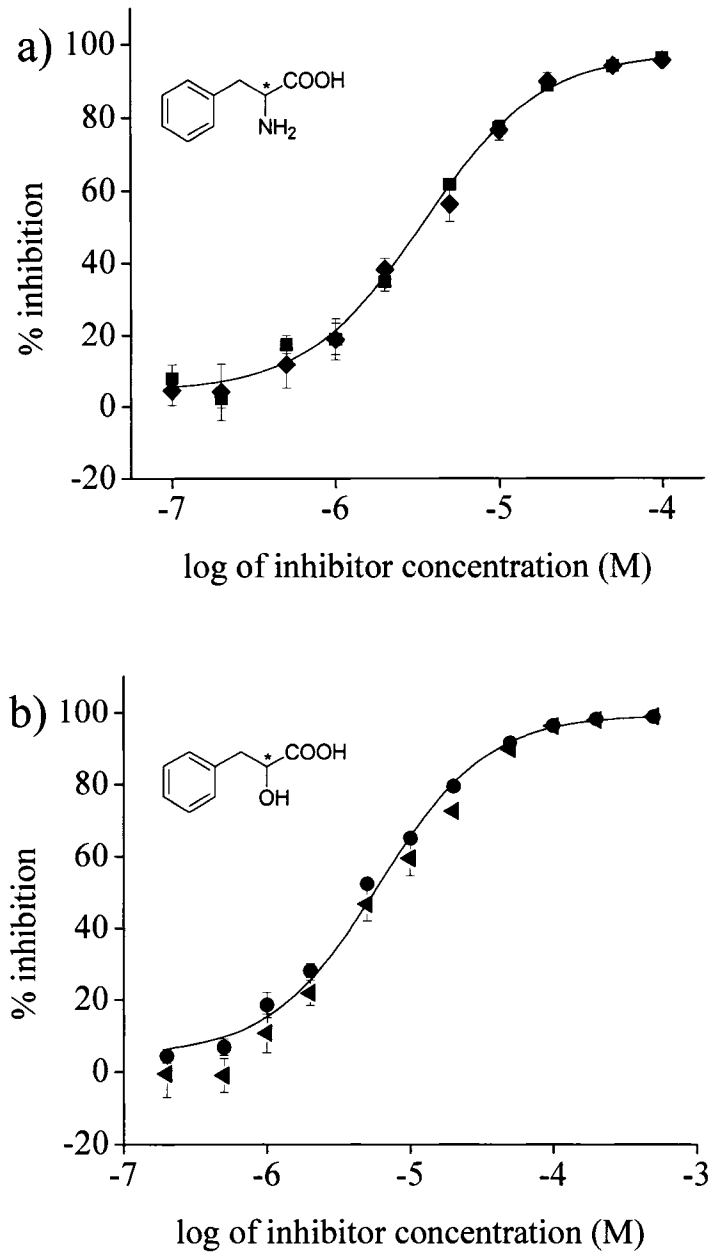

Figure 29: Competitive ELISAs with a) anti-D-AA 67.36 were carried out using varying concentrations of D-Phe in PBS (■) and D-Phe in the presence of 10 mM PLA and the anti-D-AHA 73 antibody (◆) as competitors. For competitive ELISAs with b) anti-D-AHA 73, D-PLA in PBS (●) and D-PLA in 10 mM D-Phe containing anti-D-AA 67.36 (◀) were used as competitors. Error bars indicate standard deviations of triplicate determinations. Missing error bars are obscured by symbols.

of the other antibody and competitor. However, even though the HRP-labeled secondary antibodies selectively bind to either mouse or rabbit antibodies, both secondary antibodies catalyze the production of the same colored product, making simultaneous detection impossible. In the second step of fluorescence immunoassay development, therefore, the two primary antibodies were detected simultaneously with two different fluorescently labeled secondary antibodies. Noncompetitive binding curves for both anti-D-AHA 73 and anti-D-AA 67.36 in fluorescence immunoassays did not differ substantially from those obtained in ELISAs (not shown). In the next step, in a fluorescence immunoassay, anti-D-AA 67.36 and anti-D-AHA 73 were applied in a mixture containing both antibodies at the same concentration used previously in competitive ELISAs. A mixture of both D-Phe and D-PLA at appropriate concentrations was applied as competitors. Intensity values obtained for negative controls were routinely subtracted before calculating percent inhibition values. The simultaneous competitive fluorescence immunoassay of anti-D-AA 67.36 and anti-D-AHA 73 was compared to competitive ELISAs and to competitive fluorescence immunoassays of each antibody independently measured with D-Phe and D-PLA, respectively (Figure 30). No significant difference in either inhibition curves or IC_{50} values was seen across the three formats for either antibody.

Immunoassays using fluorescently labeled secondary antibodies still limited the number of antibody/analyte pairs to a practical maximum of two. This limitation was surmounted by fluorescently labeling four primary antibodies with four distinct

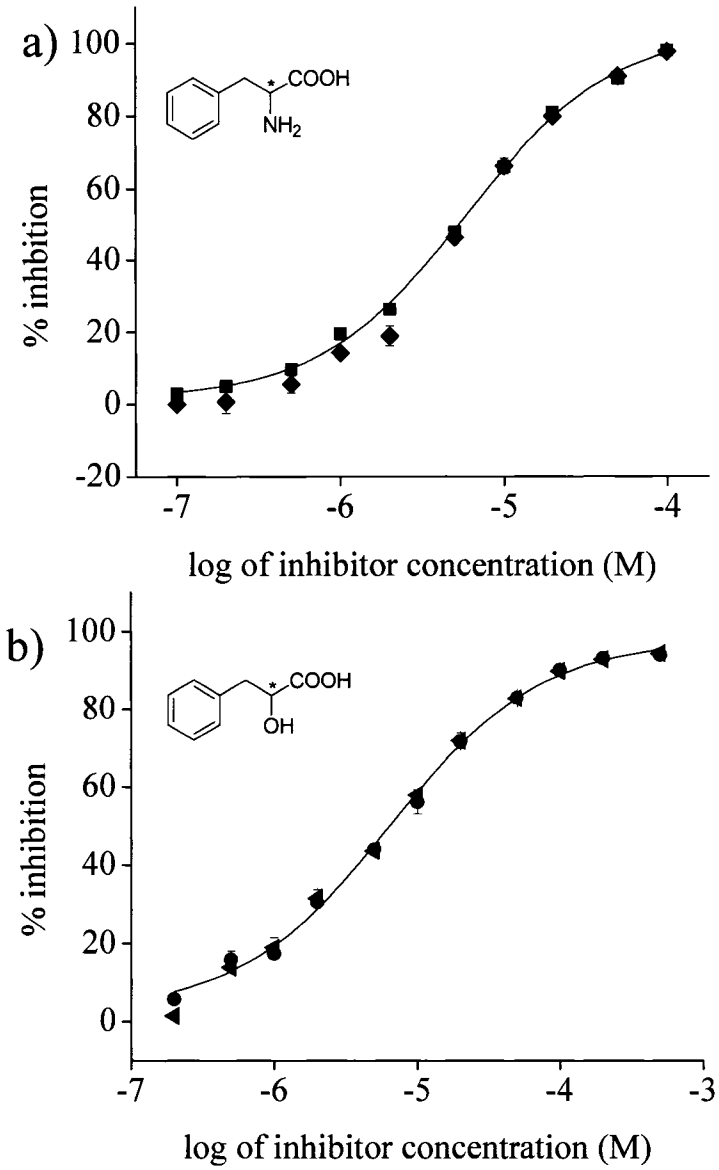

Figure 30: Competitive dual immunoassay performed with anti-D-AHA 73 and anti-D-AA 67.36 with both D-Phe and D-PLA as competitors. Two secondary antibodies labeled with distinct fluorophores were used to detect anti-D-AA 67.36 and anti-D-AHA 73. Measurement at a) 647 nm was used to detect the inhibition of anti-D-AA 67.36 by D-Phe (■). Measurement at b) 547 nm was used to detect the inhibition of anti-D-AHA 73 by D-PLA (●). Single analyte/antibody fluorescence immunoassays gave similar results (◆ and◀, respectively). Error bars indicate standard deviations of triplicate determinations. Missing error bars are obscured by symbols.

fluorophores. The four antibodies were selected and labeled as described in Chapter II, section Fluorescence Immunoassay. The ratio of fluorophore labels conjugated to each of the antibodies were calculated as described in Chapter II, section Fluorescence Immunoassay, and are presented in Table 10.

Table 10: Fluorophore-to-antibody ratios of DyLight™ conjugated antibodies

Fluorophore-antibody conjugate	number of fluorophores per antibody
anti-D-AHA 8E10 DyLight™ 547 conjugated	6
anti-L-AHA 65 DyLight™ 800 conjugated	11
anti-D-AA polyclonal antibody DyLight™ 647 conjugated	4
anti-L-AA 18.3 DyLight™ 490 conjugated	8

Noncompetitive fluorescence immunoassays were first conducted to confirm that the antibodies still selectively bound to only the correct coating after conjugation to their respective fluorophores. Microtiter plates were divided into five sections; each section was coated with one of five antigens: *p*-azo-D-PLA-BSA, *p*-azo-L-PLA-BSA, *p*-azo-D-Phe-BSA, *p*-azo-L-Phe-BSA, or BSA. All four antibodies were tested for binding to all five coatings; results are presented in Figure 31 and Figure 32. The DyLight™ 647-labeled anti-D-AA polyclonal antibody only bound to the *p*-azo-D-

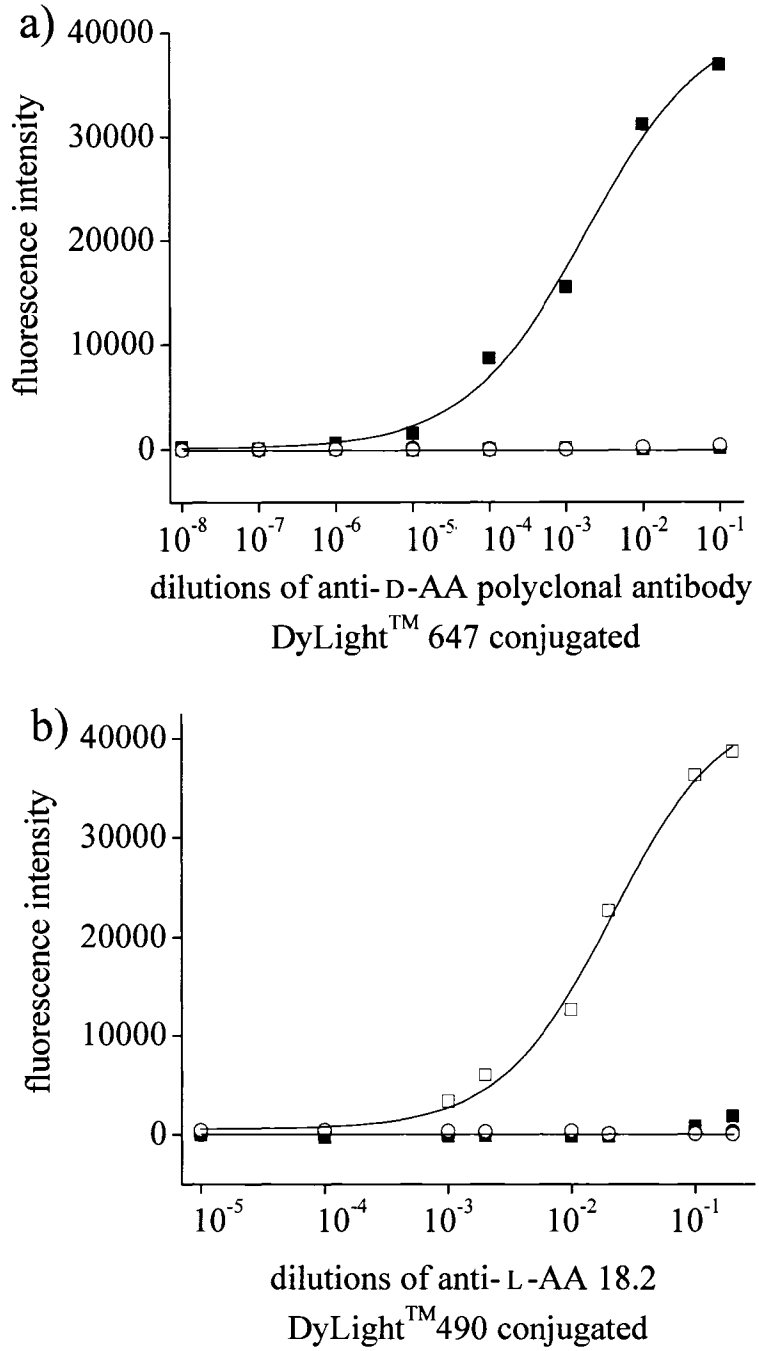

Figure 31: Noncompetitive fluorescence immunoassay results for a) anti-D-AA polyclonal antibody DyLight™ 647 conjugated (stock 0.5 mg/mL) and b) anti-L-AA 18.3 DyLight™ 490 conjugated (stock 1 mg/mL). *p*-Azo-D-Phe-BSA (■), *p*-azo-L-Phe-BSA (□), *p*-azo-D-PLA-BSA (●), *p*-azo-L-PLA-BSA (○), and BSA were used as solid-phase coatings. At each dilution, the values obtained with the BSA coating were subtracted from those obtained on the other two coatings.

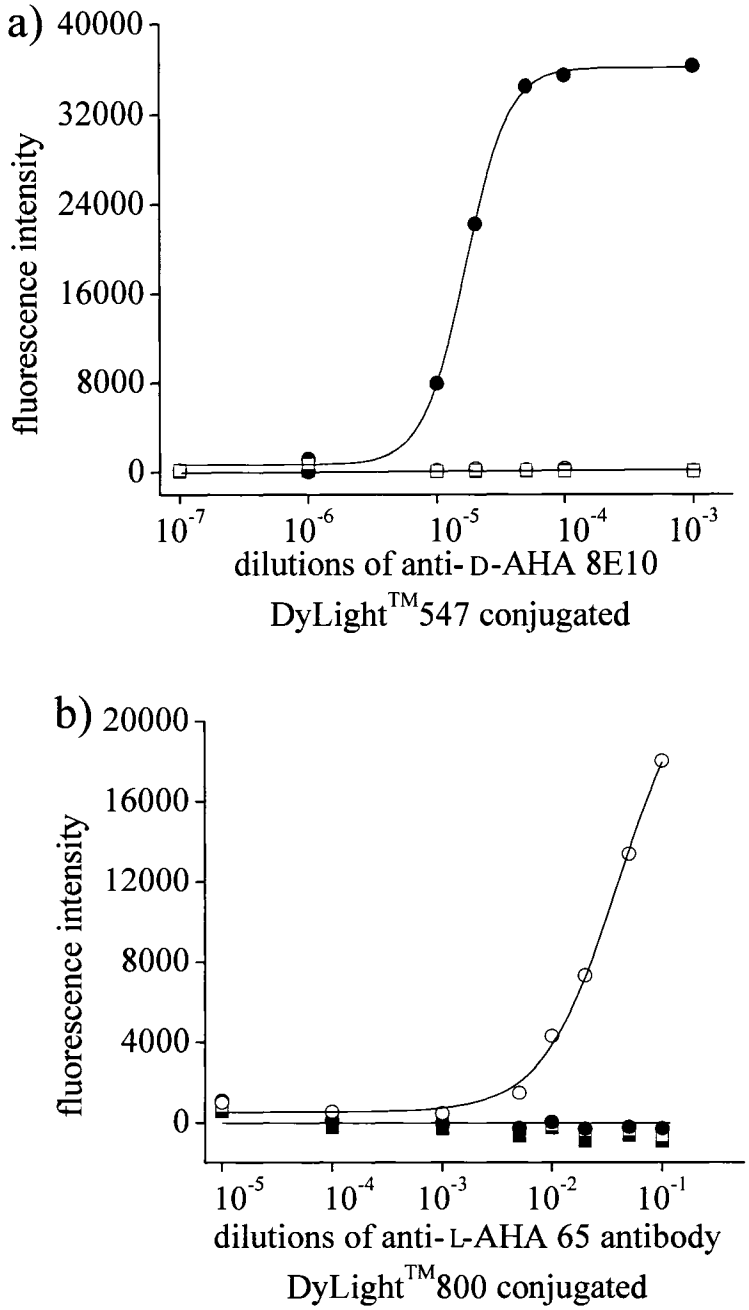

Figure 32: Noncompetitive fluorescence immunoassay results for a) anti-D-AHA 8E10 DyLight™ 547 conjugated (stock 0.5 mg/mL) and b) anti-L-AHA 65 DyLight™ 800 conjugated (stock 1 mg/mL). *p*-Azo-D-PLA-BSA (●), *p*-azo-L-PLA-BSA (○) *p*-azo-D-Phe-BSA (■), *p*-azo-L-Phe-BSA (□), and BSA were used as solid-phase coatings. At each dilution, the values obtained with the BSA coating were subtracted from those obtained on the other two coatings.

Phe-BSA coating (Figure 31a). The DyLight™ 490 -labeled anti-L-AA 18.3 bound only to the *p*-azo-L-Phe-BSA coating (Figure 31b). The anti-AHA antibodies, likewise, bound only to the "correct" coatings. The DyLight™ 547-labeled anti-D-AHA 8E10 bound only to the *p*-azo-D-PLA-BSA (Figure 32a), and the DyLight™ 800-labeled anti-L-AHA 65 bound only to the *p*-azo-L-PLA-BSA coating (Figure 32b). None of the four antibodies showed any significant binding to the BSA coating.

Competitive tests were also used to confirm that the four antibodies retained their stereoselective/class-specific binding properties after conjugation. Four so-called "single" competitive immunoassays were performed—one test for each of the four conjugated primary antibodies with its corresponding competitor having the correct structure and configuration (Figure 33 and Figure 34). For example, in the fluorescence immunoassay with DyLight™ 547-labeled anti-D-AHA 8E10, D-PLA was used as the competitor. Competitive fluorescence immunoassays were then repeated using the same four combinations of antibody/competitor in the presence of a second competitor, namely the opposite enantiomer at a constant effective concentration of 10 mM (Figure 33 and Figure 34). For example, mixtures of L-PLA at varying concentrations and D-PLA at a fixed concentration of 10 mM were used as competitors with the DyLight™ 800-labeled anti-L-AHA 65 antibody; similarly, a mixture of 10 mM L-Phe and varying concentrations of D-Phe were used as competitors with the DyLight™ 647-labeled anti-D-AA polyclonal antibody. In the final setup, referred to as the "quadruple test," competitive assays were carried out on a mixed coating containing *p*-azo-D-PLA-BSA, *p*-azo-L-PLA-BSA, *p*-azo-D-Phe-

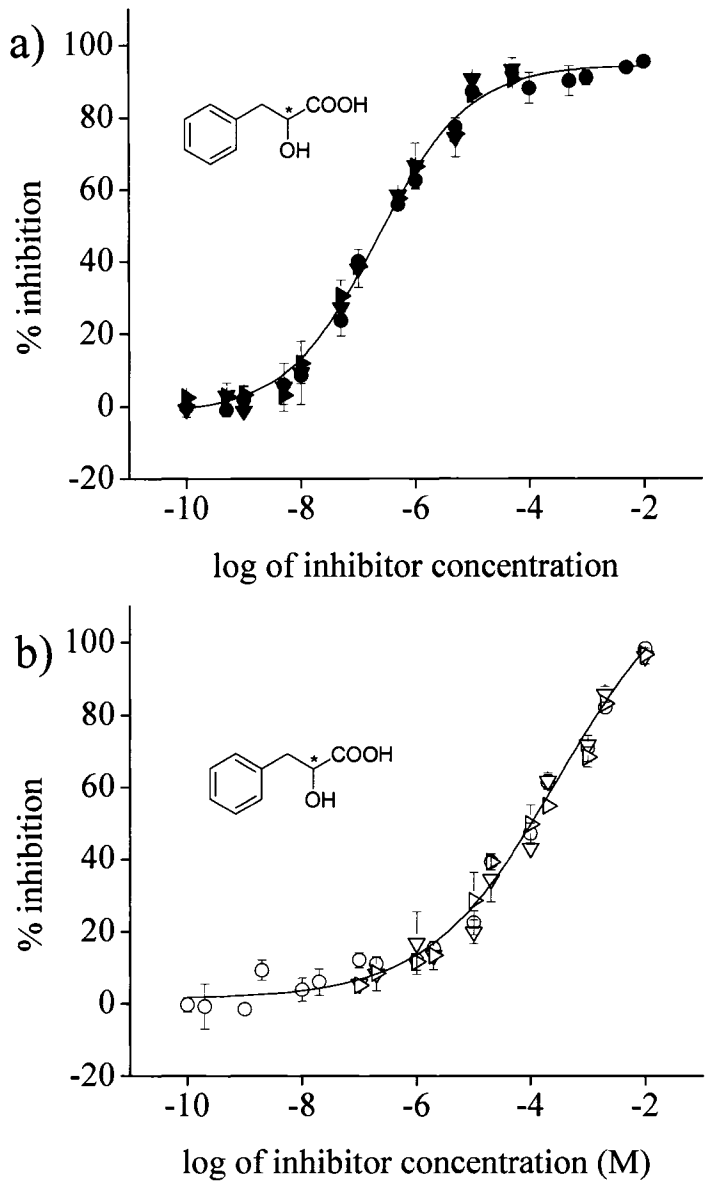

Figure 33: A quadruple competitive fluorescence immunoassay was used to simultaneously detect D- and L-PLA and D- and L-Phe using four distinctly labeled antibodies. Measurement at a) 547 nm was used to detect the inhibition of DyLight™ 547-labeled anti-D-AHA 8E10 by D-PLA while measurement at b) 774 nm was used to detect the inhibition of DyLight™ 800-labeled anti-L-AHA 65 by L-PLA. Consistent results were obtained for quadruple (●,○) and single (▼,▽) assays and for single assays in which the "opposite" enantiomer was added at a constant concentration of 10 mM (▶,▷). Closed symbols represent D-PLA and open symbols represent L-PLA. Error bars indicate standard deviations of triplicate determinations. Missing error bars are obscured by symbols.

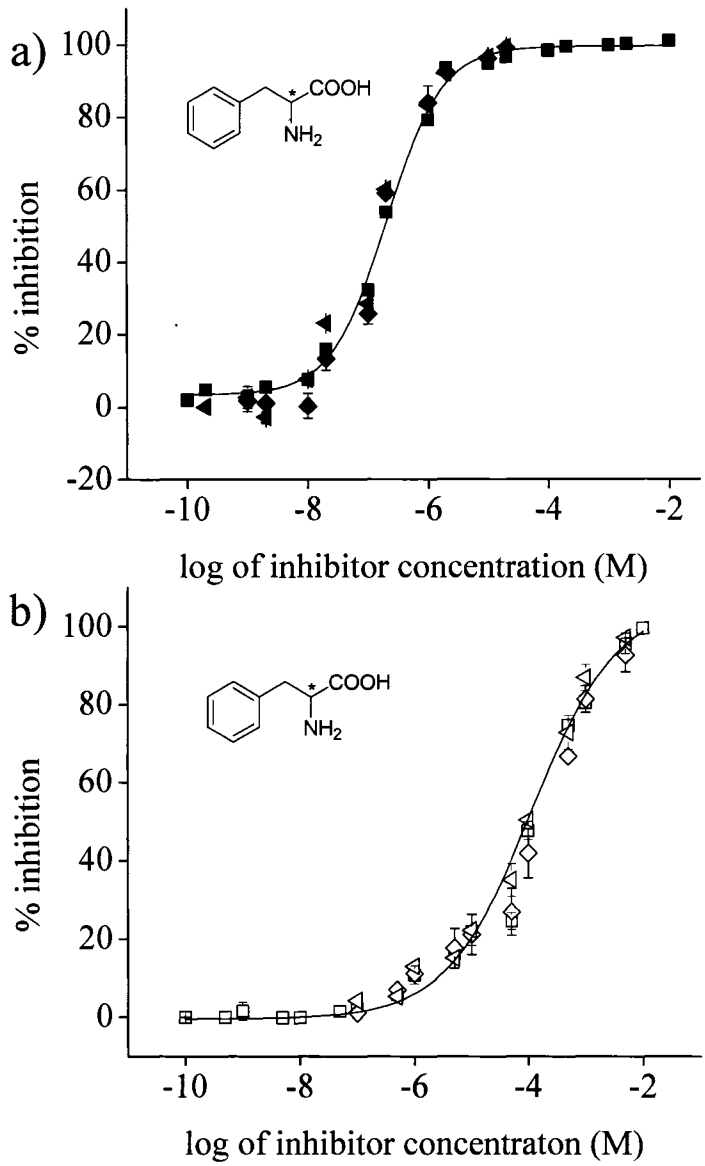

Figure 34: A quadruple competitive fluorescence immunoassay was used to simultaneously detect D- and L-Phe and D- and L-PLA using four distinctly labeled antibodies. Measurement at a) 647 nm was used to detect the inhibition of DyLight™ 647-labeled anti-D-AA polyclonal antibody by D-Phe while measurement at b) 494 nm was used to detect the inhibition of DyLight™ 490-labeled anti-L-AA 18.3 by L-Phe. Consistent results were obtained for quadruple (■,□) and single (◆,◇) assays and for single assays in which the "opposite" enantiomer was added at a constant concentration of 10 mM (◀,◁). Closed symbols represent D-Phe and open symbols represent L-Phe. Error bars indicate standard deviations of triplicate determinations. Missing error bars are obscured by symbols.

BSA, and *p*-azo-L-Phe-BSA. All four conjugated antibodies, each at a constant concentration, were applied as a mixture, and the four competitors, D- and L-PLA and D- and L-Phe, were all applied at appropriate concentrations (Figure 33 and Figure 34). For each of the four antibodies, inhibition curves were consistent among all fluorescence immunoassays conducted, yielding the same relative affinities for their corresponding binding partners. Results were, furthermore, consistent with results obtained with antibodies prior to conjugation with fluorophores.

The multianalyte fluorescence immunoassays developed in this study demonstrate the simultaneous, stereoselective, class-specific detection of four structurally closely related analytes. The exquisite selectivity of the antibodies used in these assays provides the basis for simultaneous analyte detection and high-throughput assay and array applications. Multianalyte immunoassays can simplify and expedite the analysis of complex samples and analytes typically tested in groups, thereby potentially reducing overall costs of testing.[210,212] Thus, they are ideally suited for point-of-care use in medicine and for field applications (e.g., environmental monitoring).[213] Despite the exciting potential of multianalyte immunoassays and the importance of chiral compounds (which has been discussed in Chapter I), the author has been unable to find any other multianalyte immunoassays for the detection of chiral analytes. This study for the first time demonstrates the immense potential of stereoselective antibodies for the sensitive simultaneous detection of structurally closely related chiral molecules within the same sample.

Multianalyte assays for achiral applications date back to the late 1980s. Ekins et al. developed assays based on lanthanide chelate fluorophore labels, which are now known as DELFIA, for dissociation-enhanced lanthanide fluoroimmunoassay.[212,214,215] Because four different lanthanide chelate labels are available, each with distinct emission spectra, DELFIA can be used for the simultaneous detection of four analytes.[216,217] Examples of dual-analyte detection assays have been reported using combinations of β-galactosidase with phosphodiesterase or alkaline phosphatase or of alkaline phosphatase with horseradish peroxidase as detection labels.[210] Another simultaneous detection format was the dual-label RIA conducted using ^{125}I and ^{57}Co or ^{125}I and ^{131}I tags, which can be differentiated by some gamma scintillation counters.[210] Dual-labeled simultaneous detection has been also performed using metal labels[218] and a combination of enzyme/radioisotope labels.[219]

Chiral Immunoaffinity Chromatography

In order to demonstrate that the stereoselective anti-AHA antibodies produced in this study are not only suitable for enantiomer detection but also enantiomer separation, anti-D-AHA 73 was applied as a chiral selector for the separation of PLA enantiomers in chiral immunoaffinity chromatography. Chiral immunoaffinity chromatography applies the principles of traditional affinity chromatography (which were described in Chapter III, section Production and Characterization of Polyclonal

Antibodies) to the purification of chiral target molecules using antibodies immobilized on a suitable solid phase. For example, in the first application of immunoaffinity chromatography to enantiomer separation, polyclonal antibodies raised against (*R*)-abscisic acid were immobilized on agarose and used to separate racemic abscisic acid. After the (*S*)-enantiomer was eluted, acetone was used to disrupt the interaction between the (*R*)-enantiomer and the immobilized antibody, thereby eluting the (*R*)-enantiomer.[220] Since then, a limited number of both polyclonal and monoclonal antibodies have been used for the extraction and separation of enantiomers.[35]

As with other affinity systems, conditions required to elute the bound ligand are generally harsh, which may lead to protein denaturation and, therefore, short column lifetimes. Weak affinity chromatography (WAC) overcomes these limitations. Because many biologically important processes involve weak, reversible interactions, WAC is frequently an ideal choice for the characterization of biological events in weak affinity systems, including the analysis and isolation of molecules taking part in the binding process. Such weak interactions are important in, e.g., virus-cell interactions,[221] protein-peptide interactions,[222] cell adhesion, and cell-cell interactions.[223-225] While traditional affinity chromatography involves an on/off binding process, WAC exploits weak interactions which are more readily reversible. Instead of altering mobile phase conditions to elute an immobilized ligand, isocratic conditions can be used in WAC to elute the retained binding partner in a "true chromatographic process."

Allenmark, in the early 1980s, for the first time showed the application of weak affinity systems for the separation of enantiomers under isocratic conditions using BSA as chiral selector.[226] Later, Zopf and Ohlson used monoclonal antibodies with weak affinities to an oligosaccharide in, what they termed, WAC.[227] Several chiral selectors exploit weak interactions for the separation of enantiomers; this includes cyclodextrins,[228] brush-type CSPs,[229] protein CSPs,[230,231] and even some MIPs.[232,233]

Hofstetter et al. were the first to demonstrate WAC using antibody-based CSPs.[63] They used both POROS, a polymeric high-flow-through-type support,[63,64] and silica[66,69,70] as solid supports for separation of AA enantiomers. AAs of the correct configuration bound reversibly to the antibody and were retained on the CSP, while analytes that do not interact with the antibody eluted with the void volume. Because the bound enantiomer eluted using mild isocratic conditions, the columns could be used for hundreds or even thousands of separations.[64,66] Such stable columns, which were even used typically at room temperature, are practical for routine separations of enantiomers. Various chromatographic parameters such as temperature and flow rate were shown to affect the binding strength between analyte and immobilized antibody.[64] Additionally, Hofstetter et al. were able to show that miniaturization can reduce consumption of both stationary phase material and antibody by using microbore columns.[66,69] The use of such miniaturized systems also allowed interfacing columns with mass spectrometers for detection.[66] Recently, Gübitz et al. studied the separation of enantiomers of the thyroid hormone T_3.[234]

Separations were achieved by using stereoselective antibody against L-T_3 as chiral selector in micro-HPLC. The enantiomers were separated under mild continuous isocratic elution conditions using 10 mM phosphate buffer, pH 7.4. The unretained D-enantiomer eluted with the void volume, whereas the L-enantiomer was retained by the antibody phase and eluted later.

In this study, the anti-D-AHA 73 was immobilized on silica, which had been packed in a 200 mm x 0.75 mm i.d. PEEK column as described in Chapter II, section Chiral Immunoaffinity Chromatography. A nonracemic mixture of PLA was separated under isocratic conditions at room temperature using PBS as mobile phase. The two enantiomers of PLA were separated with a resolution of 1.44 (Figure 35). Considerable peak tailing was observed on this column for the more retained enantiomer. Such peak tailing, typically observed even at low concentrations of analyte, is common on columns with protein-based stationary phases and is best explained by slow dissociation kinetics.[235]

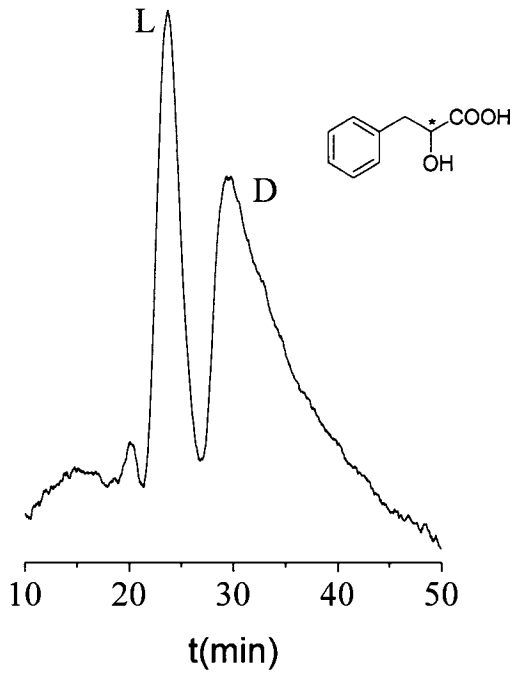

Figure 35: The enantiomers of PLA were separated using anti-D-AHA 73 as a chiral selector in a 0.75 x 200 mm microbore column packed with silica. Separations were achieved under isocratic conditions using PBS as mobile phase. Analytes were detected by measuring UV absorbance at 205 nm.

CHAPTER IV

SUMMARY

In this research, remarkably specific antibodies were produced that stereoselectively bind to the enantiomers of AHAs. In order to produce stereoselective antibodies to free AHAs, conjugates of *p*-amino-D- and -L-PLA and KLH were synthesized and used for the immunization of rabbits and mice. While polyclonal antibodies were obtained from the interstitial fluid or sera of rabbits, monoclonal antibodies were produced using hybridoma technology.

The binding characteristics and stereoselectivity of these antibodies were tested in noncompetitive and competitive ELISAs. The animals inoculated with the L-enantiomer of the hapten produced antibodies that only bind to the L-enantiomers of AHAs. Conversely, the animals inoculated with the D-enantiomer produced antibodies that only bind to the D-enantiomers of AHAs. The affinity of these antibodies to a variety of different AHAs was tested to evaluate the influence of the side chain to the overall strength of interaction. These antibodies proved effective for the sensitive, stereoselective discrimination of AHAs ranging from aromatic AHAs to aliphatic AHAs such as lactic acid. However, AHAs resembling the hapten were found to bind more strongly to the antibodies than do AHAs with aliphatic side chains.

These antibodies have been tested not only for their ability to stereoselectively bind various AHAs but also for their ability to distinguish between different classes of compounds. AHAs and AAs are similar classes of compounds that differ only in one functional group bound to the chiral carbon. Further ELISAs were performed to test the binding of an AA to the anti-AHA antibodies. Conversely, previously produced anti-AA antibodies were tested for their ability to bind to AHAs. Surprisingly, the anti-AHA antibodies do not bind at all to AAs nor do the anti-AA antibodies bind to AHAs. Neither did the anti-AHA antibodies bind to the structurally related compounds phenylpropionic acid (in which the hydroxyl group of PLA is substituted by a hydrogen atom) and PLA methyl ester (in which the carboxyl group of PLA is exchanged to a methyl ester derivative). The hydrogen/hydroxyl/carboxyl triad about the stereogenic center of AHAs is clearly essential for the interaction with the anti-AHA antibodies studied in this dissertation. A change in either hydroxyl or carboxyl functional groups resulted in a loss of all detectable interaction.

The exquisite stereoselectivity and class-specificity of the produced anti-AHA antibodies make them particularly useful for bioanalytical techniques. Enantiomer separation of PLA demonstrated the utility of the anti-AHA antibodies for chiral chromatography. The applicability of the antibodies as chiral selectors was further demonstrated in a fluorescence immunoassay that allowed the simultaneous detection of D-Phe, L-Phe, D-PLA, and L-PLA. Four antibodies, each of which binds only to analytes having the correct target structure and configuration, were conjugated to a

unique fluorophore, which enabled independent detection and quantitative measurement of the four analytes contained within the same sample.

REFERENCES

1. Pasteur, L. Mémoire sur la relation qui peut exister entre la forme crystalline et la composition chimique, et sur la cause de la polarization rotatoire. *Comptes. Rend. Hebd. Acad. Sci. Paris* **1848**, *26*, 535–538.

2. Pasteur, L. Mémoire sur la fermentation de l' acide tartrique. *Comptes. Rend. Hebd. Acad. Sci. Paris* **1858**, *46*, 615–618.

3. Fischer, E. Einfluss der Configuration auf die Wirkung der Enzyme. *Ber. Dtsch. Chem. Ges.* **1894**, *27*, 2985-2993.

4. Cushny, A. R. Atropine and the hyoscyamines—a study of the action of optical isomers. *J. Physiol.* **1904**, 176-194.

5. Holmstedt, B. The use of enantiomers in biological studies: an historical review. In *Chirality and biological activity*; Holmstedt, B.; Frank, H.; Testa, B., Eds.; Alan R. Liss: New York, 1990; pp 1-14.

6. Landsteiner, K.; van der Scheer, J. Serological differentiation of steric isomers. *J. Exp. Med.* **1928,** *48*, 315-320.

7. Piutti, A. Sur une nouvelle espece d'asparagine. *Comptes. Rend. Hebd. Acad. Sci. Paris* **1886**, *103*, 134–138.

8. Friedman, L.; Miller, J. G. Odor incongruity and chirality. *Science* **1971**, *172*, 1044-1046.

9. Walshe, J. M. Penicillamine, a new oral therapy for Wilson's disease. *Am. J. Med.* **1956**, *21*, 487-495.

10. Sheldon, R. A. *Chirotechnology: Industrial synthesis of optically active compounds*. Marcel Dekker: New York, 1993; pp 53.

11. Wainer, I. W.; Drayer, D. E. *Drug stereochemistry*. Marcel Dekker: New York, 1988; pp 253-254.

12. FDA - U.S. Food and Drug Administration, Center for Drug Evaluation and Research: FDA's policy statement for the development of new stereoisomeric drugs, 5/1/92, corrections made 1/3/97; http://www.fda.gov/cder/guidance/stereo.htm, accessed 8/2006.

13. Islam, M. R.; Mahdi, J. G.; Bowen, I. D. Pharmacological importance of stereochemical resolution of enantiomeric drugs. *Drug Safety*, **1997**, *17*, 149-165.

14. Mulzer, J. Basic Principles of EPC synthesis. In *Methods of organic chemistry: Stereoselective synthesis*, vol E 21;. Helmchen, G.; Hoffman, R.W.; Mulzer, J.; Schaumann, E., Eds.; Georg Thieme Verlag Stuttgart: New York, 2000; pp 77-85.

15. Lindner, W. Determination of enantiomeric purity via formation of diastereomers. In *Methods of organic chemistry: Stereoselective synthesis*, vol E 21a; Helmchen, G.; Hoffman, R. W.; Mulzer, J.; Schaumann, E., Eds.; Georg Thieme Verlag Stuttgart: New York, 2000; pp 225-252.

16. Lindner, W. Chiral Liquid Chromatography. In *Methods of organic chemistry: Stereoselective synthesis*, vol E 21a; Helmchen, G.; Hoffman, R. W.; Mulzer, J.; Schaumann, E., Eds.; Georg Thieme Verlag Stuttgart: New York, 2000; pp 193-224.

17. Chankvetadze, B. Chiral separation. Elsevier: Amsterdam; 2001.

18. Liu, Y.; Lantz, A. W.; Armstrong, D. W. High efficiency liquid and super-subcritical fluid-based enantiomeric separations: An overview. *J. Liq. Chromatogr. R. T.* **2004**, *27*, 1121-1178.

19. Chankvetadze, B.; Blaschke, G. Enantioseparations in capillary electromigration techniques: recent developments and future trends. *J. Chromatogr. A*, **2001**, *906*, 309-363.

20. Duddeck, H. Determination of relative configuration by nuclear magnetic resonance methods. In *Methods of organic chemistry: Stereoselective Synthesis*; vol E 21a; Helmchen, G.; Hoffman, R. W.; Mulzer, J.; Schaumann. E., Eds.; Georg Thieme Verlag Stuttgart: New York, 2000; pp 293-377.

21. Schug, K. A.; Lindner, W. Chiral molecular recognition for the detection and analysis of enantiomers by mass spectrometric methods. *J. Sep. Sci.* **2005**, *28*, 1932-1955.

22. Korbel, G. A.; Lalic, G.; Shair, M. D. Reaction microarrays: A method for rapidly determining the enantiomeric excess of thousands of samples. *J. Am. Chem. Soc.* **2001**, *123*, 361-362.

23. Maier, N.; Franco, P.; Lindner, W. Separation of enantiomers: needs, challenges, perspectives. *J. Chromatogr. A*, **2001**, *906,* 3-33.

24. Booth, T. D.; Azzaoui K.; Wainer I. W. Prediction of chiral chromatographic separations using combined multivariate regression and neural networks. *Anal. Chem.* **1997**, *69*, 3879-3883.

25. Arshady, R.; Mosbach, K. Synthesis of substrate-selective polymers by host-guest polymerization. *Makromol. Chem.* **1981**, *182*, 687-692.

26. Wulff, G.; Minarik, M. Enzyme-analogue built polymers Part XX. Pronounced effect of temperature on racemic resolution using template-imprinted polymeric sorbents. *HRC & CC, J. High Resolut. Chromatogr. Chromatogr. Commun.* **1986,** *9*, 607-608.

27. Sellergren, B.; Lepistö, M.; Mosbach, K. Highly enantioselective and substrate-selective polymers obtained by molecular imprinting utilizing noncovalent interactions. NMR and chromatographic studies on the nature of recognition. *J. Am. Chem. Soc.* **1988**, *110*, 5853-5860.

28. Michaud, M.; Jourdan, E.; Villet, A.; Ravel, A.; Grosset, C.; Peyrin, E. A DNA aptamer as a new target-specific chiral selector for HPLC. *J. Am. Chem. Soc.* **2003**, *125*, 8672-8679.

29. Michaud, M.; Jourdan, E.; Ravelet, C.; Villet, A.; Ravel, A.; Grosset, C.; Peyrin, E. Immobilized DNA aptamers as target-specific chiral stationary phases for resolution of nucleoside and amino acid derivative enantiomers. *Anal. Chem.* **2004**, *76*, 1015-1020.

30. Ravelet, C.; Boulkedid, R.; Ravel, A.; Grosset, C.; Villet, A.; Fize, J.; Peyrin, E. A L-RNA aptamer chiral stationary phase for the resolution of target and related compounds. *J. Chromatogr. A* **2005**, *1076*, 62-70.

31. Ruta, J.; Ravelet, C.; Grosset, C.; Fize, J.; Ravel, A.; Villet, A.; Peyrin, E. Enantiomeric separation using an L-RNA aptamer as chiral additive in partial-filling capillary electrophoresis. *Anal. Chem.* **2006**, *78*, 3032-3039.

32. Ravelet, C.; Peyrin, E. Recent developments in the HPLC enantiomeric separation using chiral selectors identified by a combinatorial strategy. *J. Sep. Sci.* **2006**, *29*, 1322-1331.

33. Andre, C.; Berthelot, A.; Thomassin, M.; Guillaume, Y-C. Enantioselective aptameric molecular recognition material: Design of novel chiral stationary phase for enantioseparation of a series of chiral herbicides by capillary electrochromatography. *Electrophoresis* **2006**, *27*, 3254-3262.

34. Ruta, J.; Ravelet, C.; Grosset, C.; Fize, J.; Villet, A.; Ravel, A.; Peyrin, E. Chiral resolution of histidine using an anti-D-histidine L-RNA aptamer microbore column. *J. Chromatogr. B* **2007**, *845*, 186-190.

35. Hofstetter, H.; Hofstetter, O. Antibodies as tailor-made chiral selectors for detection and separation of stereoisomers. *TRAC-Trend. Anal. Chem.* **2005**, *24*, 869-879.

36. Andersson, L. I. Molecular imprinting: developments and applications in the analytical chemistry field. *J. Chromatogr. B* **2000**, *745*, 3-13.

37. Henery, O. Y. F.; Cullen, D. C.; Piletsky, S. A. Optical interrogation of molecularly imprinted polymers and development of MIP sensors: a review. *Anal. Bioanal. Chem.* **2005**, *382*, 947-956.

38. Spegel, P.; Schweitz, L.; Nilsson, S. Molecularly imprinted polymers in capillary electrochromatography: Recent developments and future trends. *Electrophoresis.* **2003**, *24*, 3892-3899.

39. Turiel, E.; Martin-Esteban, A. Molecularly imprinted polymers: towards highly selective stationary phases in liquid chromatography and capillary electrophoresis. *Anal. Bioanal. Chem.* **2004**, *378*, 1876-1886.

40. Sellergren, B. Imprinted chiral stationary phases in high-performance liquid chromatography. *J. Chromatogr. A* **2001**, *906*, 227-252.

41. Famulok, M.; Szostak, J. W. Stereospecific recognition of tryptophan agarose by in vitro selected RNA. *J. Am. Chem. Soc.* **1992**, *114*, 3990-3991.

42. Famulok, M. Molecular recognition of amino acids by RNA-aptamers: An L-citruline binding RNA motif and its evolution into an L-arginine binder. *J. Am. Chem. Soc.* **1994**, *116*, 1698-1706.

43. Williams, K. P.; Liu, X. H.; Schumacker, T. N. M.; Lin, H. Y.; Ausiello, D. A.; Kim, P. S.; Bartel, D. P. Bioactive and nuclease-resistant L-DNA ligand of vasopressin. *Proc. Natl. Acad. Sci.* **1997**, *94*, 11285-11290.

44. Geiger, A.; Burgstaller, P.; Eltz, H.; Roeder, A.; Famulok, M. RNA aptamers that bind L-arginine with sub-micromolar dissociation constants and high enantioselectivity. *Nucleic. Acids. Res.* **1996**, *24*, 1029-1036.

45. Proske, D.; Blank, M.; Buhmann, R.; Resch, A. Aptamers-basic research, drug development, and clinical applications. *Appl. Microbiol. Biot.* **2005**, *69*, 367-374.

46. Turner, R.J. *Immunology: A comparative approach*; Wiley: Chichester, UK; 1994.

47. Nezlin, R. *The immunoglobuins: structure and functions*; Academic Press: New York, 1998; pp 5.

48. Nezlin, R. *The immunoglobuins: structure and functions*; Academic Press: New York, 1998; pp 18-20.

49. Nezlin, R. *The immunoglobuins: structure and functions*; Academic Press: New York, 1998; pp 19-21.

50. Nezlin, R. *The immunoglobuins: structure and functions*; Academic Press: New York, 1998; pp 21-22.

51. Landsteiner, K. *The specificity of serological reactions*; Dover Publications: New York, 1962.

52. Harlow, E.; Lane, D. *Antibodies: A Laboratory Manual.* Cold Spring Harbor Laboratory: Cold Spring Harbor, New York, 1988.

53. Köhler, G.; Milstein, C. Continuous cultures of fused cells secreting antibody of predefined specificity. *Nature* **1975**, *256*, 495-497.

54. Köhler, G.; Milstein, C. Fusion between immunoglobulin-secreting and nonsecreting myeloma cell lines. *Eur. J. Immun.* **1976**, *6*, 511-519.

55. Galfre, G.; Howe, S. C.; Milstein, C.; Butcher, G. W.; Howard, J. C. Antibodies to major histocompatibility antigens produced by hybrid cell lines. *Nature* **1977**, *266*, 550-552.

56. Goding, J. W. *Monoclonal Antibodies: Principles and Practice*. Academic Press: San Diego, 1996.

57. Fitzpatrick, J.; Fanning, L.; Hearty, S.; Leonard, P.; Manning, B. M.; Quinn, J. G.; O'Kennedy, R. Applications and recent developments in the use of antibodies for analysis. *Anal. Lett.* **2000**, *33*, 2563-2609.

58. Landsteiner, K. *The Specificity of serological reactions*; Dover Publications: NewYork, 1962; pp 172-173.

59. Hofstetter, O.; Hofstetter, H.; Schurig, V.; Wilchek, M.; Green, B. S. Antibodies can recognize the chiral center of free α-amino acids. *J. Am. Chem. Soc.* **1998**, *120*, 3251-3252.

60. Hofstetter, O.; Hofstetter, H.; Wilchek, M.; Schurig, V.; Green, B. S. Production and application of antibodies directed against the chiral center of α-amino acids. *Int. J. Bio-Chromatogr.* **2000**, *5*, 165-174.

61. Hofstetter, O.; Hofstetter, H.; Schurig, V.; Wilchek, M.; Green, B. S. Chiral discrimination using an immunosensor. *Nat. Biotechnol.* **1999**, *17*, 371-374.

62. Hofstetter, O.; Hofstetter, H.; Schurig, V.; Wilchek, M.; Green, B. S. An immunochemical approach for the determination of trace amounts of enantiomeric impurities. *Chem. Commun.* **2000**, 1581-1582.

63. Hofstetter, O.; Lindstrom, H.; Hofstetter, H. Direct resolution of enantiomers in high-performance immunoaffinity chromatography under isocratic conditions. *Anal. Chem.* **2002**, *74*, 2119-2125.

64. Hofstetter, O.; Lindstrom, H.; Hofstetter, H. Effect of the mobile phase on antibody-based enantiomer separations of amino acids in high-performance liquid chromatography. *J. Chromatogr. A* **2004**, *1049*, 85-95.

65. Hofstetter, O.; Hertweck, J. K; Hofstetter, H. Detection of enantiomeric impurities in a simple membrane-based optical immunosensor. *J. Biochem. Bioph. Meth.* **2005**, *63*, 91-99.

66. Zeleke, J. M.; Smith, G. B.; Hofstetter. H.; Hofstetter, O. Enantiomer separation of amino acids in immunoaffinity micro LC-MS. *Chirality* **2006**, *18*, 544-550.

67. Tsourkas, A.; Hofstetter, O.; Hofstetter, H.; Weissleder, R.; Josephson, L. Magnetic relaxation switch immunosensors detect enantiomeric impurities. *Angew. Chem. Int. Edit.* **2004**, *43*, 2395-2399.

68. Dutta, P.; Tipple, C. A.; Lavrik, N. V.; Datskos, P. G.; Hofstetter, H.; Hofstetter, O.; Sepaniak, M. J. Enantioselective sensors based on antibody-mediated nanomechanics. *Anal. Chem.* **2003**, *75*, 2342-2348.

69. Hofstetter, H.; Cary, J. R.; Eleniste, P. P.; Hertweck, J. K.; Lindstrom, H. J.; Ranieri, D. I.; Smith, G. B.; Undesser, L. P.; Zeleke, J. M.; Zeleke, T. K.; Hofstetter, O. New developments in the production and use of stereoselective antibodies. *Chirality* **2005**, *17*, S9-S18.

70. Franco, E. J.; Hofstetter, H.; Hofstetter, O. A comparative evaluation of random and site-specific immobilization techniques for the preparation of antibody-based chiral stationary phases. *J. Sep. Sci.* **2006**, *10*, 1458-1469.

71. Zhang, S.; Ding, J.; Liu, Y.; Kong, J.; Hofstetter, O. Development of a highly enantioselective capacitive immunosensor for the detection of alpha-amino acids. *Anal. Chem.* **2006**, *78*, 7592-7596.

72. Tubbs, P. K. The metabolism of D-α-hydroxy acids in animal tissues. *Ann. NY Acad. Sci.* **1965**, *119*, 920-926.

73. Gordon, R. S. Metabolism of other D- and L-hydroxy acids. *Ann. NY Acad. Sci.* **1965**, *119*, 927-941.

74. Roberts, S. M. In *Comprehensive Organic Chemistry*, vol 2; Barton, D.; Ollis, W. D., Eds.; Pergamon: Oxford, 1979; pp739.

75. Ewaschuk, J. B.; Zello, G. A.; Naylor, J. M.; Brocks, D. R. Metabolic acidosis: separation methods and biological relevance of organic acids and lactic acid enantiomers. *J. Chromatogr. B* **2002**, *781*, 39-56.

76. Fall, P. J.; Szerlip, H. M. Lactic acidosis: From sour milk to septic shock. *J. Intensive Care Med.* **2005**, *20*, 225-271.

77. Calza, L.; Manfredi, R.; Chiodo, F. Hyperlactataemia and lactic acidosis in HIV-infected patients receiving antiretroviral therapy. *Clin. Nutr.* **2005**, *24*, 5-15.

78. Tripuraneni, N. S.; Smith, P. R.; Weedon, J.; Rosa, U.; Sepowitz, D. Prognostic factors in lactic acidosis syndrome caused by nucleoside reverse transcriptase inhibitors: Report of eight cases and review of the literature. *AIDS Patient Care St.* **2004**, *18*, 379-384.

79. Podebrad, F.; Heil, M.; Leib, S.; Geier, B.; Beck, T.; Mossandi, A.; Sewell, A. C.; Böhels, H. Analytical approach in diagnosis of inherited metabolic diseases: Maple syrup urine disease (MSUD) – simultaneous analysis of metabolites in urine by enantioselective multidimensional capillary gas chromatography-mass spectrometry (enantio-MDGC-MS). *J. High Res. Chromatog.* **1997**, *20*, 355-362.

80. Griffiths, C. E. M. Drug treatment of photoaged skin. *Drug Aging* **1999**, 14, 289-301.

81. Kaidbey, K.; Suntherland, B.; Bennett, P.; Wamer, W. G.; Barton, C.; Dennis, D.; Kornhauser, A. Topical glycolic acid enhances photodamage by ultraviolet light. *Photodermatol. Photo.* **2003**, 19, 21-27.

82. FDA - U.S. Food and Drug Administration, Center for Food Safety and Applied Nutrition, Office of Cosmetics and Colors: FDA Backgrounder: Alpha hydroxy acids in cosmetics, 6/3/97; http://www.cfsan.fda.gov/~dms/cos-aha.html, accessed 8/2006.

83. Heymann, L. A. The Cosmetic/drug dilemma: FDA regulation of alpha-hydroxy acids. *Food Drug Law J.* **1997**, 52, 357-375.

84. Scott, J. W. In *Asymmetric synthesis*, vol 4; Morrison, J. D.; Scott, J. W.; Eds.; Academic Press: New York, 1984.

85. Coppla, G. M.; Schuster, H. F. *α-Hydroxy acids in enantioselective synthesis*. Academic Press: Weinheim, 1997.

86. Kim, H. O.; Lum, C.; Lee, M. S. Malic Acid: A convenient precursor for the synthesis of peptide secondary structure mimetics. *Tetrahedron Lett.* **1997**, *38*, 4935-4938.

87. Christoffers, J.; Rößler, U. Novel synthesis of chiral, enantiomerically pure thiodiglycols and diglycols. *Tetrahedron-Asymmetr.* **1998**, *9*, 2349-2357.

88. Christoffers, J.; Rößler, U. Novel bi- and tridentate phosphane and thioether ligands derived from chiral α-hydroxy acids. *Tetrahedron-Asymmetr.* **1999**, *10*, 1207-1215.

89. Valentekovich, R. J.; Schreiber, S. L. Enantiospecific total synthesis of the protein phosphatase inhibitor motuporin. *J. Am. Chem. Soc.* **1995**, *117*, 9069-9070.

90. Boeckman Jr., R. K.; Yoon, S. K.; Heckendorn, D. K. Synthetic studies directed toward the eremantholides. 2. A novel application of the Ramberg-Baecklund rearrangement to a highly stereoselective synthesis of (+)-eremantholide A. *J. Am. Chem. Soc.* **1991**, *113*, 9682-9684.

91. Niwa, H.; Miyachi, Y.; Okamoto, O.; Uosaki, Y.; Kuroda, A.; Ishiwata, H.; Yamada, K. Total synthesis of optically active integerrimine, a twelve-membered dilactonic pyrrolizidine alkaloid of retronecine type. *Tetrahedron* **1992**, *48*, 393-412.

92. Niwa, H.; Ogawa, T.; Okamoto, O.; Yamada, K. Total synthesis of optically active moncrotaline,a carcinogenic pyrrolizidine alkaloid possessing an eleven-membered retronecine dilactone. *Tetrahedron* **1992**, *48*, 10531-10548.

93. Piskin, E. Biodegradable polymers as biomaterials. *J. Biomat. Sci-Polym. E.* **1995**, *6*, 775-795.

94. Ogawa, Y. Injectable microcapsules prepared with biodegradable poly(α-hydroxy) acids for prolonged release of drugs. *J. Biomat. Sci-Polym. E.* **1997**, *8*, 391-409.

95. Jain, R. A. The manufacturing techniques of various drug loaded biodegradable poly(lactide-co-glycolide) (PLGA) devices. *Biomaterials* **2000**, *21*, 2475-2490.

96. Rokkanen, P. U.; Bostman, O.; Hirvensalo, E.; Makela, E. A.; Partio, E. K.; Patiala, H.; Vainionpaa, S. I.; Vihtonen, K.; Tormala, P. Bioabsorbable fixation in orthopaedic surgery and traumatology. *Biomaterials* **2000**, *21*, 2607-2613.

97. Sawhaney, A. S.; Pathak, C. P.; Hubbell, J. A. Bioerodible hydrogels based on photopolymerized poly(ethylene glycol)-co-poly(α-hydroxy acid) diacrylate macromers. *Macromolecules* **1993**, *26*, 581-587.

98. Smith, K. L.; Schimpf, M. E.; Thompson, K. E. Bioerodible polymers for delivery of macromolecules. *Adv. Drug Deliver. Rev.* **1990**, *4*, 343-357.

99. Saulnier, B.; Ponsart, S.; Coudane, J.; Garreau, H.; Vert, M. Lactic acid-based functionalized polymers via copolymerization and chemical modification. *Macromol. Biosci.* **2004**, *4*, 232-237.

100. Taguchi, K.; Yano, S.; Hiratani, K.; Minoura, N.; Okahata, Y. Ring-opening polymerization of 3(*S*)-[(benzyloxycarbonyl)methyl]-1,4-dioxane-2,5-dione: A new route to a poly (α-hydroxy acid) with pendant carboxy groups. *Macromolecules* **1988**, *21*, 3338-3340.

101. Wong, C-H.; Matos, J. R. Enantioselective oxidation of 1,2-diols to L-α-hydroxy acids using coimmobilized alcohol and aldehyde dehydrogenases as catalysts. *J. Org. Chem.* **1985**, *50*, 1992-1994.

102. Wong, C-H.; Whitesides, G. M. Enzymes in synthetic organic chemistry. In *Tetrahedron organic chemistry series*, vol 12; Pergamon: Tarrytown; 1994.

103. Kim, M. J.; Whitesides, G. M. L-Lactate dehydrogenase: Substrate specificity and use as a catalyst in the synthesis of homochiral 2-hydroxy acids. *J. Am. Chem. Soc.* **1988**, *110*, 2959-2964.

104. Simone, E. S.; Plante, R.; Whitesides, G. M. *Appl. Biochem. Biotechnol.* **1989**, *22*, 169.

105. Nakamura, K.; Inoue, K.; Ushio, K.; Oka, S.; Ohno, A. Stereochemical control on yeast reduction of α-keto esters. Reduction by immobilized Bakers' yeast in hexane. *J. Org. Chem.* **1988**, *53*, 2589-2593.

106. Effenberger, F. Synthesis and reactions of optically active cyanohydrins. *Angew. Chem. Int. Ed.* **1994**, *33*, 1555-1564.

107. Pansare, S. V.; Ravi, R. G. Asymmetric reactions of α-ketoacid-derived hemiacetals: Stereoselective synthesis of α-hydroxy acids. *Tetrahedron* **1998**, *54*, 14549-14564.

108. Akiyama, T.; Nishimoto, H.; Ozaki, S. Diastereoselective reduction of α-keto esters bearing *chiro*-inositol derivatives as chiral auxiliaries. *Tetrahedron Lett.* **1991**, *32*, 1335-1336.

109. Evans, D. A.; Morrissey, M. M.; Dorow, R. L. Asymmetric oxygenation of chiral imide enolates. A general approach to the synthesis of enantiomerically pure alpha-hydroxy carboxylic acid synthons. *J. Am. Chem. Soc.* **1985**, *107*, 4346-4348.

110. Aladro, F. J.; Guerra, F. M.; Moreno-Dorado, F. J.; Bustamante, J. M.; Jorge, Z. D.; Massanet, G. M. Enantioselective synthesis of α-hydroxy acids through oxidation of terminal alkenes with AD-mix/TEMPO. *Tetrahedron Lett.* **2000**, *41*, 3209-3213.

111. Burk, M. J.; Kalberg, C. S.; Pizzano, A. Rh-DuPHOS-catalyzed enantioselective hydrogenation of enol esters. Application to the synthesis of highly enantioenriched α-hydroxy esters and 1,2-diols. *J. Am. Chem. Soc.* **1998**, *120*, 4345-4353.

112. Mashima, K.; Kusano, K.; Sato, N.; Matsumura, Y.; Nozaki, K.; Kumobayashi, H.; Sayo, N.; Hori, Y.; Ishizaki, T.; Akutagawa, S.; Takaya, H. Cationic BINAP-Ru(II) halide complexes: Highly efficient catalysts for stereoselective asymmetric hydrogenation of α- and β-functionalized ketones. *J. Org. Chem.* **1994**, *59*, 3064-3076.

113. Deechongkit, S.; You, S-L.; Kelly, J. W. Synthesis of all nineteen appropriately protected chiral α-hydroxy acid equivalents of the α-amino acids for boc solid-phase despi-peptide synthesis. *Org. Lett.* **2004**, *6*, 497-500.

114. Schmid, M. G.; Grobuschek, N.; Lecnik, O.; Gübitz, G. Chiral ligand-exchange capillary electrophoresis. *J. Biochem. Bioph. Meth.* **2001**, *48*, 143-154.

115. Berthod, A.; Chen, X.; Kullman, J. P.; Armstrong, D. W.; Gasparrini, F.; D'Acquarica, I.; Villani, C.; Carotti, A. Role of the carbohydrate moieties in chiral recognition on teicoplanin-based LC stationary phases. *Anal. Chem.* **2000**, *72*, 1767-1780.

116. Welch, C. J. Evolution of chiral stationary phase design in the Pirkle laboratories. *J. Chromatogr. A* **1994**, *666*, 3-20.

117. Andersson, S.; Allenmark, S.; Erlandsson, P.; Nilsson, S. Direct liquid chromatographic separation of enantiomers on immobilized protein stationary phases: VIII. A comparison of a series of sorbents based on bovine serum albumin and its fragments. *J. Chromatogr.* **1990**, *498*, 81-91.

118. Dotsevi, G.; Soga, Y.; Cram, D. J. Chromatographic optical resolution through chiral complexation of amino ester salts by a host covalently bound to silica. *J. Am. Chem. Soc.* **1975**, *97*, 2342-2348.

119. Brandt, R.; Siegel, S.; Waters, M.; Bloch, M. Spectrophotometric assay for D-(−)-lactate in plasma. *Anal. Biochem.* **1980**, *102*, 39-46.

120. McKendry, R.; Theoclitou, M-E.; Rayment, T,; Abell, C. Chiral discrimination by chemical force microscopy. *Nature* **1998**, *391*, 566-568.

121. Tabachnik, M.; Sobotka, H. Azoproteins. I. Spectrophotometric studies of amino acid azo derivatives. *J. Biol. Chem.* **1959**, *234*, 1726-1730.

122. Wilchek, M.; Miron, T. Activation of sepharose with *N,N'*-disuccinimidyl carbonate. *Appl. Biochem. Biotechnol.* **1985**, *11*, 191-193.

123. Erlanger, B. F. The preparation of antigenic hapten-carrier conjugates: A survey. *Method. Enzymol.* **1980**, *70*, 85-104.

124. Hermanson, G. T. *Bioconjugate techniques*. Academic press: San Diego,1996; pp 419-455.

125. Sela, M.; Fuchs, S.; Arnon, R. Studies on the chemical basis of the antigenicity of proteins. 5. Synthesis, characterization and immunogenicity of some multichain and linear polypeptides containing tyrosine. *Biochem. J.* **1962**, *85*, 223-235.

126. Sela, M. Antigenicity: Some molecular aspects. *Science* **1969**, 166, 1365-1374.

127. Atassi, M. Z.; Singhal, R. P. Immunochemistry of sperm whale myoglobin. XI. Modification of two glutamic acid residues and their role in the antigenic reactivity. *Immunochemistry* **1972**, *9*, 1057-1062.

128. Crumpton, M. J. In *The Antigens*, vol. 2; Sela M. Ed.; Academic Press: New York, 1974; pp 1.

129. Arnon, R. A selective fractionation of anti-lysozyme antibodies of different determinant specificities. *Eur. J. Biochem.* **1968**, *5*, 583-589.

130. Arnon, R.; Sela, M. Antibodies to a unique region in lysozyme provoked by a synthetic antigen conjugate. *Proc. Nat. Acad. Sci.* **1969**, *62*, 163-170.

131. Arnon, R.; Maron, E.; Shiozawa, C.; Sela, M. Chemical and immunological characterization of a unique antigenic region in lysozyme. *Biochemistry* **1971**, *10*, 763-771.

132. Blake, C. C. F.; Koenig, D. F.; Mair, G. A.; North, A. C. T.; Phillips, D. C.; Sarma, V. R. Structure of hen egg-white lysozyme: A Three-dimensional Fourier synthesis at 2 Å resolution. *Nature* **1965**, *206*, 757-760.

133. Deshpande, S. S. *Enzyme immunoassays: From concept to product development*; Chapman & Hall: New York, 1996; pp 117-130.

134. Got, P. A.; Scherrmann, J. M. Stereoselectivity of antibodies for the bioanalysis of chiral drugs. *Pharm. Res.* **1997**, *14*, 1516-1523.

135. Cook, C. E. Enantiomer analysis by competitive binding methods. In *Drug stereochemistry*; Wainer, I. W.; Drayer, D. E. Eds.; Marcel Dekker: New York, 1993; pp 35-64.

136. Hermanson, G. T. *Bioconjugate techniques*. Academic Press: San Diego, 1996; pp 446-449.

137. Landsteiner, K. *The Specificity of serological reactions*; Dover Publications: NewYork, 1962; pp 160.

138. Klause, G. G. B.; Cross, A. M. The influence of epitope density on the immunological properties of hapten-protein conjugates. *Cell. Immunol.* **1974**, *14*, 226-241.

139. Malaitsev, V. V.; Azhipa, O. Y. Influence of epitope density on the immunogenic properties of hapten-protein conjugates. *Bull. Exp. Biol. Med.* **1993**, *115*, 726-728.

140. Harlow, E.; Lane, D. *Antibodies: A Laboratory Manual*. Cold Spring Harbor Laboratory: Cold Spring Harbor, NY, 1988; pp 298-299.

141. Björck, L. Protein L - a novel bacterial cell wall protein with affinity for immunoglobulin light chains. *J. Immunol.* **1988**, *140*, 1194-1197.

142. Sjodal, J. Structural studies on the four repetitive Fc-binding regions in protein A from Staphylococcus aureus. *Eur. J. Biochem.* **1977**, *78*, 471-490.

143. Deshpande, S. S. *Enzyme immunoassays: From concept to product development*; Chapman & Hall: New York, 1996; pp 46.

144. Eliasson, M.; Olson, A.; Palmcrantz, E.; Wiberg, K.; Inganas, M.; Guss, B.; Linberg, M.; Uhlen, M. Chimeric IgG-binding receptors engineered from staphylococcal protein A and streptococcal protein G. *J. Biol. Chem.* **1988**, *263*, 4323-4327.

145. Cuatrecasas, P.; Wilchek, M.; Anfinsen, C. B. Selective enzyme purification by affinity chromatography. *Proc. Natl. Acad. Sci.* **1968**, *61*, 636-643.

146. Hofstetter, O. *Stereoselektive Antikörper gegen Aminosäuren*. Doctoral Dissertation: University of Tübingen, Germany; 1999.

147. Singh, K. V.; Kaur, J.; Raje, M. An ELISA-based approach to optimize elution conditions for obtaining hapten-specific antibodies. *Anal. Bioanal. Chem.* **2003**, 377, 220-224.

148. Harlow, E.; Lane, D. *Antibodies: A Laboratory Manual*. Cold Spring Harbor Laboratory: Cold Spring Harbor, NY, 1988; pp 291.

149. Deshpande, S. S. *Enzyme immunoassays: From concept to product development*; Chapman & Hall: New York, 1996; pp 145.

150. Yalow, R. S.; Berson, S. A. Assay of plasma insulin in human subjects by immunological methods. *Nature* **1959**, *184*, 1648-1649.

151. Yalow, R. S.; Berson, S. Immunoassay of endogenous plasma insulin in man. *J. Clin. Invest.* **1960**, *39*, 1157-1175.

152. Engvall, E.; Perlmann, P. Enzyme-linked immunosorbent assay (ELISA). Quantitative assay of immunoglobulin G. *Immunochemistry* **1971**, *8*, 871-874.

153. van Weeman, B. K.; Schuurs, A. H. W. N. Immunoassay using antigen-enzyme conjugates. *FEBS Lett.* **1971**, *15*, 232-236.

154. Nossal, G. J. V.; Lederberg, J. Antibody production by single cells. *Nature* **1958**, *181*, 1419-1420.

155. Jerne, N. K.; Nordin, A. A. Plaque formation in agar by single antibody-producing cells. *Science* **1963**, *140*, 405.

156. Mäkelä, O. The specificity of antibodies produced by single cells. *Cold Spring Harbor Symp. Quant. Biol.* **1967**, *32*, 423-430.

157. Green, I.; Vassill, P.; Nussenzweig, V.; Benacerraf, B. Specificity of the antibodies produced by single cells following immunization with antigens bearing two types of antigenic determinants. *J. Exp. Med.* **1967**, *125*, 511-526.

158. Klinman, N. R. Antibody with homogeneous antigen binding produced by splenic foci in organ culture. *Immunochemistry* **1969**, *6*, 757-759.

159. Klinman, N. R. Mechanism of antigenic stimulation of primary and secondary clonal precursor cells. *J. Exp. Med.* **1972**, *136*, 241-260.

160. Köhler, G.; Milstein, C. Derivation of specific antibody-producing tissue culture and tumor lines by cell fusion. *Eur. J. Immun.* **1976**, *6*, 511-519.

161. Briles, D. E.; Davie, J. M. Clonal nature of the immune response. II. The effect of immunization on clonal commitment. *J. Exp. Med.* **1980**, *152*, 151-160.

162. Tijssen, P. *Practice and theory of enzyme immunoassays*. Elsevier: Amsterdam, 1985.

163. Roitt, I. M.; Brostoff, J.; Male, D. *Immunology*. Gower Medical Publishing: London, 1989.

164. Day, E. D. *Advanced immunochemistry*. Wiley-Liss: NY, 1990; pp 355.

165. Eisen, H. N.; Little, J. R.; Osterland, C. K.; Simms, E. S. A myeloma protein with antibody activity. *Cold Spring Harbor Symp. Quant. Biol.* **1967**, *32*, 75-81.

166. Eisen, H. N.; Simms, E. S.; Potter, M. Mouse myeloma proteins with antihapten antibody activity: The protein produced by plasma cell tumor MOPC-315. *Biochemistry* **1968**, *7*, 4126-4134.

167. Jaffe, B. M.; Eisen, H. N.; Simms, E. S.; Potter, M. Myeloma proteins with anti-hapten antibody activity: ε-2,4-dinitrophenyl lysine binding by the protein produced by mouse plasmacytoma MOPC-460. *J. Immunol.* **1969**, *103*, 872-874.

168. Terry, W. D.; Ashman, R. F.; Metzger, H. Human IgA-myeloma protein which binds nitrophenyl ligands. *Immunochemistry* **1970**, *7*, 257-260.

169. Michaelides, M. C.; Eisen, H. N. The strange cross-reaction of menadione (vitamin K_3) and 2,4-dintrophenyl ligands with a myeloma protein and some conventional antibodies. *J. Exp. Med.* **1974**, *140*, 687-702.

170. Potter, M.; Boyce, C. R. Induction of plasma cell neoplasms in strain BALB/c mice with mineral oil adjuvants. *Nature* **1962**, *193*, 1086-1087.

171. Potter, M. Immunoglobulin-producing tumors and myeloma proteins of mice. *Physiol. Rev.* **1972**, *52*, 631-719.

172. Deshpande, S. S. *Enzyme immunoassays: From concept to product development*. Chapman & Hall: New York, 1996; pp 141.

173. Ringertz, N. R.; Savage, R.E. *Cell hybrids*. Academic Press: New York, 1976.

174. Pontecorvo, G. Production of indefinitely multiplying mammalian somatic cell hybrids by polyethylene glycol (PEG) treatment. *Somatic. Cell Genet.* **1976**, *1*, 397-400.

175. Galfrè, G.; Milstein, C. Preparation of monoclonal antibodies: strategies and procedures. *Meth. Enzym.* **1981**, *73*, 3-46.

176. Vienken, J.; Zimmermann, U.; Fouchard, M.; Zagury, D. Electrofusion of myeloma cells on the single cell level. *FEBS Lett.* **1983**, *163*, 54-56.

177. Vienken, J.; Zimmermann, U. An improved electrofusion technique for production of mouse hybridoma cells. *FEBS Lett.* **1985**, *182*, 278-279.

178. Deshpande, S. S. *Enzyme immunoassays: From concept to product development.* Chapman & Hall: New York, 1996; pp 32.

179. Tiselius, A.; Kabat, E. An electrophoretic study of immune serums and purified antibody preparations. *J. Exp. Med.* **1939**, *69*, 119-131.

180. Steward, M. W. *Antibodies: Their structure and function.* Chapman and Hall: New York, 1984.

181. Potter, M.; Lieberman, R. Genetics of immunoglobulin in the mouse. *Adv. Immunol.* **1967**, *7*, 92-145.

182. Harlow, E.; Lane, D. *Antibodies: A Laboratory Manual.* Cold Spring Harbor Laboratory: Cold Spring Harbor, NY, 1988; pp 231.

183. Harlow, E.; Lane, D. *Antibodies: A Laboratory Manual.* Cold Spring Harbor Laboratory: Cold Spring Harbor, NY, 1988; pp 291.

184. Deshpande, S. S. *Enzyme immunoassays: From concept to product development.* Chapman & Hall: New York, 1996; pp 145.

185. Berzofsky, J.A.; Schechter, A.N. The concepts of crossreactivity and specificity in immunology. *Mol. Immunol.* **1981**, *18*,751–763.

186. van Regenmortel, M.H.V. From absolute to exquisite specificity. Reflections on the fuzzy nature of species, specificity and antigenic sites. *J. Immunol. Meth.* **1998**, *216*: 37–48.

187. Kubinyi, H. Chemical similarity and biological activity. *J. Braz. Chem. Soc.* **2002**, *13*, 717-726.

188. Thornber, C. W. Isosterism and molecular modification in drug design. *Chem. Soc. Rev.* **1979**, *8*, 563-580.

189. Lipinski, C. A. Bioisosterism in drug design. *Ann. Rep. Med. Chem.* 1986, 21, 283-291.

190. Lima, L. M.; Barreiro, E. J. Bioisosterism: A useful strategy for molecular modification and drug design. *Curr. Med. Chem.* **2005**, *12*, 23-49.

191. Arrhenius, S. *Immunochemistry: The application of the principles of physical chemistry to the study of the biological antibodies*. The Macmillan Company: NewYork, 1907.

192. Pressman, D.; Siegel, M. The binding of simple substances to serum proteins and its effect on apparent antibody-hapten combination constants. *J. Am. Chem. Soc.* **1953**, 75, 686-693.

193. Benveniste, R.; Davies, J. Structure-activity relationships among the aminoglycoside antibiotics: role of hydroxyl and amino groups. *Antimicrob. Agents. Ch.* **1973**, *4*, 402-409.

194. Nagabhushan, T. L.; Daniels, P. J. L. Synthesis and biological properties of 6'-amino-6'-deoxygentamicin A. *J. Med. Chem.* **1994**, *17*, 1030-1031.

195. Mingeot-Leclercq, M. P.; Glupczynski, Y.; Tulkens, P. M. Aminoglycosides: Activity and Resistance. *Antimicrob. Agents. Ch.* **1999**, *43*, 727-737.

196. Eustice, D. C.; Wilhelm, J. M. Mechanisms of action of animoglycoside antibiotics in eukaryotic protein synthesis. *Antimicrob. Agents. Ch.* **1984**, *26*, 53-60.

197. Chaires, J. B.; Satyanarayana, S.; Suh, D.; Fokt, I.; Prewloka, T.; Priebe, W. Parsing the fee energy of anthracycline antibiotic binding to DNA. *Biochemistry* **1999**, *35*, 2047-2053.

198. Bailly, C.; Qu, X.; Anizon, F.; Prudhomme, M.; Riou, J-F; Chaires, J. B. Enhanced binding to DNA and topoisomerase I inhibition by an analog of the antitumor antibiotic rebeccamycin containing an amino sugar residue. *Mol. Pharmacol.* **1999**, *55*, 377-385.

199. Capranico, G.; Supino, R.; Binaschi, M.; Capolongo, L.; Grandi, M.; Suarato, A.; Zunino, F. Influence of structural modifications at the 3' and 4' positions of doxorubicin on the drug ability to trap topoisomerase II and to overcome multidrug resistance. *Mol. Pharmacol.* **1994**, *45*, 908-915.

200. Kati, W. M.; Montgomery, D.; Maring, C.; Stoll, V. S.; Giranda, V.; Chen, X.; Laver, G.; Kohlbrenner, W.; Norbeck, D. W. Novel α- and β-amino acid inhibitors of influenza virus neuraminidase. *Antimicrob. Agents. Ch.* **2001**, *45*, 2563-2570.

201. Smith, B. J.; Colman, P. M.; Itzstein, M. V.; Danylec, B.; Varghese, J. N. Analysis of inhibitor binding in influenza virus neuraminidase. *Protein Sci.* **2001**, *10*, 689-696.

202. Szajnman, S. H.; Ravaschino, E. L.; Docampo, R.; Rodriguez, J. B. Synthesis and biological evaluation of 1-amino-1,1-bisphosphonates derived from fatty acids against *Trypanosoma cruzi* targeting farnesyl pyrophosphate synthase. *Bioorg. Med. Chem. Lett.* **2005**, *15*, 4685-4690.

203. Hope, D. B.; Wälti, M. [1-(L-2-Hydroxy-3-mecaptopropanoic acid)]-oxytocin, a highly potent analogue of oxytocin not bound by neurophysin. *Biochem. J.* **1971**, *125*, 909-911.

204. Teplyakov, A.; Obmolova, G.; Badet-Denisot, M-A.; Badet, B. The mechanism of sugar phosphate isomerization by glucosamine 6-phosphate synthase. *Protein Sci.* **1999**, *8*, 596-602.

205. Bieling, P.; Beringer, M.; Adio, S.; Rodnina, M, V. Peptide bond formation does not involve acid-base catalysis by ribosomal residues. *Nat. Struct. Mol. Biol.* **2006**, *13*, 423-428.

206. Coons, A. H.; Creech, H. J.; Jones, R. N. Immunological properties of an antibody containing a fluorescent probe. *P. Soc. Exp. Biol. Med.* **1941**, *47*, 200-202.

207. Coons, A. H.; Creech, H. J.; Jones, R. N.; Berliner, E. The demonstration of pneumococcal antigen in tissues by the use of fluorescent antibody. *J. Immunol.* **1942**, *45*, 159-170.

208. Hemmilä, I. A. *Applications of fluorescence in immunoassays*. Wiley: New York, 1991; pp 21.

209. Ekins, R. P. Multi-analyte immunoassay. *J. Pharm. Biomed. Anal.* **1989**, *7* 155–168.

210. Kricka, L. J. Simultaneous multianalyte immunoassays. In *Immunoassay*; Diamandis, E. P.; Christopoulos, T. K., Eds.; Academic Press: New York, 1996; pp 389-404.

211. Ekins, R. P.; Chu, F. W. Multianalyte microspot immunoassay—microanalytical "compact disk" of the future. *Clin. Chem.* **1991**, *37*, 1955-1967.

212. Ekins, R. P. Ligand assays: from electrophoresis to miniaturized microarrays. *Clin. Chem.* **1998**, *44*, 2015-2030.

213. Brecht, A.; Abuknesha, R. Multi-analyte immunoassays application to environmental analysis. *TRAC-Trend. Anal. Chem.* **1995**, *14*, 361-371.

214. Marshall, N. J.; Dakubu, S.; Jackson, T.; Ekins, R. P. Pulsed light, time resolved fluoroimmunoassay. In *Monoclonal antibodies and developments in immunoassay*; Albertini, A.; Ekins, R. P., Eds.; Elsevier: Amsterdam, 1981; pp 101-108.

215. Soini, E.; Lövgren, T.; Reimer, C. B. Time-resolved fluorescence of lanthanide probes and applications in biotechnology. *Crit. Rev. Anal. Chem.* **1987**, *18*, 105-154.

216. Xu, Y-Y.; Pettersson, K.; Blomberg, K.; Hemmilä, I.; Mikoa, H. Lövgren, T. Simultaneous quadruplelabel fluorometric immunoassay of thyroid-stimulating hormone, 17 α-hydroxyprogestrone, immunoreactive trypsin, and creatine kinase MM isoenzyme in dried blood spots. *Clin. Chem.* **1992**, *38*, 2038-2043.

217. Wood, P.; Barnard, G. Fluoroimmunoassay. In *Principles and practice of immunoassay*, Price, C. P.; Newman, D. J., Eds.; Macmillan Referecne Ltd.: New York, 1997; pp104-402.

218. Salamain, M.; Vessieres, A.; Brossier, P.; Jaouen, G. Use of Fourier transform infrared spectroscopy for the simultaneous quantitative detection of metal carbonyl tracers suitable for multilabel immunoassays. *Anal. Biochem.* **1993**, *208*, 117-120.

219. DeMars, D. D.; Katzmann, J. A.; Kimlinger, T. K. Simultaneous measurement of total and IgA-conjugated alpha 1-microglobulin by a combined immunoenzyme/immunoradiometric assay technique. *Clin. Chem.* **1989**, *35*, 766-772.

220. Mertens, R.; Stüning, M.; Weiler, E. W. Metabolism of titrated enantiomers of abscisic acid prepared by immunoaffinity chromatography. *Naturwissenschaften* **1982**, 69, 595-597.

221. Haywood, A. M. Virus receptors: Binding, adhesion strengthening, and changes in viral structure. *J. Virol.* **1994**, *68*, 1-5.

222. Fairchild, P. J.; Wraith, D. C. Lowering the tone: mechanisms of immunodominance among epitopes with low affinity for MHC. *Immunol. Today* **1996**, *17*, 80-85.

223. Hakomori, S. I. Structure and function of sphingoglycolipids in transmembrane signaling and cell-cell interactions. *Biochem. Soc. Trans.* **1993**, *21*, 583-595.

224. Van der Merwe, P. A.; Brown, M. H.; Davis, S. J.; Barclay, A. N. Affinity and kinetic analysis of the interaction of the cell adhesion molecules rat CD2 and CD8. *EMBO J.* **1993**, *12*, 4945-4954.

225. Reilly, P. L.; Woska, J. R.; Jeanfavre, D. D.; McNally, E.; Rothlein, R.; Bormann, B. J. The native structure of intercellular adhesion molecule-1 (ICAM-1) is a dimer. *J. Immunol.* **1995**, *155*, 529-532.

226. Allenmark, S. Enantioselective binding of small ligands to proteins and its use for direct separation of optical antipodes by isocratic liquid affinity chromatography. *Chem. Scr.* **1982**, *20*, 5-10.

227. Zopf, D.; Ohlson, S. Weak-affinity chromatography. *Nature* **1990**, *346*, 87-88.

228. Armstrong, D.; Ward, T.; Armstrong, R.; Beesley, T. Separation of drug stereoisomers by the formation of β-cyclodextrin inclusion complexes. *Science* **1986**, *232*, 1132-1135.

229. Perrin, S. R.; Pirkle, W. H. Commercially available brush-type chiral selectors for the direct resolution of enantiomers. *ACS Symp. Ser.* **1991**, *471*, 43-46.

230. Allenmark, S.; Andersson, S. Chromatographic resolution of chiral compounds by means of immobilized proteins. In *Molecular Interactions in Bioseparations*; Ngo, T. T., Ed.; Plenum: New York, 1993; pp 179-187.

231. Loun, B.; Hage, D. S. Chiral separation mechanisms in immobilized protein affinity columns: Binding of R- and S-warfarin in human serum albumin. *J. Mol. Reconit.* **1995**, *8*, 235.

232. Kemple, M.; Mosbach, K. Binding studies on substrate- and enantio-selective molecularly imprinted polymers. *Anal. Lett.* **1991**, *24*, 1137-1145.

233. Andersson, H. S.; Koch-Schmidt, A. C.; Ohlson, S.; Mosbach, K. Study of the nature of recognition in molecularly imprinted polymers. *J. Mol. Reconit.* **1996**, *9*, 675-682.

234. Koidl, J.; Schmid, M. G.; Konrad, M.; Petschauer, G.; Kostner, G. M.; Gübitz, G. Chiral separation of T_3 enantiomers using stereoselective antibodies as a selector in micro-HPLC. *J. Biochem. Bioph. Meth.* **2006**, *69*, 33-42.

235. Fornstedt, T.; Zhong, G.; Bensentiti, Z.; Guiochon, G. Experimental and theoretical study of the adsorption behavior and mass transfer kinetics of propanolol enantiomers on cellulose protein as the selector. *Anal. Chem.* **1996**, *68*, 2370-2378.

APPENDIX

BUFFER AND CELL CULTURE MEDIA PREPARATION

Phosphate-Buffered Saline

A stock solution of 20x PBS is prepared by dissolving 48 g of sodium phosphate dibasic, 8 g of potassium phosphate monobasic, 8 g of potassium chloride, and 320 g of sodium chloride in two liters of water. PBS is made by diluting the stock solution of 20x PBS by a factor of 20 with water.

Carbonate Buffer

Sodium bicarbonate (2.1 g) and sodium carbonate (2.65 g) are each dissolved in 500 mL of water to make 50 mM sodium bicarbonate and 50 mM sodium carbonate solutions, respectively. Carbonate buffer is prepared by adding 50 mM sodium carbonate to 500 mL of 50 mM sodium bicarbonate until the pH of the buffer is 9.6.

Citrate-Phosphate Buffer

Stock solutions of 100 mM citric acid and 200 mM sodium phosphate dibasic are made by dissolving 19.2 g of citric acid and 3.56 g of sodium phosphate dibasic, respectively, in 100 mL of water each. Stock solutions are stored at 4°C until needed. Citrate-phosphate buffer is made by mixing 4.8 mL of 100 mM citric acid, 5.2 mL of 200 mM sodium phosphate dibasic, and 10 mL of water.

Tris/HCl Buffer

One hundred mM Tris buffer is made by adding 6.05 g of Trizma base to 500 mL of water and adjusting the pH to 7.0 with HCl.

PBS/Tween 20

PBS/Tween 20 buffer is made by adding 1 mL of Tween 20 to two liters of PBS.

OPD ELISA Substrate

Citric acid (0.1 M, 4.8 mL) and sodium phosphate dibasic (0.2 M, 5.2 mL) are combined with 10 mL of water, then 8 mg of 1,2-phenylenediamine are added. After mixing thoroughly, 13μL of 30% hydrogen peroxide are added.

Cell Culture Medium

Cell culture medium is prepared by dissolving 10.4 g of RPMI-1640 medium powder in 750 mL of ultrapure water. The pH is transiently (for approximately 20 minutes) lowered to 4.0 with 1 N hydrochloric acid to aid in dissolving the medium. After readjusting the pH to 7.2 with 1 N sodium hydroxide, 2.5 g of glucose, 1.5 g of sodium bicarbonate, and 2.4 g of HEPES are added to the medium. More ultrapure water is added to bring the volume to 840 mL. Under sterile conditions, 10 mL of sodium pyruvate is added. The medium is filtered, stored at 4°C, and warmed up to 37°C before feedings.

The medium for myeloma cells is supplemented with horse serum and antibiotic-antimycotic. Before feeding, 1 mL of antibiotic-antimycotic and 15 mL of horse serum are added to 86 mL of RPMI medium. The medium for hybridoma cells is supplemented with HAT, horse serum, and antibiotic-antimycotic. One vial of 50x HAT media supplement is dissolved in 10 mL of prepared medium. Before feeding, 2 mL of HAT, 1 mL of antibiotic-antimycotic, and 15 mL of horse serum are added to 84 mL of RPMI medium.